LIBRARIES
UNIVERSITY OF WISCONSIN–MADISON

Hydrodynamics and associated chemical species transport calculations performed in analysis of the Exxon/Crandon infiltration test site. 1981

[s.l.]: [s.n.], 1981

https://digital.library.wisc.edu/1711.dl/OCW2JKUNULB258K

http://rightsstatements.org/vocab/InC/1.0/

For information on re-use see:
http://digital.library.wisc.edu/1711.dl/Copyright

The libraries provide public access to a wide range of material, including online exhibits, digitized collections, archival finding aids, our catalog, online articles, and a growing range of materials in many media.

When possible, we provide rights information in catalog records, finding aids, and other metadata that accompanies collections or items. However, it is always the user's obligation to evaluate copyright and rights issues in light of their own use.

728 State Street | Madison, Wisconsin 53706 | library.wisc.edu

UNIVERSITY LIBRARY
UW-STEVENS POINT

TD
194.66
.W62
C708
no.27

RECEIVED
JAN 30 1981
EXXON MINERALS
CRANDON PROJECT

HYDRODYNAMICS AND ASSOCIATED CHEMICAL SPECIES TRANSPORT CALCULATIONS PERFORMED IN ANALYSIS OF THE EXXON/CRANDON INFILTRATION TEST SITE

Prepared by

DAMES & MOORE
1626 Cole Boulevard
Golden, Colorado 80401

Dames & Moore

Job No. 08837-090-07
January 1981

ANCHORAGE · ATLANTA · BOSTON · CHICAGO · CINCINNATI · DENVER · HONOLULU · HOUSTON · LEXINGTON, KY · NEW HAVEN · PITTSBURGH · SALT LAKE CITY · SAN FRANCISCO · SANTA BARBARA · SEATTLE · SYRACUSE · WASHINGTON, D.C. · WHITE PLAINS

DAMES & MOORE

CONSULTANTS IN THE ENVIRONMENTAL AND APPLIED EARTH SCIENCES

JAKARTA · KUWAIT · LONDON · MADRID · PERTH · RIYADH · TEHRAN · TOKYO · TORONTO · VANCOUVER

1626 COLE BOULEVARD · GOLDEN, COLORADO 80401 PHONE (303) 232-6262
TWX 910-931-2600

January 26, 1981

EXXON Minerals Company
P.O. Box 813
655 Washington Street
Rhinelander, Wisconsin 54501

Attn: Mr. D.L. Rastetter

Dear Mr. Rastetter:

Please find attached two copies of our final report "Hydrodynamics and Associated Chemical Species Transport Performed in Analysis of the Exxon/Crandon Infiltration Test Site and Hypothetical Seepage Pond". This report describes mathematical model calculations relating to liquid waste disposal at the Crandon Prospecting Program Site. It includes work performed in April, 1980 and described in a preliminary draft report on November 6, 1980. In addition it includes a recent study of a hypothetical pond and its flow and chemical effects upon the underlying aquifer. The scope of this latter work was agreed upon by us in several verbal discussions and in our letter to you dated December 9, 1980.

It has been a pleasure working on this exciting project for Exxon. Please do contact us if you have any questions.

Very truly yours,

DAMES & MOORE

Devraj Sharma

Dr. Devraj Sharma
Manager, Advanced Technology Group

TABLE OF CONTENTS

LIST OF FIGURES AND TABLES

1.0 METHODOLOGY FOR ANALYSIS OF THE INFILTRATION BED

1.1 INTRODUCTION

The problem considered in this study is the prediction of vertical flow through an unsaturated soil zone towards the water table. The flow is generated by the injection of waste fluid via an infiltration bed. Since the governing equation of unsaturated flow is highly nonlinear, the problem is most tractable to numerical modelling techniques rather than analytical solution procedures.

The mathematical model utilized in this investigation is a one-dimensional finite-difference model which solves the governing unsaturated flow equations for the two main variables: pressure and chemical species concentration. A number of such species may be handled simultaneously. A semi-implicit solution algorithm is used to ensure that, provided reasonable selections of calculation-grid, time-step, iteration scheme, and numerical parameters such as relaxation factors are made, the solutions will converge monotonically. The resulting solutions generally have an acceptable degree of accuracy at all stages of the calculations. Details of the model and the numerical solution procedure it employs are provided in Appendix A.

1.2 INITIAL CONDITIONS

The supply of reasonable initial conditions for pressure head, ψ, is important in ensuring the realism and accuracy of predictions in the early stages of calculation. At this point, the effect of infiltration is just beginning to be felt.

To provide such initial conditions consistent with the properties of the site being considered, the following procedure was adopted. The algebraic notation and nomenclature are explained in Appendix A.

The vertical flow velocity may be written as:

$$W = -K_r K_z \left\{\frac{\partial \psi}{\partial z} + 1\right\} \qquad (1)$$

Three flow conditions may occur. Each is considered separately below. For present purposes, the flow condition corresponding to that at the Exxon-Crandon site is the first to be discussed.

(i) Small Infiltration Rates

Expressing the precipitation-induced infiltration rate as $\dot{q}''_I$, equation (1), may be written as:

$$\dot{q}''_I = K_r K_z \left\{\frac{\partial \psi}{\partial z} + 1\right\} \tag{2}$$

When infiltration rates are assumed to be small and steady, then:

$$\frac{\dot{q}''_I}{K_r K_z} << 1 \tag{3}$$

Equation (3) together with equation (2) implies that:

$$\frac{\partial \psi}{\partial z} < 0 \tag{4}$$

or the pressure heads are negative, i.e., below atmospheric pressure since $\psi = 0$ at $Z = 0$, and equation (2) gives:

$$\frac{\partial \psi}{\partial z} = \frac{\dot{q}''_I}{K_r K_z} - 1 \tag{5}$$

where K_r may be expressed (see Appendix A) as:

$$K_r = \{1 + [a_{ok}(-\psi)]^{a1k}\}^{a2k}, \quad -\infty < \psi < 0 \tag{6}$$

Equation (5) is highly non-linear and for arbitrary values of the constants must be solved by iterative techniques. The resulting ψ distribution will provide unsaturated zone pressure heads which are a function of both depth and infiltration rate.

(ii) Moderate-to-Large Infiltration Rates

Assuming that infiltration rates are steady and moderate, such that:

$$\frac{\dot{q}''_I}{K_r K_z} \geq 1 \qquad (7)$$

then either:

$$\frac{\partial \psi}{\partial z} > 0$$

or

$\psi = \psi_0$ everywhere, since pressures cannot exceed atmospheric values without man-made influences.

In other words, the soil is just saturated.

(iii) No-Flow Conditions

In the case that no infiltration is occuring:

$$W = 0$$

which implies:

$$\frac{\partial \psi}{\partial z} + 1 = 0 \qquad (8)$$

This can be simply integrated and allows one to write:

$$\psi - \psi_0 = -(Z - Z_0) \qquad (9)$$

Equation (9) implies that the pressure head above the water table are everywhere negative, i.e., hydrostatic and below atmospheric, if one defines $\psi_0 = 0$ at the water table, and $Z_0 = 0$ at the water table.

Since the rainfall-induced infiltration at the site under consideration is small, the initial pressure head distribution was obtained from equations (5) and (6), and utilized in all consequent predictions.

1.3 INFORMATION SUPPLIED TO THE MODEL

In this subsection, the information supplied to the mathematical model is listed according to category. Two such categories are considered, viz. geometric and hydrodynamic. The information thus listed is derived mainly from field measurements conducted at or near the proposed site as well as from laboratory measurements. Wherever necessary, this information has been supplemented with data gleaned from published literature.

In order to be representative of the scatter in available data for each of the quantities required to be supplied to the mathematical model, a parametric form of data supply has been selected. In this form the data on any quantity actually supplied, to each model run, fall within the recorded band width of variation of that quantity. Thus, the sensitivity of results predicted by the model to the variation in each such parameter, is evaluated through numerical "experiments."

1.3.1 Geometric Parameters

(a) Location of the infiltration bed

The approximate location, in plan view, of the proposed infiltration bed is indicated in Figure 1.1. An enlargement of the region in the proximity of grid lines R12-13 East and T34-35 North is provided in Figure 1.2 and the borings in this vicinity are also indicated. The boring DMI-7 is located at the approximate geometric center of the proposed infiltration bed at which point the local ground water elevation is located at approximately 1590 feet and the ground surface elevation at approximately 1630 feet.

It has been presumed that the proposed infiltration bed is located vertically at a point approximately 6 to 8 feet below the ground surface.

(b) Horizontal area of infiltration bed: A_z

The horizontal area of the proposed infiltration bed has been selected by other consultants to Exxon so as to provide a uniform vertical seepage flow under saturated conditions. A contingency of 25 percent above the maximum flow rate required has also been provided for. Thus:

$$A_z = \frac{(1 + 0.25)\dot{Q}_{b,\ max}}{W} \qquad (10)$$

where the vertical seepage velocity W is presumed to occur in a steady saturated flow under unit (or purely gravity-induced) head gradient. Accordingly,

$$W = K_z \qquad (11)$$

where K_z is the vertical permeability whose maximum measured value is 0.0049 cm/sec.

The above "design" area A_z has been selected by Exxon; it may have to be altered based upon the results of the hydrodynamic calculations to follow.

(c) Depth to water table: L

The water table elevation has been shown, on the basis of earlier field measurements (Dames & Moore, 1980), to curve gently away from the site of the proposed infiltration bed. In Table 1.1, the elevations of ground surface and water table are listed for selected borings in the vicinity of the proposed infiltration bed; and, the deduced values of L, the depth to the water table are also provided. It may be observed that this depth is variable, ranging from approximately 8 feet to 70 feet with a mean of approximately 32 feet.

However, since data on elevations precisely at the proposed infiltration bed site are not available, L will be treated as a variable ranging from 32 feet to about 48 feet. This is justified by the fact that the values of L closest to the site (DMI-1 and DMI-2) are of the order of 40 feet.

The conceptual diagram of the problem to be investigated is depicted in Figure 1.3. In this figure the significance of the above-mentioned parameters is illustrated.

1.3.2 Hydrodynamic Parameters

Certain soil properties required for the hydrodynamic calculations were obtained by laboratory measurements on soil samples taken at borings close to the site. The measured parameters were:

W_T : total weight of wet sample (g);
W_S : weight of dry soil in sample (g); and
V_T : total volume of wet sample (cc).

From the above, the following quantities were deduced. The ratio of weight of water in wet sample to weight of dry soil in same sample,

$$f_w = \frac{W_T - W_S}{W_S} \tag{12}$$

Volume of solid in the wet soil sample, using an assumed value of soil dry density, ρ_S,

$$V_S = \frac{W_S}{\rho_S} = \frac{W_T}{(1 + f_w)\rho_S} \tag{13}$$

Volume of voids in the wet soil sample,

$$V_V = V_T - V_S \tag{14}$$

Using the quantities so deduced the required hydrodynamic parameters were calculated.

(a) Porosity: n

The porosity n was calculated, thus

$$n = \frac{V_V}{V_T} = 1 - \frac{W_T}{V_T[(1+f_w)\rho_S]} \tag{15}$$

(b) Initial degree of saturation: $S_{r,i}$

The initial degree of saturation, defined as the ratio of volume of voids occupied by water to the total void volume, was calculated as follows.

$$S_{r,i} = \frac{V_w}{V_v} = \frac{W_T\{1 - (\frac{1}{1+f_w})\}}{\rho_w\{V_T - \frac{W_T}{(1+f_w)\rho_s}\}} \qquad (16)$$

where ρ_w is the density of water.

Using soil samples collected at locations in the unsaturated region close to the ground surface, values of n and S_r were calculated. The former quantity was found to lie in the range:

$$0.270 < n < 0.375, \text{ and}$$

the latter quantity in the range:

$$0.285 < S_{r,i} < 0.571$$

The calculated values are presented in Table 1.2.

(c) Initial moisture content: θ_i

Using the standard definition, the initial moisture content was calculated as:

$$\theta_i = nS_{r,i}$$

(d) Flow rate supplied to infiltration bed: $\dot{Q}_b$

The range of flow rates $\dot{Q}_b$ expected to be supplied to the infiltration bed were supplied, as design conditions, by Exxon. The values of $\dot{Q}_b$ lie in the range

$$67.3 < \dot{Q}_b < 190.5 \text{ gpm}$$

(e) Rainfall-induced infiltration: $\dot{q}''_I$

The infiltration rate $\dot{q}''_I$ caused by precipitation on the ground surface is an extremely variable quantity; at any specific location it is strongly dependent upon:

- o time-dependent precipitation rates;
- o runoff and all the above-ground parameters such as ground slope which influence it;
- o evapo-transpiration rates and the mechanisms which control them; and
- o the initial condition of unsaturated soils at that location.

In view of the complexities inherent in the determination of $\dot{q}''_I$, a reasonable supposition is to supply a uniform value compatible with a static water balance for sites close to the infiltration bed. The local precipitation rate is 30.78 inches/year, or 0.214 cm/day, based upon rainfall data, compiled over the last 68 years, from Nicolet College, which is about 30 miles west of Crandon.

The rainfall-induced infiltration rate was estimated to be 20% of the total rainfall, that is 6.154 inches/year, or 0.043 cm/day.

(f) Vertical hydraulic conductivity: K_z

The saturated value of vertical hydraulic conductivity, K_z, is not easily measurable under in-situ conditions. At the site in question, the soil above the water table is known to consist mainly of non-calcareous sandy soils together with some fines and clay lenses. A single measurement of conductivity would therefore not be strictly representative of all points in a column vertically below the infiltration bed. Therefore, it is reasonable to employ a spatially constant value of K_z in each calculation but examine the effects of a range of values through separate calculations. The values used, as supplied by Exxon in March, 1980, and backed up by Soil Testing Service in-situ measurements at depths of 5 to 9 feet, are as follows:

$$1 \times 10^{-3} < K_z < 5 \times 10^{-3} \text{ cm/sec}$$

(g) Variation of hydrodynamic parameters with suction pressure head: K_r, S_r

For convenience, the effective values of hydraulic conductivity and the saturation have been defined as:

$K \equiv K_r K_z$ where K_z is the saturated value and K_r is the value relative to saturation

$S \equiv S_r$ where S_r is degree of saturation.

The relationship between K_r, S_r and pressure head, ψ, may only be determined experimentally for any particular type of soil (see for instance, Gillham, Klute and Heermann, 1976). Many such experiments have been conducted (see for example Bouwer, 1964); from such measurements a selection of properties for soils similar to those at the site of the infiltration bed was made. The measurements specifically adopted are due to Van Genuchten et al. (1976). The hydraulic properties of the soil are plotted in Figure 1.4 and are described by the following empirical relations:

$$K_r = \{1 + [a_{0k}(-\psi)]^{a_{1k}}\}^{a_{2k}} \quad (17)$$

$$S_r = \frac{\theta_r}{\theta_s} + \left(1 - \frac{\theta_r}{\theta_s}\right)\{1 + [a_{0s}(-\psi)^{a_{1s}}]\}^{a_{2s}} \quad (18)$$

where a_{0k}, a_{1k}, a_{2k}, a_{0s}, a_{1s}, a_{2s} are parameters determined through careful regression analyses. Also, θ_r is the residual moisture content and, θ_s is the saturated moisture content. The values of these quantities supplied to the model are listed in Table 1.3.

1.4 TEST CASES CONSIDERED

Since fluid flow in the unsaturated zone is biased towards being vertical due to the influence of gravity the assumption was made that a one-dimensional vertical pattern of flow exists. Calculation-grids and test cases were selected accordingly.

As a first step, modelling runs were carried out in order to determine the optimum numerical calculation-grid, timestep-size and iteration scheme to be adopted. Necessary tests to ensure proper convergence of the solution and therefore accuracy of predicted results were also conducted. The calculation-grid thus selected is shown schematically in Figure 1.5. The cells are each 30 cm in depth, and of width and length each 1750 cm, to correspond to the area of 306.25 m^2 of the infiltration bed. The infiltration pipes were situated at 210 cm (6.89 ft.) below the ground surface, and the water table is 960 cm (31.5 ft.) below the ground surface. This grid was used in all the test cases discussed below.

In order to investigate a set of test cases which illustrate the effects of a range of parameter variations described in the previous subsection, "best" and "worst" case situations were first defined and then utilized in choosing suitable test-case problem parameters. The "worst" case was defined as the situation in which the wetting front would reach the water table in the shortest time, with correspondingly largest fluid velocities, given the ranges of problem parameters available. Conversely, the "best" case was taken as the situation in which the wetting front would reach the water table in the longest possible period of time. These rather loose definitions were employed since the "worst" case would imply that the vertical fluid velocities were at their maximum, and hence the residence time of chemicals in the unsaturated zone is at its minimum. In this way decay, reaction and adsorption time for such chemicals is more limited, and thus the concentrations reaching the water table will be greater than in any other postulated test case. Correspondingly, the "best" case will permit the longest residence time for chemical species, with consequent lessened concentrations at and below the water table.

Four major test cases were selected for consideration in the hydrodynamics portion of the study, the parameters and figures applicable to each being listed in Table 1.4.

Test case 1 was chosen to represent "average" conditions, that is material properties mid-way in the ranges of measured property values, and with an injection rate in the infiltration bed of the maximum expected, 25 percent being added as extra for contingencies.

Test case 2 was selected to represent the "worst" conditions which could be expected, given the probable range of each problem parameter. That is, the smallest value in the range of measured porosities, and the largest value in the range of vertical hydraulic conductivities were chosen to achieve minimum storage in the unsaturated zone and maximum speed of the wetting front. Also, the largest expected value for the injection rate of fluid was selected.

Test case 3 is the reverse of case 2 that is, it represents the "best" conditions with a high value for porosity, low conductivity soil, and injection of fluids at an average rate.

The last test case, no. 4, illustrates the effect that lateral transport of injected flow would have upon the overall flow. In test case 4 it was arbitrarily assumed that the horizontal area of the vertical column increased uniformly by ten percent from the infiltration bed to the water table. It must be emphasized that neglect of lateral movement of injected fluids leads to conservatism in the predicted results. This is so because lateral flow results in increased residence times as well as reduced chemical concentrations in the transporting fluid. The mathematical treatment of three-dimensional unsaturated flow which would be required to predict this lateral movement, besides being extremely expensive, would not be expected to provide results substantially different from those of test case 4.

The results predicted by each of these test cases are discussed in detail in the following section.

2.0 PREDICTED RESULTS OF ANALYSIS OF THE INFILTRATION BED

2.1 FLOW RATES WITHIN THE UNSATURATED ZONE

The results predicted by the model are summarized, in the main, by Figures 2.1 to 2.16, which illustrate the vertical profiles of each of the main variables--pressure head, moisture content, degree of saturation, and vertical fluid velocity as a function of time for each test case. In reference to these figures, one may make interpretations of the flow through the unsaturated zone. The flow rates, as predicted, are important results to note because they will determine the residence time of the chemicals in any one part of the soil column below the infiltration bed. Hence, the velocity profiles determine, to a large extent, the final concentrations which will reach the water table at any particular time.

The velocity profiles generally mark the position of the wetting front by discontinuities as noticeable as any of the other variables plotted. The differences between test cases therefore mainly consist of the difference of velocity of the wetting front, which is discussed in the following section, and peak vertical fluid velocities predicted at any particular instant of time.

At times up to 300 days, the velocity profiles are similar for test cases 1, 2, and 4. However, test case 3 with the smallest conductivity and injection rate shows much smaller peak velocities, at 50 cm/day as compared to 200 to 300 cm/day in the other cases.

At times greater than 300 days, the peak velocities in any profile appear, looking at Figures 2.4, 2.8, and 2.16, to be similar to each other, and the final vertical velocity at the water table is close to that velocity implied by the rate of infiltration and the area of the infiltration bed. That is, for cases 1, 2, and 4, where the injection rate is 190.5 gpm, corresponding to a vertical flow of 4.9×10^{3}cm/sec, the final downward velocities are 6.37×10^{3}cm/sec, 5.67×10^{3}cm/sec

and 7.29 x 10^3cm/sec, respectively. Similarly for test case 3, where the inflow rate is 67.3 gpm, implying a downward flow of 1.39 x 10^3cm/sec, the predicted vertical velocity at the water table is 1.97 x 10^3cm/sec. In all the test cases the infiltration rate may not be exactly compared to the predicted vertical velocities because the model accounts for rainfall-induced infiltration in addition to the effects of the man-made infiltration bed.

2.2 PROGRESS OF WETTING FRONT

The wetting front is a well-defined front at which pore-pressure, saturation, moisture content and vertical fluid velocity all exhibit rapid changes.

A summary of the progression of the wetting fronts as shown in Figures 2.1 to 2.16 is presented in Figure 2.17. This figure illustrates the progression of the wetting front and the total time taken for that front to reach the water table.

The following problem parameters were shown to influence the speed of the front and the total time taken to reach the water table.

(i) The depth to water table, L which was not varied between test cases. The plots in Figure 2.17 show that the extension of the graphs for greater values of L would be simple since the plots become almost linear. In general, the greater the distance between the infiltration bed and the water table, the greater the time required for the wetting front to progress from the one to the other.

(ii) The vertical hydraulic conductivity which is greatest in test case 2, at 5 x 10^{-3}cm/sec, and leads to the wetting front reaching the water table in the shortest time, that is 445 days since the start of infiltration.

(iii) The injection rate into the infiltration bed which affects the pressure distribution causing vertical flows and influences the rate of progress downwards of the wetting front. In test case 3, in which the infiltration rate is at the average rate of 67.3 gpm, the time to reach the water table is considerably greater, ie., 1780 days, than the remaining cases with greater infiltration rates.

(iv) The lateral transport of fluid, which is empirically provided for in test case 4, illustrates how horizontal flow delays the wetting front. Upon comparing the results of test cases 2 and 4 in Figure 2.17 it may be observed that the assumption of no horizontal flow applied in test cases 1, 2, and 3 is indeed conservative.

2.3 PRESSURE HEADS WITHIN THE INFILTRATION BED

Figure 2.18 is a plot of the maximum pressure heads, that is, pressure head within the infiltration bed, as a function of time for each test case. Since extreme cases have been selected as the "best" and "worst" conditions in test cases 3 and 2, respectively, all likely conditions are expected to fall between these two. In this way, one may determine the likely range of pressure heads within the infiltration bed itself. From Figure 2.18 one may observe that the maximum expected pressure is approximately 1700 cm of water above atmospheric pressure, while the minimum expected pressure is approximately -700 cm of water, a range of 2400 cm of pressure.

2.4 CONCLUSIONS

The conclusions which may be drawn from the results discussed in the previous subsections and illustrated in Figures 2.1 to 2.18 are twofold.

Firstly, the pumping pressure requirements for injection, i.e. disposal of a given volumetric rate of fluid in the infiltration bed are shown to range up to 1700 cm of water above atmospheric pressure for flow rates of 190.5 gpm through an area of 306.25 m^2. If this requirement

is to be reduced for a given flow rate then the area of the infiltration bed must be increased.

Secondly, and more importantly, the effect of various problem parameters upon the residence time of chemical species in the unsaturated zone may be deduced. Since greater attenuation is achieved during longer residence periods, the greatest possible time before the wetting front reaches the water table is preferable.

Disregarding material properties, which will be site-specific and invariant, the parameters which will determine the time to reach the water table are depth to water table, rate of injection of fluid, and area of infiltration bed. To increase the residence time of chemicals in the unsaturated zone, one could select a site with a greater depth to the water table. Alternatively one could increase the area of the infiltration bed, or adopt a combination of these.

3.0 METHODOLOGY FOR ANALYSIS OF THE SEEPAGE POND

3.1 INTRODUCTION

The following two sections describe the numerical modelling of a hypothetical seepage pond located at the Exxon/Crandon site. A schematic diagram of the pond is shown in Figure 3.1.

The objectives of this study were to determine the amounts and quality of seepage from a hypothetical mining wastewater pond. The impact of seepages from the pond upon the underlying aquifer over a 15 year period of operation was to be determined.

The specific problem considered consisted of modelling the groundwater flow and the transport by convective and reactive mechanisms of selenium (Se) and sulfate ions (SO_4^{-2}) from the pond to the surrounding soil during the first 15 years of operation of the pond.

The pond was modelled numerically by means of 2 Dames & Moore computer programs. One program modelled the pond during the temporarily unsaturated conditions which are assumed to exist immediately prior to flooding of the pond. This is the program which was used to model the infiltration bed, as described in the previous two sections, and is discussed in Appendix A. The other program modelled the pond after saturated conditions were reached, i.e. after the wetting-front had reached the water-table. This program is described in Appendix B.

3.2 INFORMATION SUPPLIED TO THE MODELS

In this sub-section, the information supplied to the models is listed according to three categories. These categories are geometric, hydrodynamic, and chemical species transport.

3.2.1 Geometric Parameters

(a) Pond dimensions

The pond is assumed to be unlined, 5-feet deep, and has an area of 275 feet by 275 feet. These parameters were picked fairly arbitrarily,

but were based on typical waste-water pond geometries previously analyzed.

(b) Depth to water-table

A 30 foot layer of non-calcareous soil lies directly beneath the pond. This depth is approximately the mean of the values observed in selected borings close to the pond, as listed in Table 1.1.

(c) Saturated Thickness

Below the water-table, which exists at 30 feet beneath the pond, the soil is calcareous and is assumed to extend to an average depth of 60 feet below the elevation of the pond. A regional ground water gradient of 0.0075 feet/feet from northeast to southwest is assumed to exist, and so the saturated thickness varies from place to place in the domain, the average thickness being 30 feet. Below the calcareous saturated layer a horizontal impermeable layer of bedrock is assumed to exist; this layer forms the base of the saturated model.

3.2.2 Hydrodynamic Parameters

(a) Porosity, soil density and degree of saturation

The hydrodynamic parameters applicable to this site have already been discussed in sub-section 1.3.2. The values for most parameters used in this study were approximately the same as those used previously, and are listed in Table 3.1. That is, the porosity is assumed to be 0.25; the dry density of the soil is 110 lb/ft^3, and the initial degree of saturation in the non-calcareous soil is 57.1%. The degree of saturation was chosen to be the most conservative, i.e., the wettest in the range observed, in order that the maximum rate of transport of chemicals to the water-table might be modelled.

(b) Variation of permeability and degree of saturation with suction pressure head

The relationships described in equations (17) and (18) and Table 1.3 were again used to approximate the variations of permeability and degree of saturation with suction pressure head.

(c) Horizontal and vertical hydraulic conductivities

Vertical hydraulic conductivity (permeability) K_z is difficult to measure under in-situ conditions, and the value for K_z used in modelling the infiltration bed was based on observed infiltration rates at depths of 5 to 9 feet below ground. The data available concerning horizontal hydraulic conductivity, based upon many pumping tests carried out in borings in the area, is summarized in Figure 3.2. As may be seen, these values range over more than 3 orders of magnitude. Because of the large variation in observed values of horizontal permeability, K_x, and the uncertainty in K_z, for modelling purposes the same value was used for each, that is an average permeability was assumed to apply to both:

$$K_x = K_z = 2 \times 10^{-4} \text{ cm/sec.}$$

3.2.3 Chemical Transport Parameters

The values used for the chemical transport parameters are summarized in Table 3.2.

(a) Background chemical species concentrations

The background chemical species concentrations were taken to be average values from observations at the nearby piezometer DMA-19, test-well TW-1, and water-well WW-2. The location of these borings is given in Figure 1.2.

In the case of sulfate, 25 observations led to an average value for local background concentration of 8.8 mg/l.

For selenium, 7 observations were made, each showing levels of selenium below the detection limit of 0.001 mg/l. It was therefore assumed that the background concentration of selenium is 0.0005 mg/l.

(b) Chemical species concentrations within the pond

Based upon the design for the water treatment plant at the Exxon/ Crandon prospecting project, as described by Exxon in December 1980, the

effluent would have an estimated water-quality corresponding to 2480 mg/l concentration of sulfate and 0.65 mg/l concentration of selenium.

(c) Chemical reactions

The soil beneath the pond and in the underlying aquifer will adsorb some of the chemicals which seep from the pond. In this way the concentrations in the ground water are gradually reduced. Laboratory analyses of the behavior of the species of concern were carried out, both for the calcareous and non-calcareous soil-types. Based upon the results of these tests, and, in the case of sulfate, upon observations at other Dames & Moore field sites and reports in the literature, the following conclusions were drawn. The Freundlich isotherm was found to best describe the behavior of selenium and sulfate, that is an equation of the form:

$C_s = K_d C^m$ where C_s is the concentration on the soil (mg/g);

K_d is the adsorption distribution coefficient $(\frac{mg^{(1-m)}\,l^m}{g})$;

C is the concentration in the ground water (mg/l);

m is the exponent of C;

could be applied to both. The values for K_d and m vary for different soil-types and are summarized in Table 3.2. Use of this form of reaction equation is a simplification of the behavior of the chemicals as they are transported. The competition between various chemicals to be adsorbed, and the upper limits on adsorption due to the solubility of a species or due to the local ground water pH have been neglected. However, the absence of laboratory or in-situ observations of these details of the soil behavior necessitates the simplifying assumption of a reversible one-step reaction to be made.

3.3 TEST CASE CONSIDERED

One test case was considered in this portion of the study. In this test case it was assumed that the pond, which is unlined, has an

operating period of 15 years and that it was modelled for that length of time.

The purpose of the test case was to predict, using both saturated and unsaturated ground water flow and transport analyses, the impacts that the pond will have upon the underlying ground water in terms of both flow-patterns and water-quality. With this purpose in mind, and utilizing the data described in the previous sub-section, the results described on the following pages were obtained.

4.0 PREDICTED RESULTS OF ANALYSIS OF THE SEEPAGE POND

The transient ground water flow and reacting chemical transport from the pond was predicted by means of the 2 Dames & Moore computer programs described in Appendices A and B. The program discussed in Appendix A was used to model the pond and underlying soil when unsaturated conditions will exist beneath the pond, i.e., when the pond first becomes operational. The second program was used to model the pond and underlying aquifer after the soil becomes fully saturated.

4.1 UNSATURATED MODEL PREDICTED RESULTS

A one-dimensional vertical model of the pond and underlying non-calcareous soil was used to predict the rate at which the soil beneath the pond will become saturated and to predict how long it will take the sulfate and selenium fronts to reach the existing water-table.

The column of 32 finite-difference cells shown in Figure 4.1 represents a 30 foot column of initially unsaturated non-calcareous s directly beneath the pond. The pressure head along the top boundary was fixed to a value of 5 feet (152.4cm), i.e., the average pond depth, for the entire analysis. And, the pressure head along the bottom boundary was maintained at a value of 0. feet. That is, atmospheric pressure was assumed to exist at the base of the non-calcareous soil which coincides with the pre-existing water table.

The one-dimensional unsaturated analysis indicates that the wetting front will reach the water-table soon after operation of the pond begins. The sulfate and selenium fronts will follow: each will vary according to its own concentration gradient and rate of adsorption. The predicted arrival times of the concentration and wetting fronts are summarized in Table 4.1. The entire column of non-calcareous soil will become saturated within 17 days of the start of pond operation. The term concentration front is henceforth defined as the 100% pond concentration front. Profiles of pressure head, sulfate concentration and selenium concentration at various times are plotted in Figures 4.2, 4.3, and 4.4.

The results of this analysis were then used as input to the two-dimensional, horizontal model, the results of which are described in the following sub-section.

4.2 SATURATED MODEL PREDICTED PRESULTS

A two-dimensional horizontal model of the saturated region below the pond was used to predict the transport of the chemical species and the ground water flow patterns after the wetting front from the pond had reached the water-table.

A finite-difference grid of 36 by 31 cells of variable size, illustrated in Figure 4.5, covering an area of 4000 ft. by 3000 ft, was used in this analysis. The boundary conditions were as follows: the NW and SE boundaries were treated as impermeable boundaries, since the regional ground water flow is parallel to those boundaries. The NE and SW boundaries were fixed head and chemical species concentration boundaries, fixed such that the head gradient between them was 0.0075 ft./ft. The initial head distribution was chosen to be a uniform flow-field of fixed gradient, and the initial chemical species concentrations were at background concentration levels.

The flow is averaged with depth in the vertical direction, and the base of the aquifer (an average over the domain of 60 feet below the pond) is assumed to be impermeable, i.e., no leakage or recharge from any underlying aquifers is taken into account.

At a time 17 days after the pond operation commences (which is when the wetting front reaches the water-table) the pre-existing unconfined aquifer starts to feel the influence of the pressure-head exerted by the pond. Thirty-five and forty days after the start of pond operation the sulfate and selenium concentration fronts respectively reach the original position of the water-table, and the chemicals start to move horizontally, at a rate determined by the local head-gradient, concentration-gradient and rate of adsorption.

The predictions of the transient hydraulic head contours and concentration distributions for sulfate and selenium after 1, 5, 10, and 15 years of pond operation are presented as Figures 4.6 to 4.17. The head contours illustrate the ground water mound beneath the pond flattening with time as the water-table rises around the pond. Between 10 years (Figure 4.12) and 15 years (Figure 4.15) the head distributions change little, indicating that a steady-state ground water flow pattern is being approached.

The sulfate spreads out from the pond rapidly at first, due to the large lateral pressure gradients, and then more slowly as the concentration and pressure gradients lessen.

In the case of selenium the over-riding factor determining the concentration distribution is the rate of adsorption, which is to be expected since its distribution coefficient is fairly large. Consequently the rate of expansion of the concentration plume does not vary much with variations in concentration and pressure-gradient.

After 15 years of pond operation the ground water mound has expanded to influence ground water flow 1200 feet away from the pond, and the 200 mg/l sulfate front has travelled some 850 (horizontal) feet from the pond, while the 0.005 mg/l selenium front has travelled only 390 feet from the pond, horizontally.

The rate of seepage from the pond was also calculated, and is shown in Figure 4.18. This graph shows that initially the rate of seepage is rapid, but that this rate drops with time, and, if one extrapolates the curve, becomes almost constant at a rate of about 13 gpm.

4.3 CONCLUSIONS

Three sets of conclusions may be drawn from the results described in the foregoing sub-sections.

Firstly, the convective and reactive transport of chemicals from a seepage pond may be adequately modelled by means of coupling a one-dimensional unsaturated model to a two-dimensional saturated model.

Secondly, the pond, as hypothetically designed in this study, would be insufficient in size to handle the average water treatment plant effluent flow-rate of 60 gpm. However, hydrodynamic modelling of a similar nature to that described in this report could be used to design such a pond.

Lastly, the use of adsorption isotherms as postulated in this study is known to be a simplification of the ground water soil interactions which are known to occur but have rarely been accurately observed. Due to the lack of observations, and not to any inherent simplification in the mathematical models employed, the assumption of this type of soil-water interaction was made. The validity of this assumption must be established with reference to field measurements.

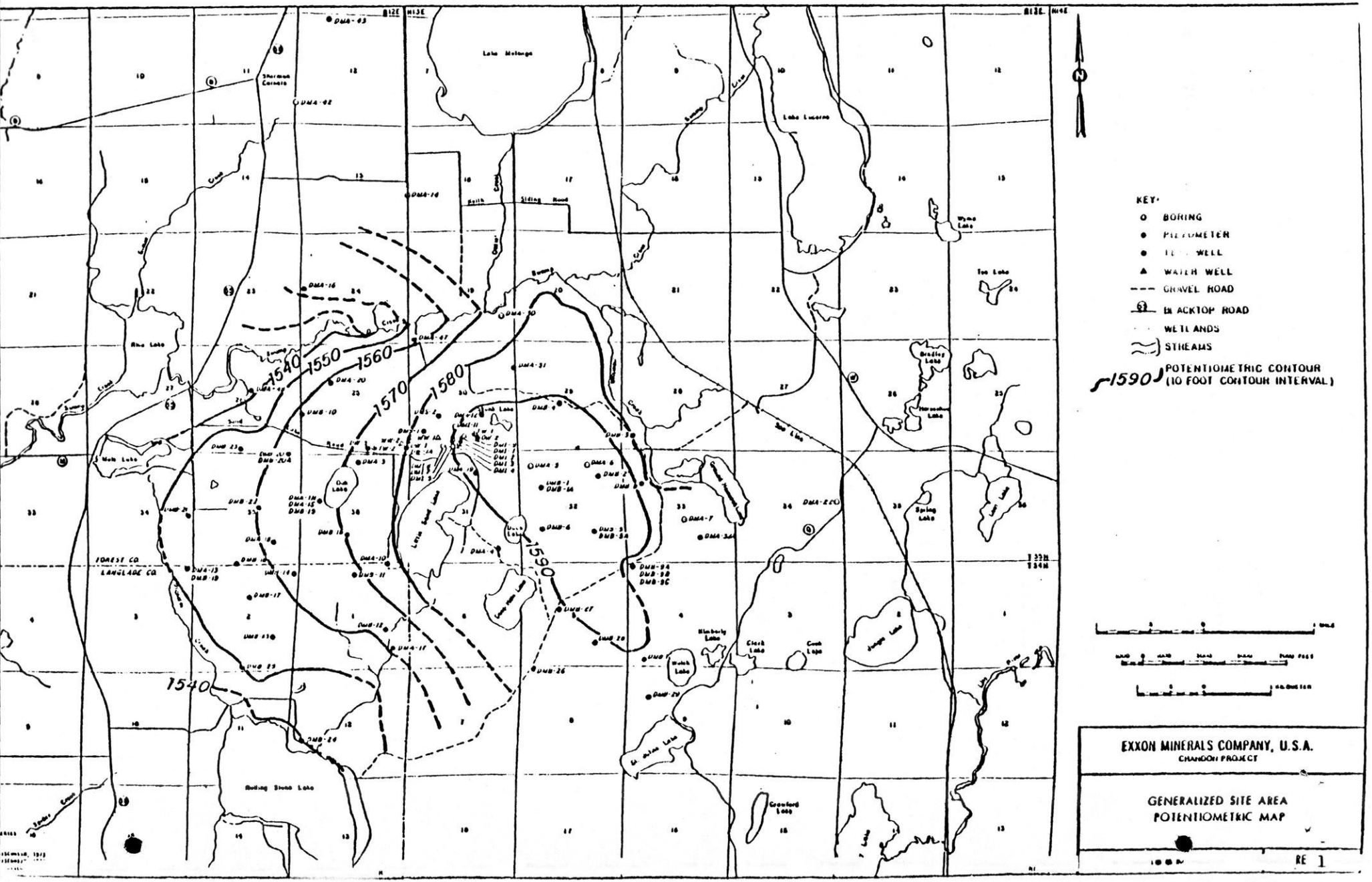
KEY:
BORING
PIEZOMETER
TEST WELL
WATER WELL
GRAVEL ROAD
BLACKTOP ROAD
WETLANDS
STREAMS
1590 POTENTIOMETRIC CONTOUR (10 FOOT CONTOUR INTERVAL)
1540
1550
1560
1570
1580
1590
Lake Melange
Lake Lucerne
Rhue Lake
Oak Lake
Duck Lake
Spring Lake
Kimberly Lake
Clark Lake
Cook Lake
Rolling Stone Lake
Crawford Lake
FOREST CO.
LANGLADE CO.
EXXON MINERALS COMPANY, U.S.A.
CHANDON PROJECT
GENERALIZED SITE AREA
POTENTIOMETRIC MAP
RE 1

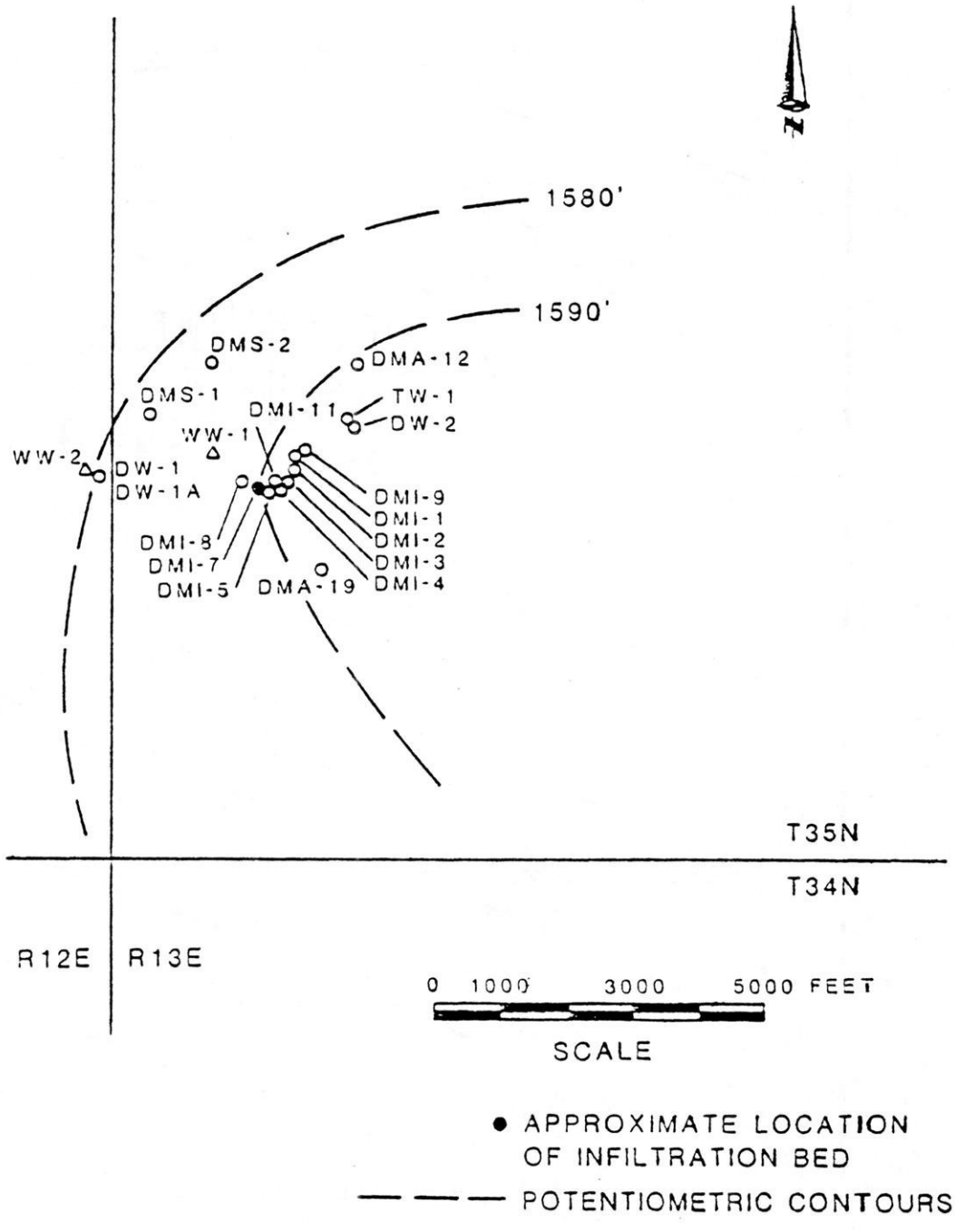

Fig. 1.2 Borings in the vicinity of the infiltration bed

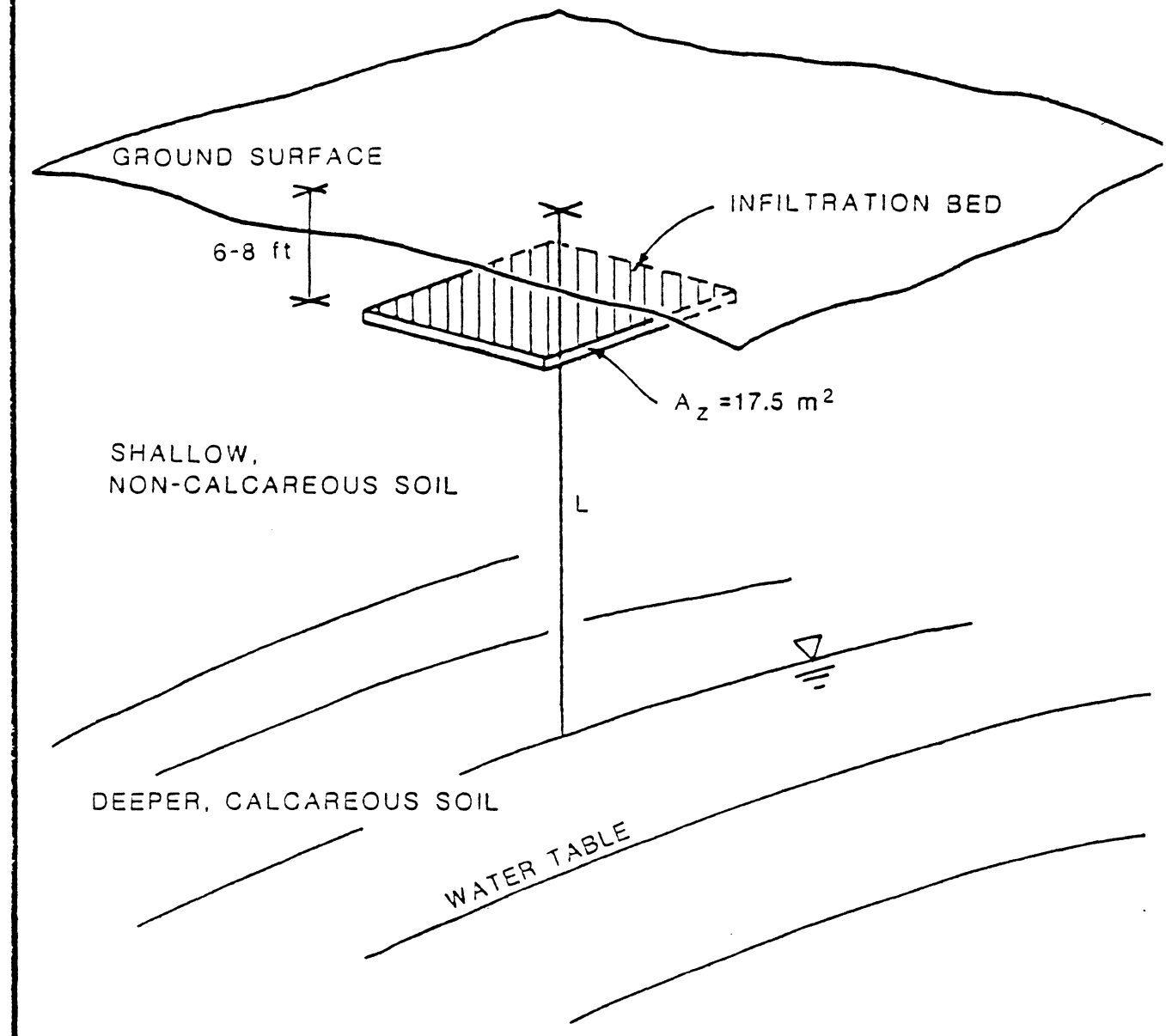

Fig. 1.3 Conceptual diagram of problem

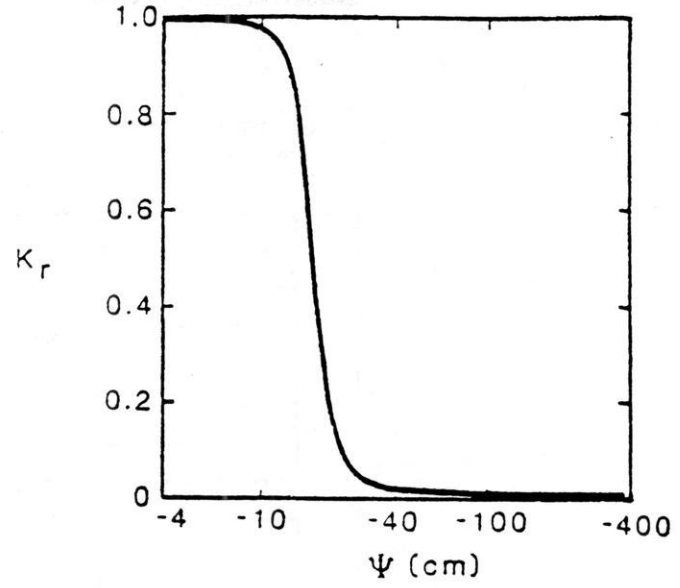

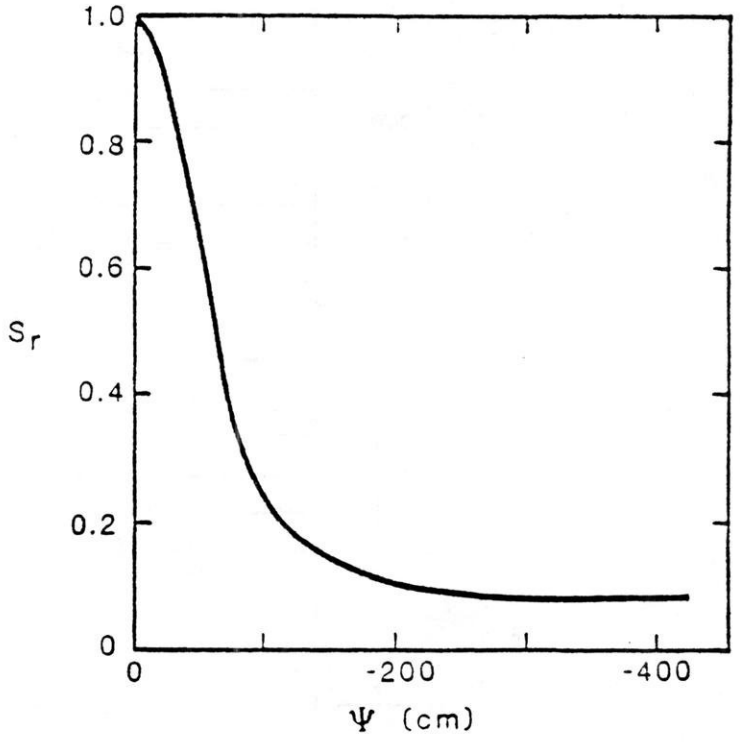

Fig. 1.4 Relationships between hydraulic conductivity and pressure head, and degree of fluid saturation and pressure head

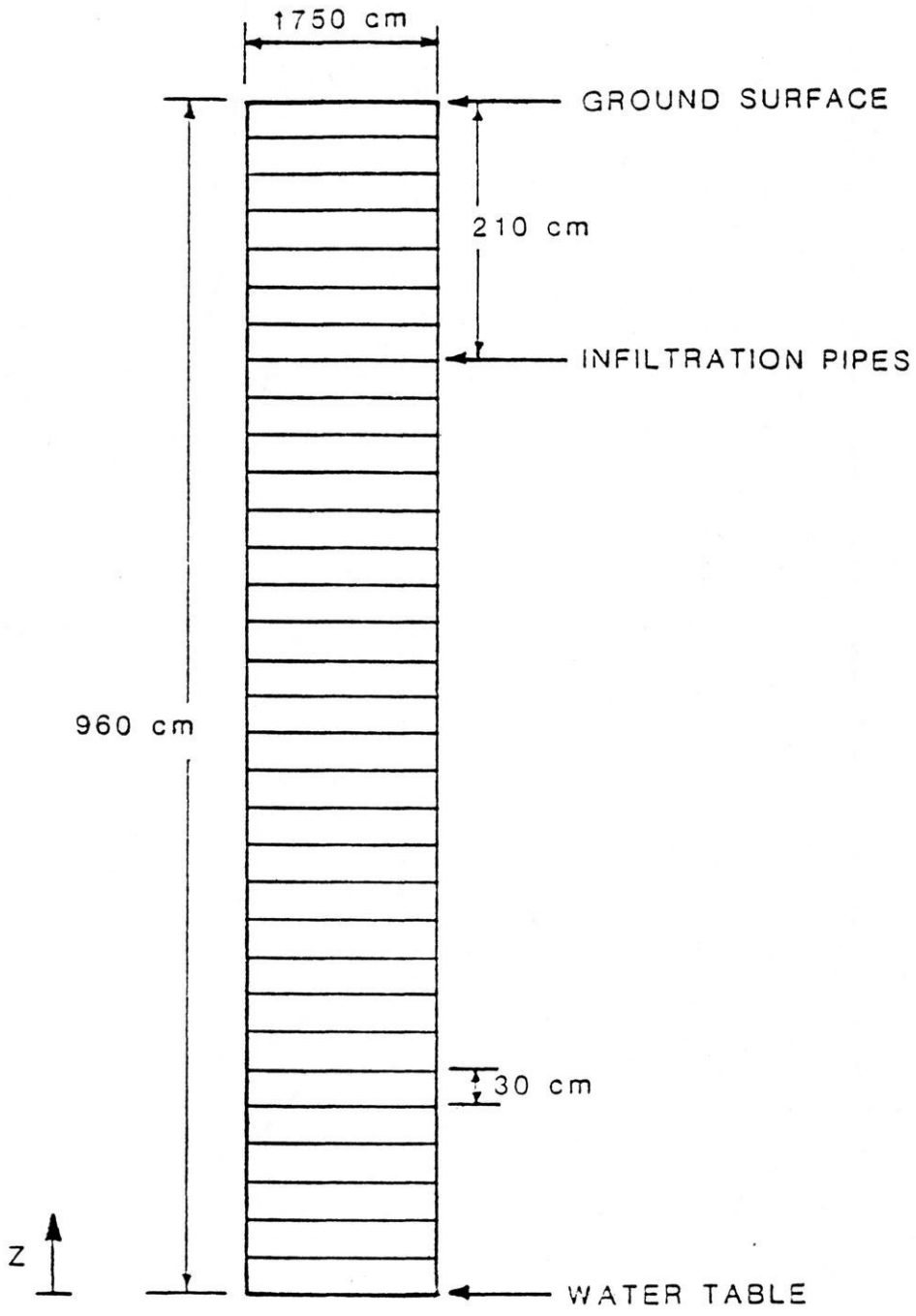

Fig. 1.5 Calculation grid

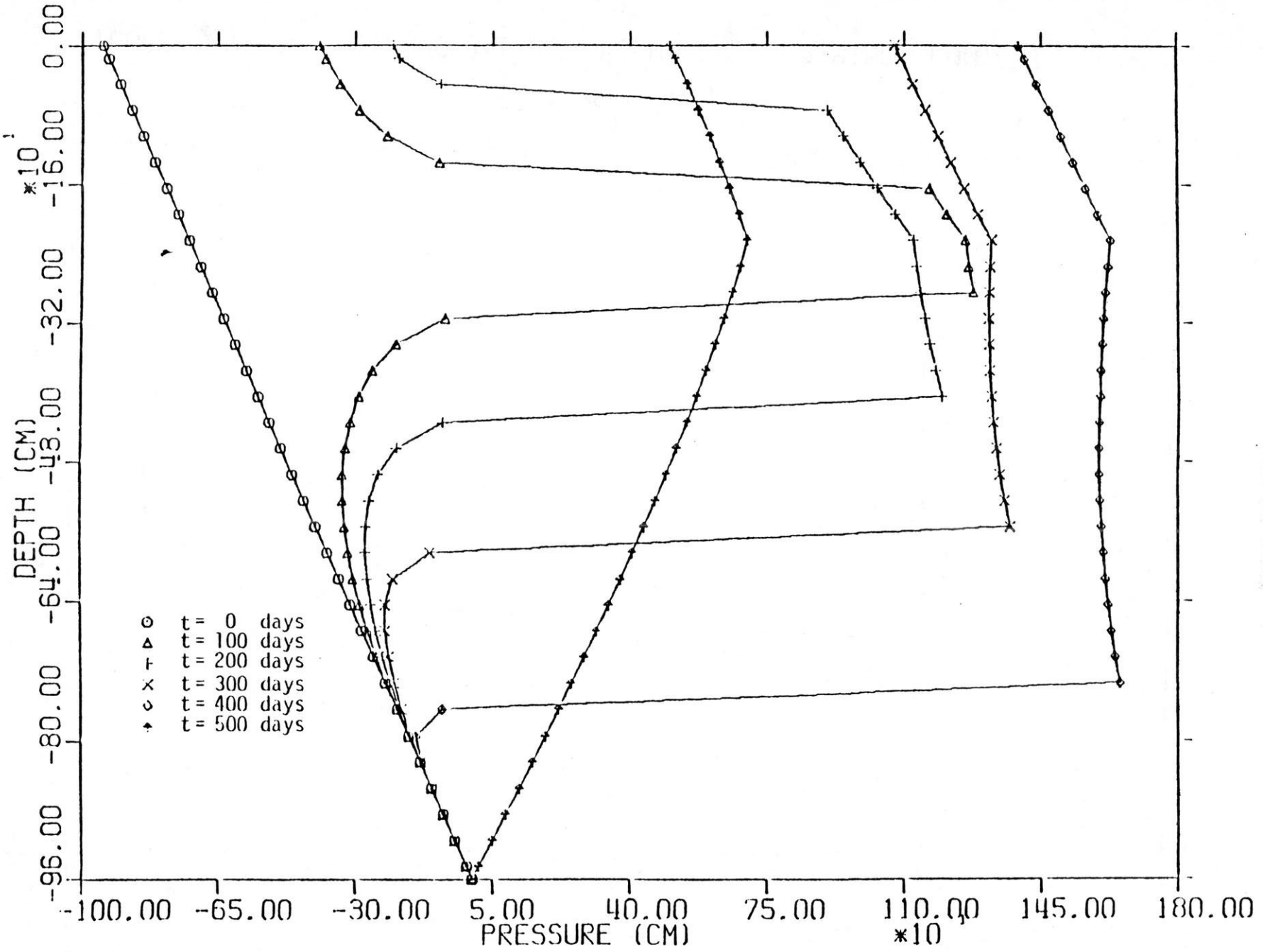

FIGURE 2.1 PROFILES OF PORE-WATER PRESSURE Test Case 1

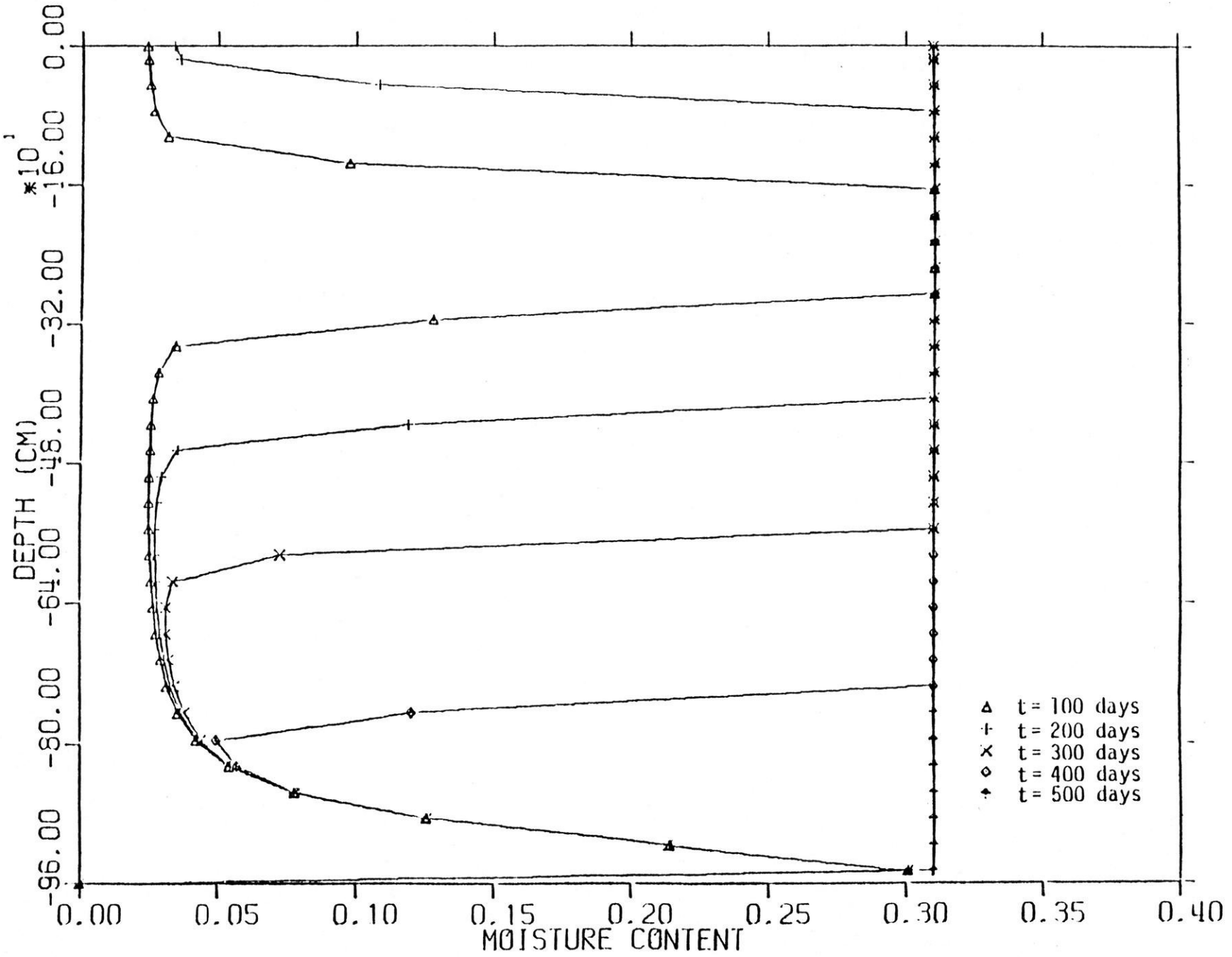

FIGURE 2.2 PROFILES OF VOLUMETRIC MOISTURE CONTENT Test Case 1

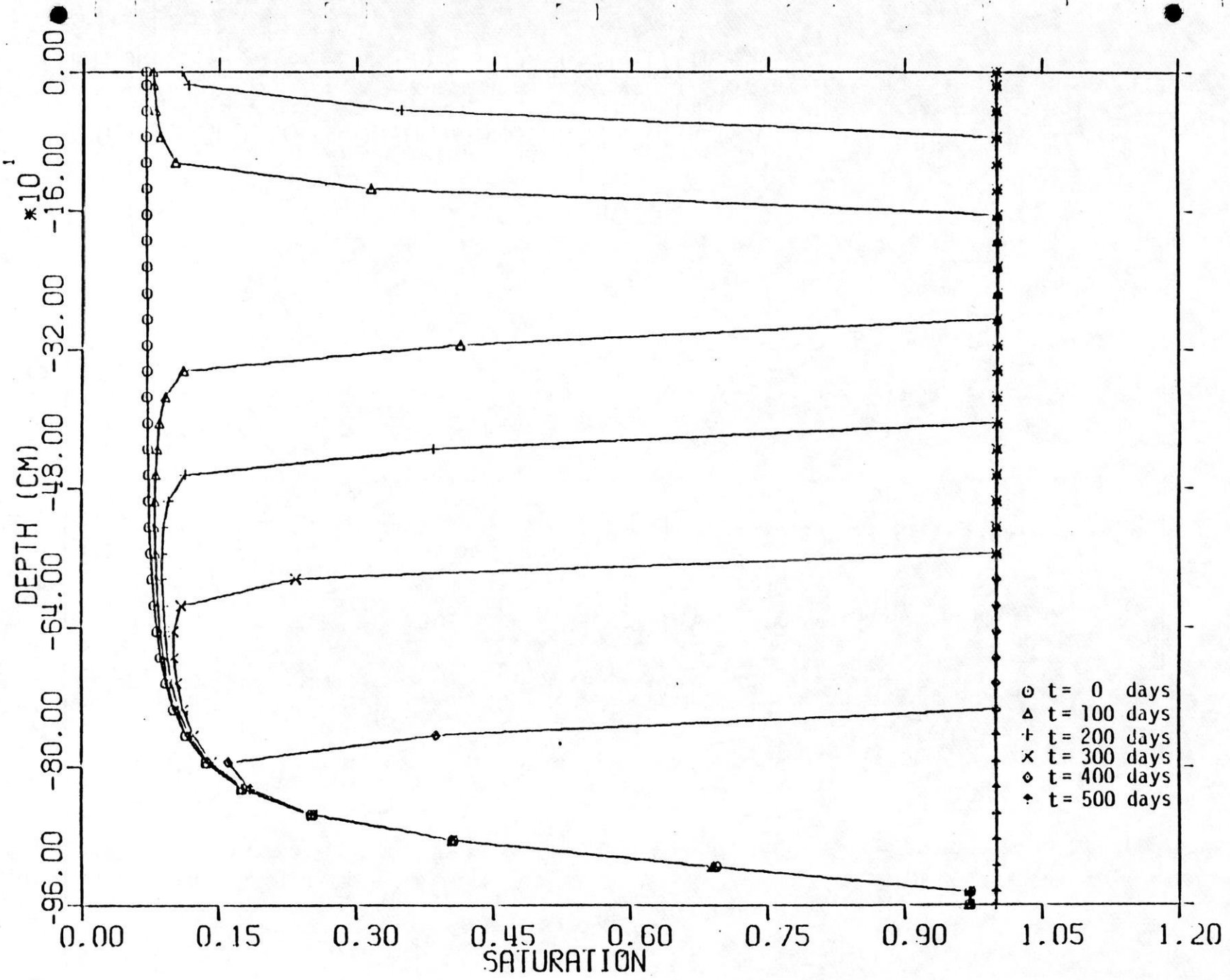

FIGURE 2.3 PROFILES OF DEGREE OF SATURATION Test Case 1

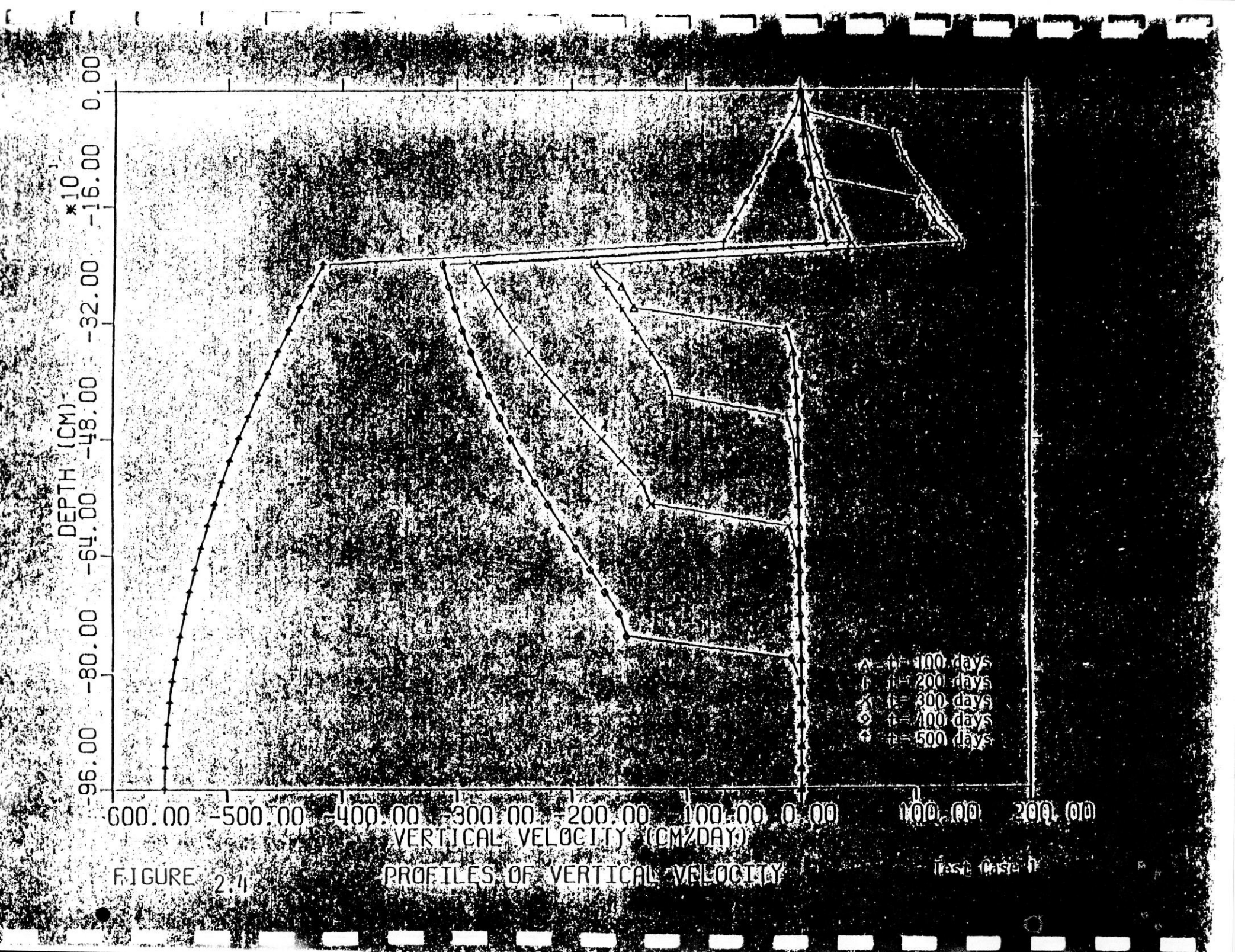

FIGURE 2.4 PROFILES OF VERTICAL VELOCITY

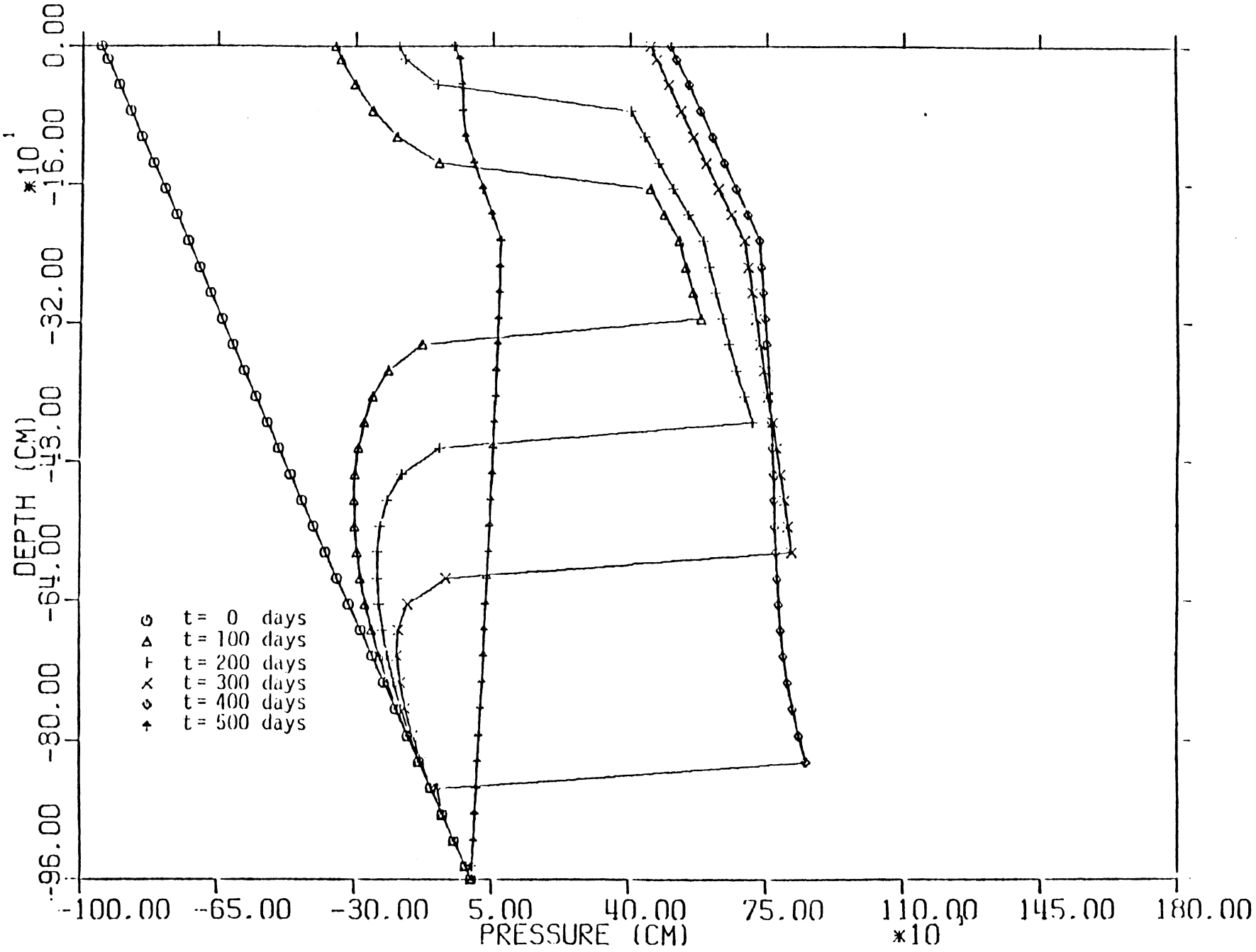

FIGURE 2.5 PROFILES OF PORE-WATER PRESSURE Test Case 2

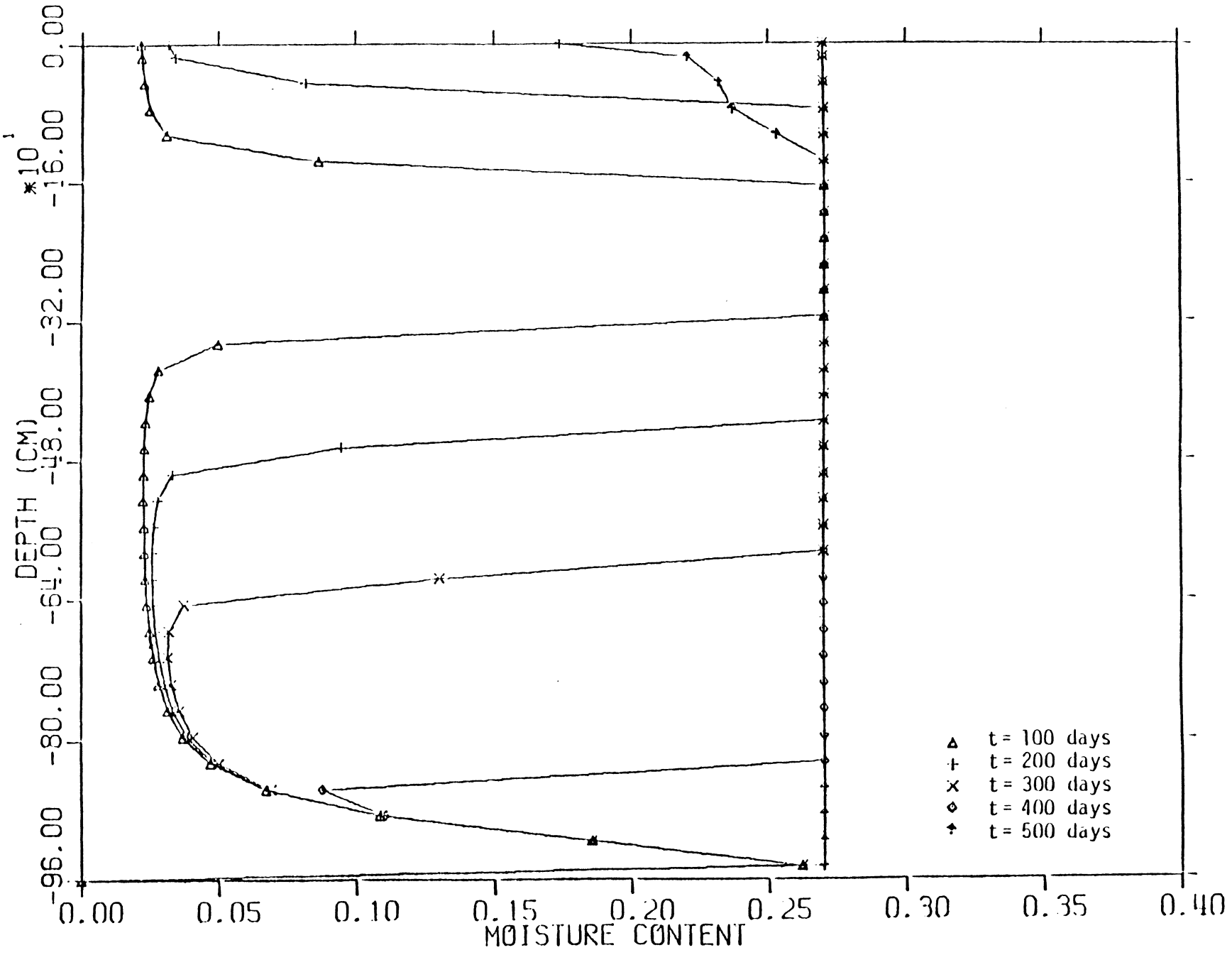

FIGURE 2.6 PROFILES OF VOLUMETRIC MOISTURE CONTENT Test Case 2

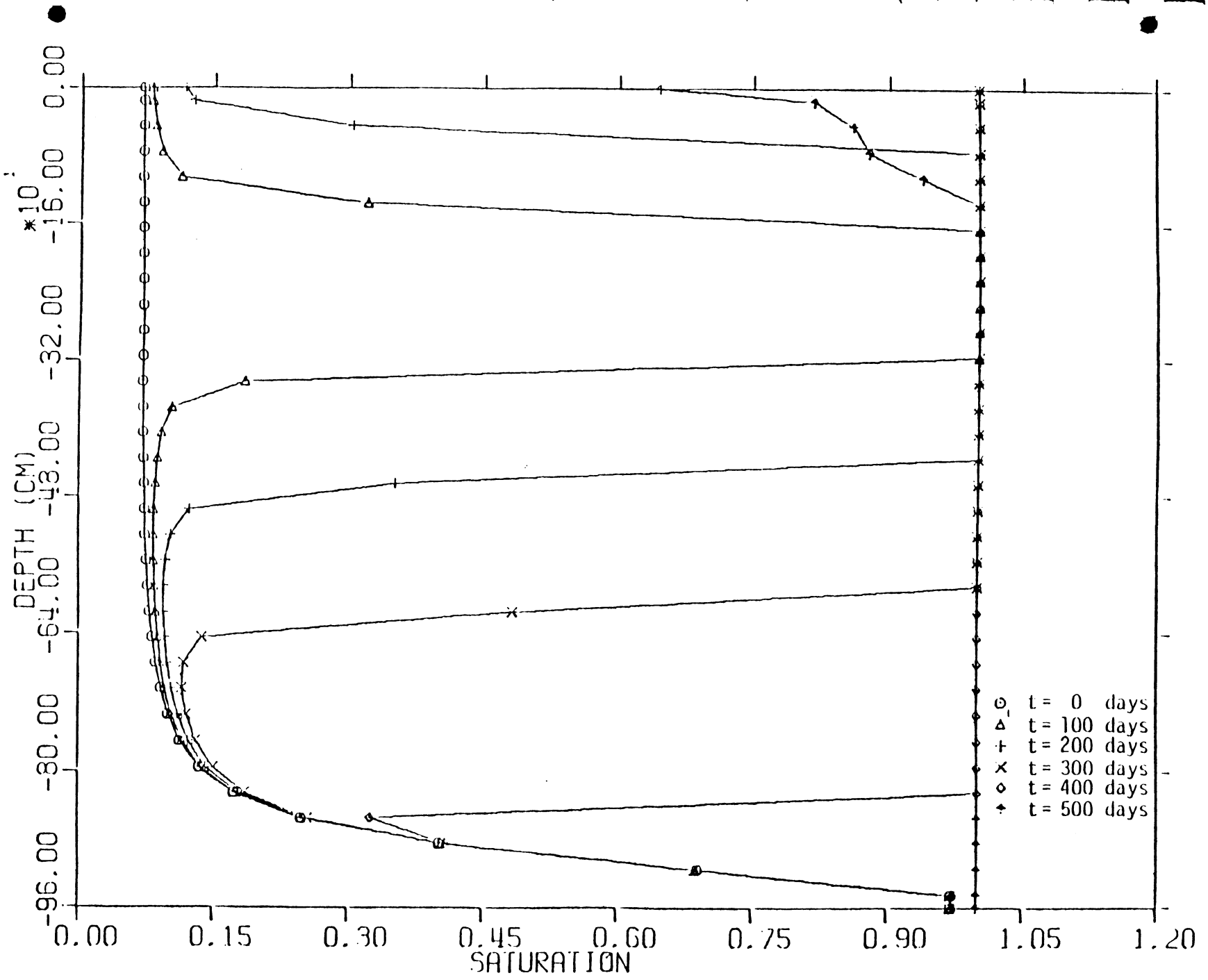

FIGURE 2.7 PROFILES OF DEGREE OF SATURATION Test Case 2

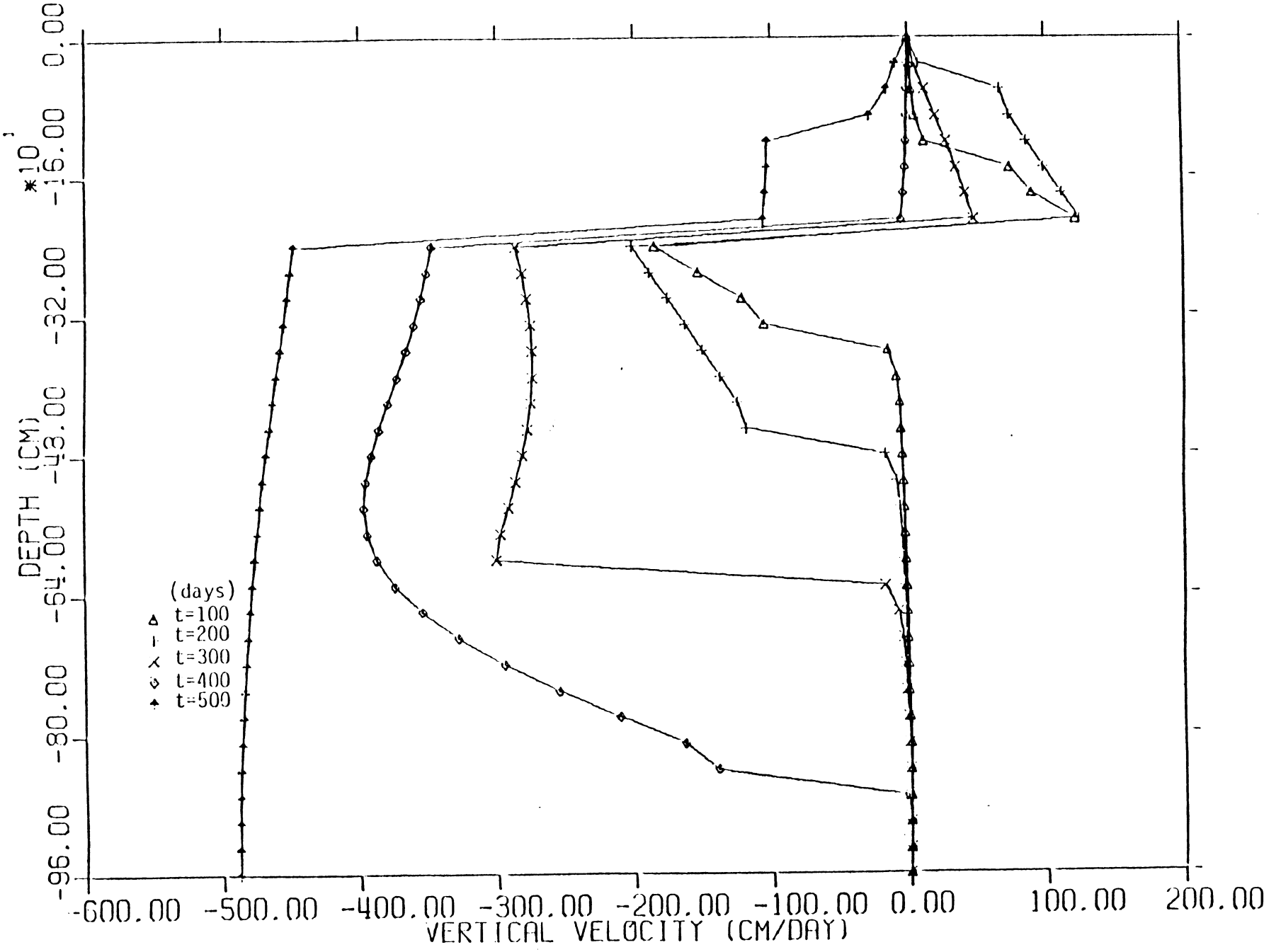

FIGURE 2.8 PROFILES OF VERTICAL VELOCITY Test Case 2

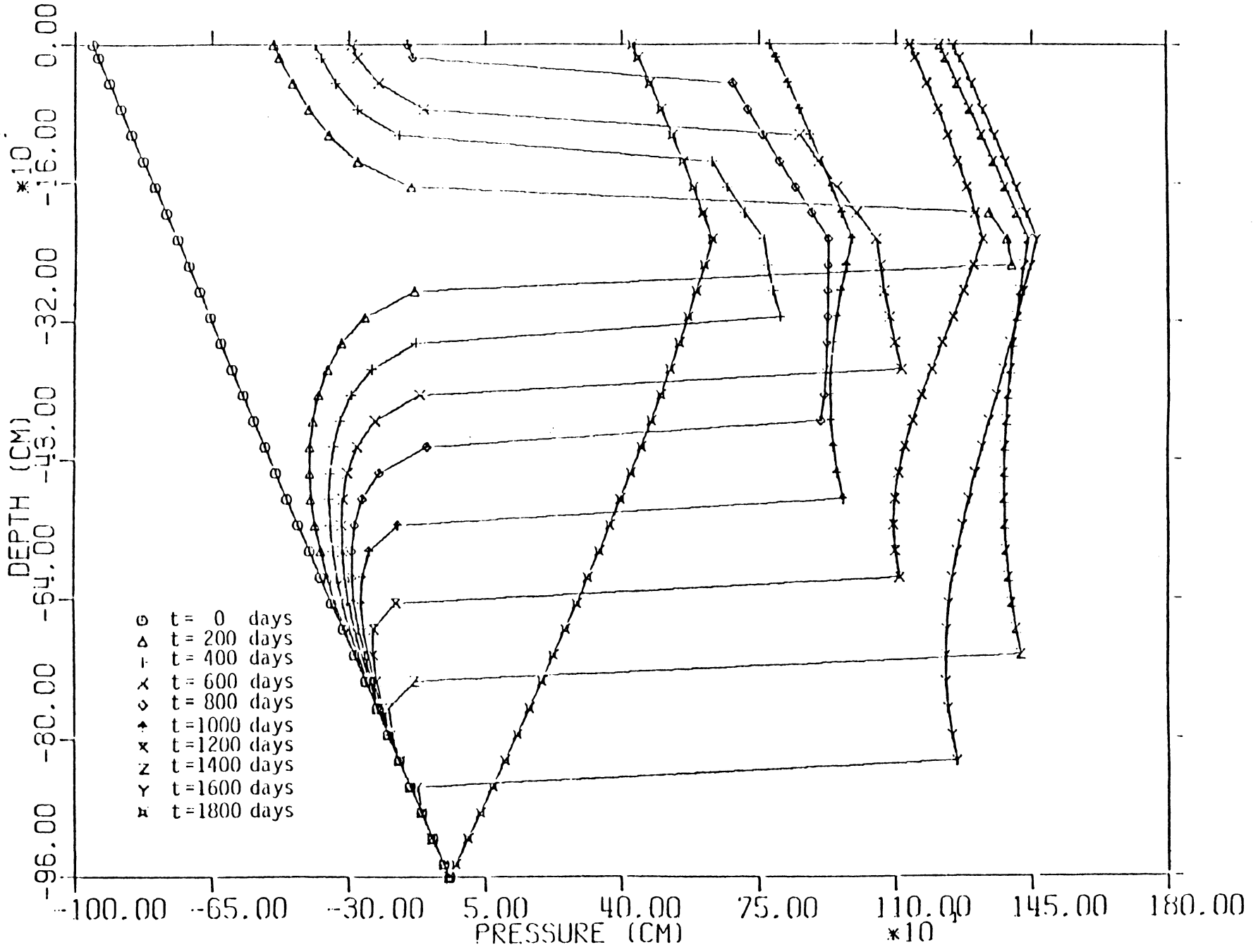

FIGURE 2.9 PROFILES OF PORE-WATER PRESSURE Test Case 3

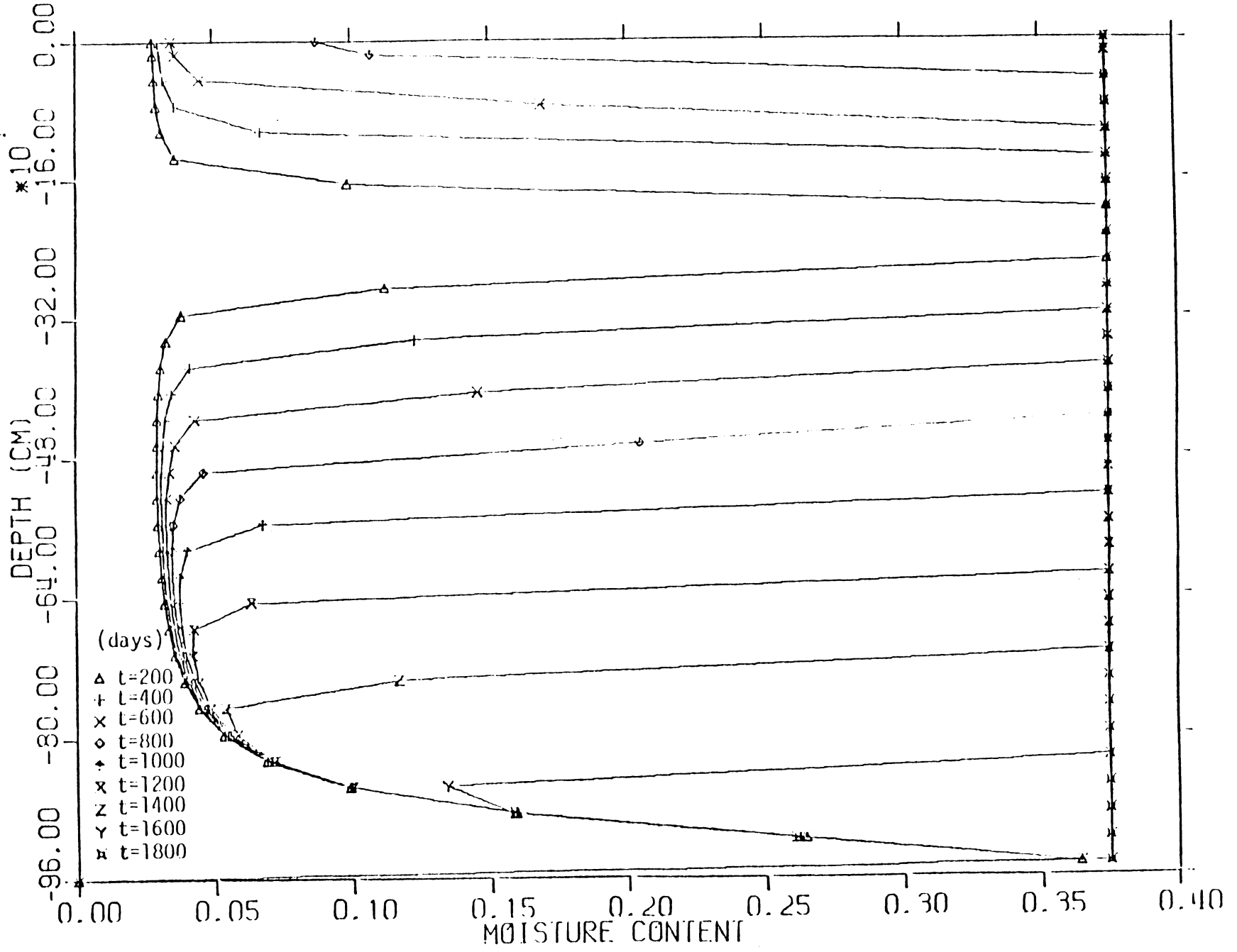

FIGURE 2.10 PROFILES OF VOLUMETRIC MOISTURE CONTENT Test Case 3

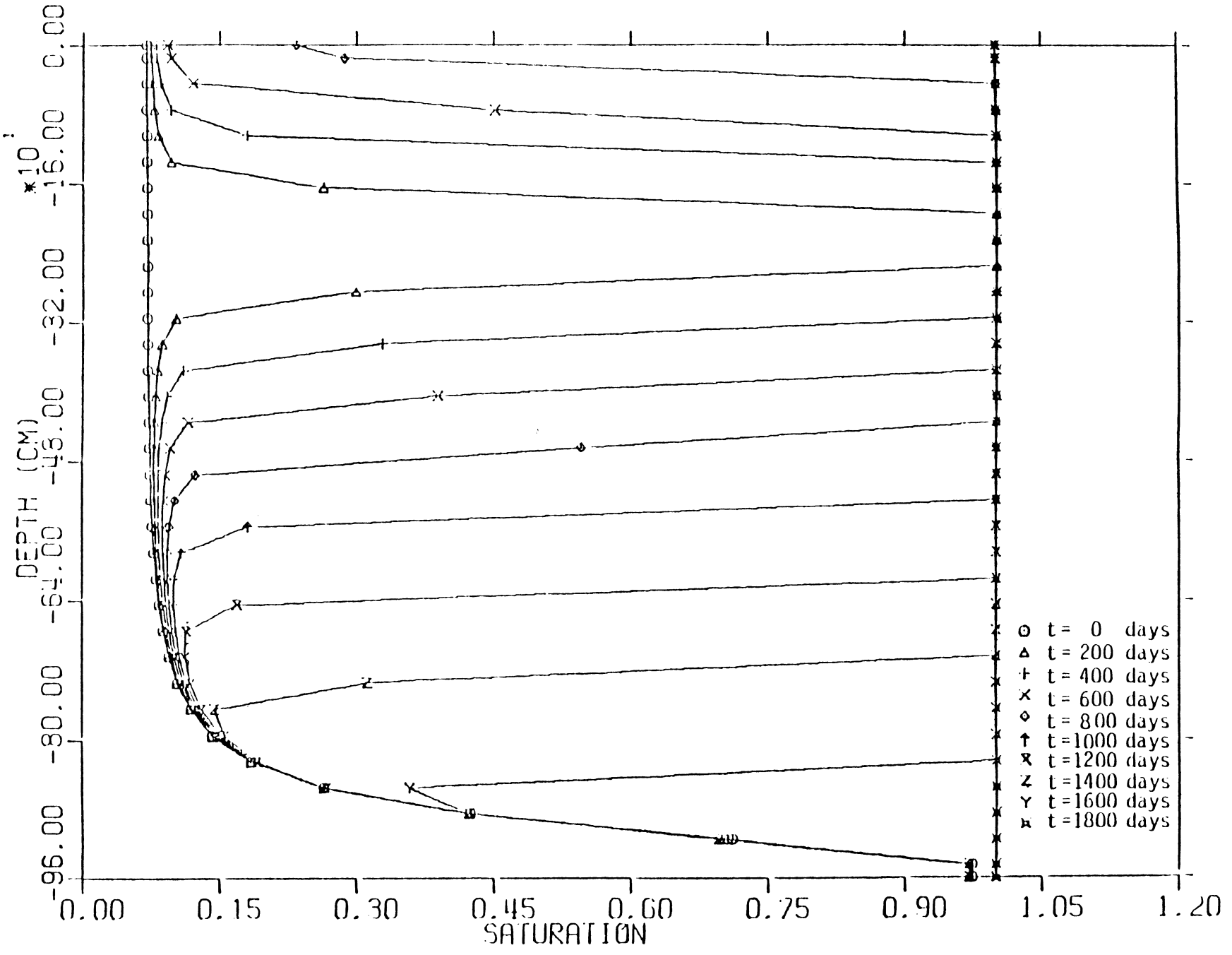

FIGURE 2.11 PROFILES OF DEGREE OF SATURATION Test Case 3

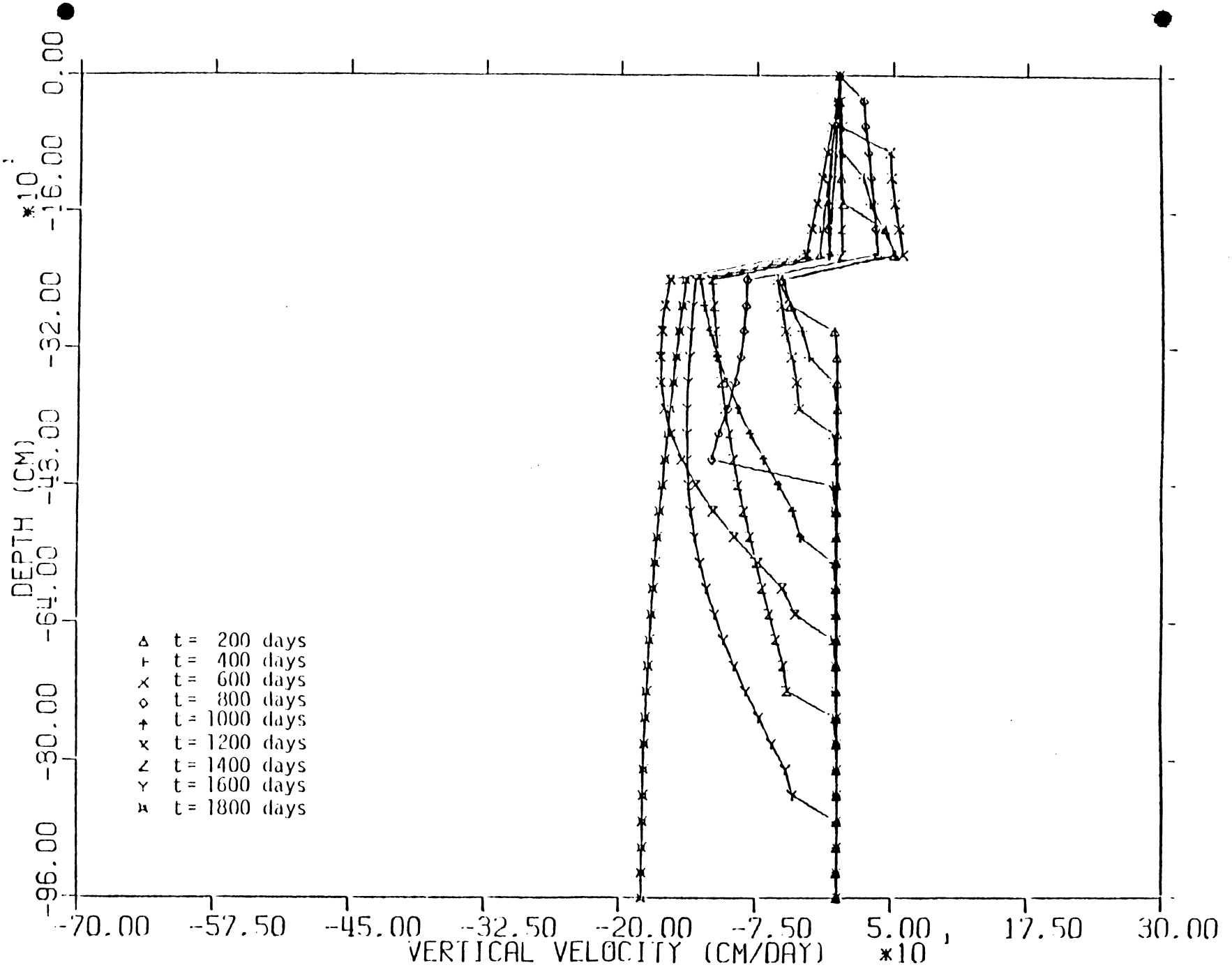

FIGURE 2.12 PROFILES OF VERTICAL VELOCITY Test Case 3

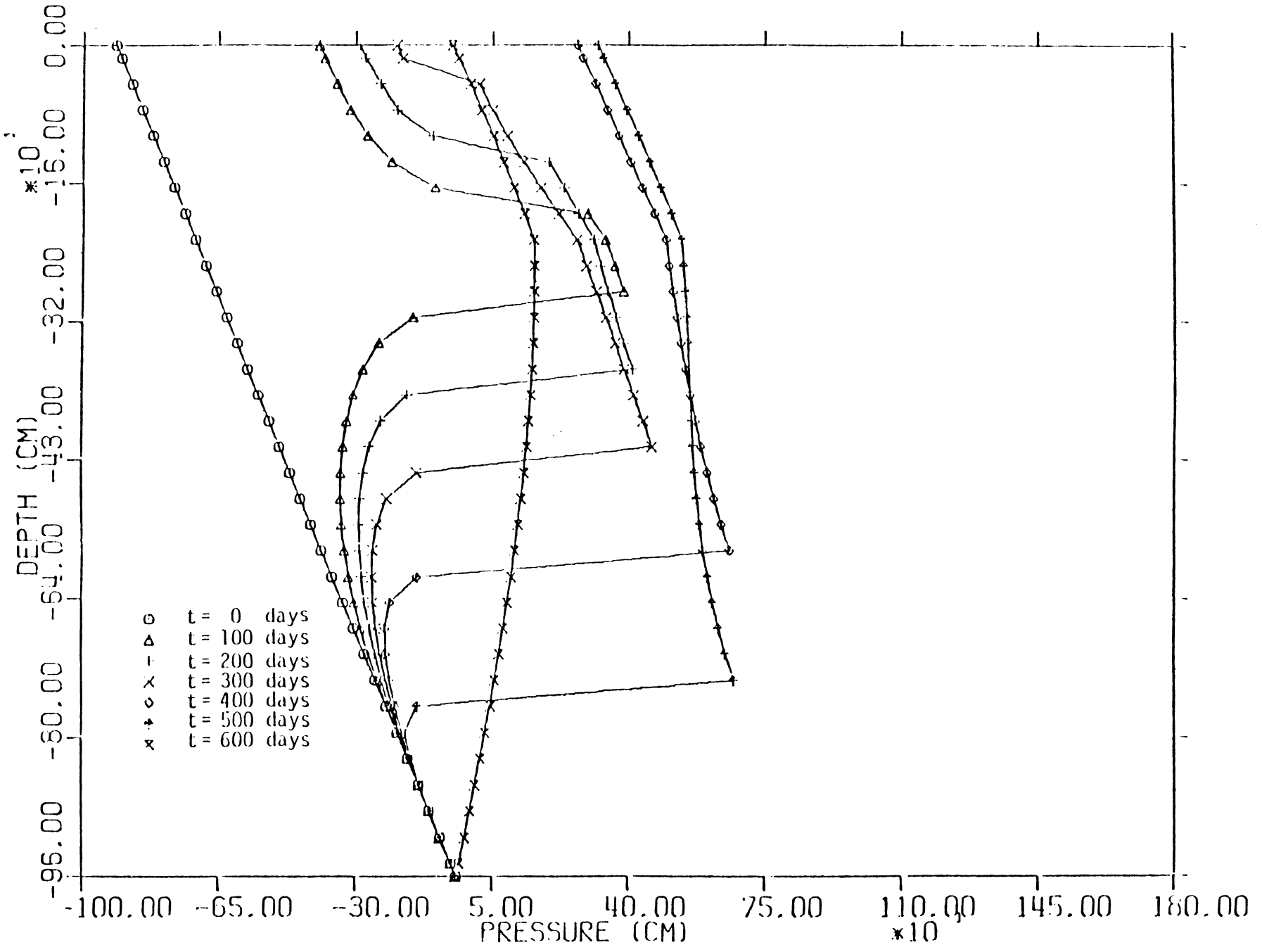

FIGURE 2.13 PROFILES OF PORE-WATER PRESSURE Test Case 4

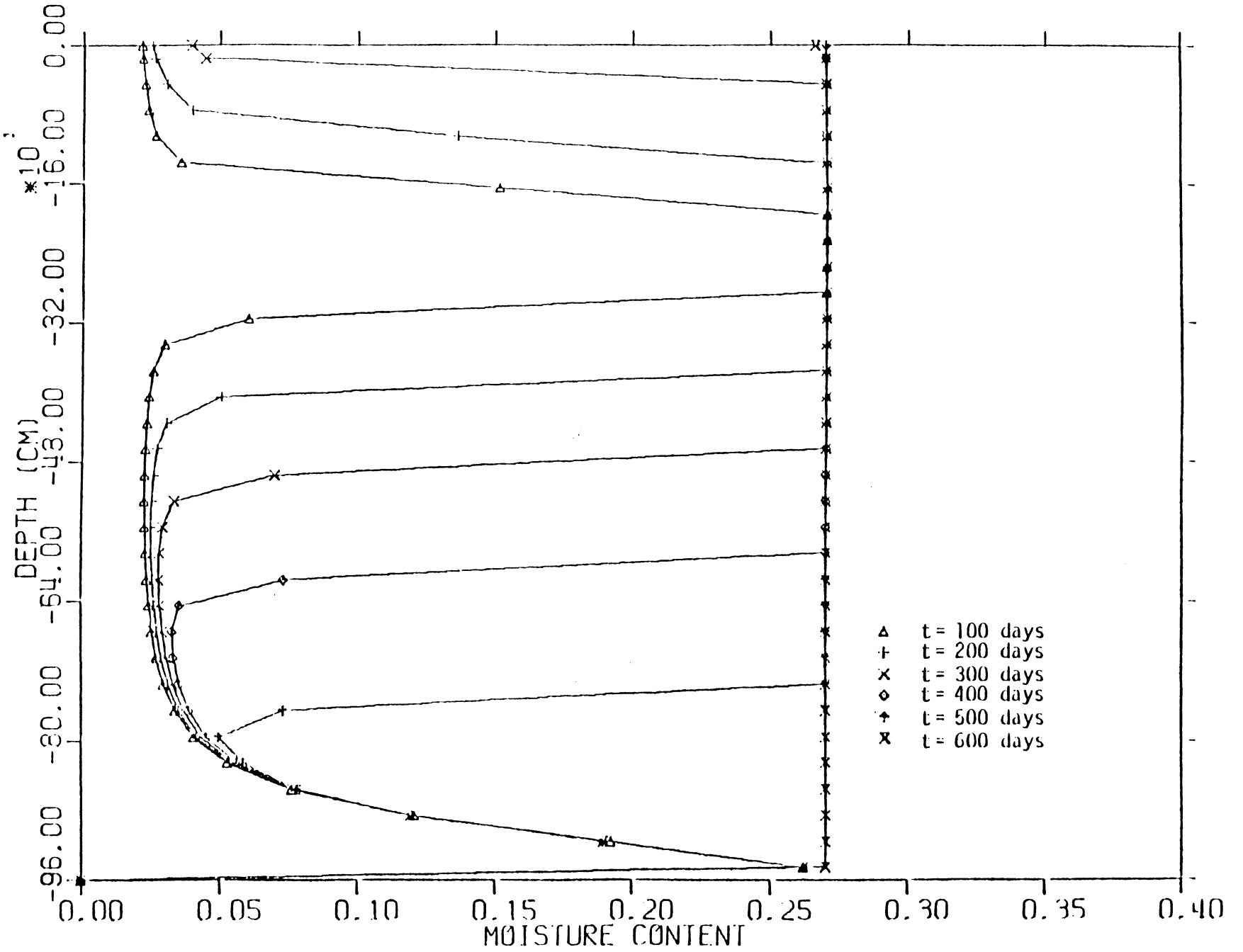

FIGURE 2.14 PROFILES OF VOLUMETRIC MOISTURE CONTENT Test Case 4

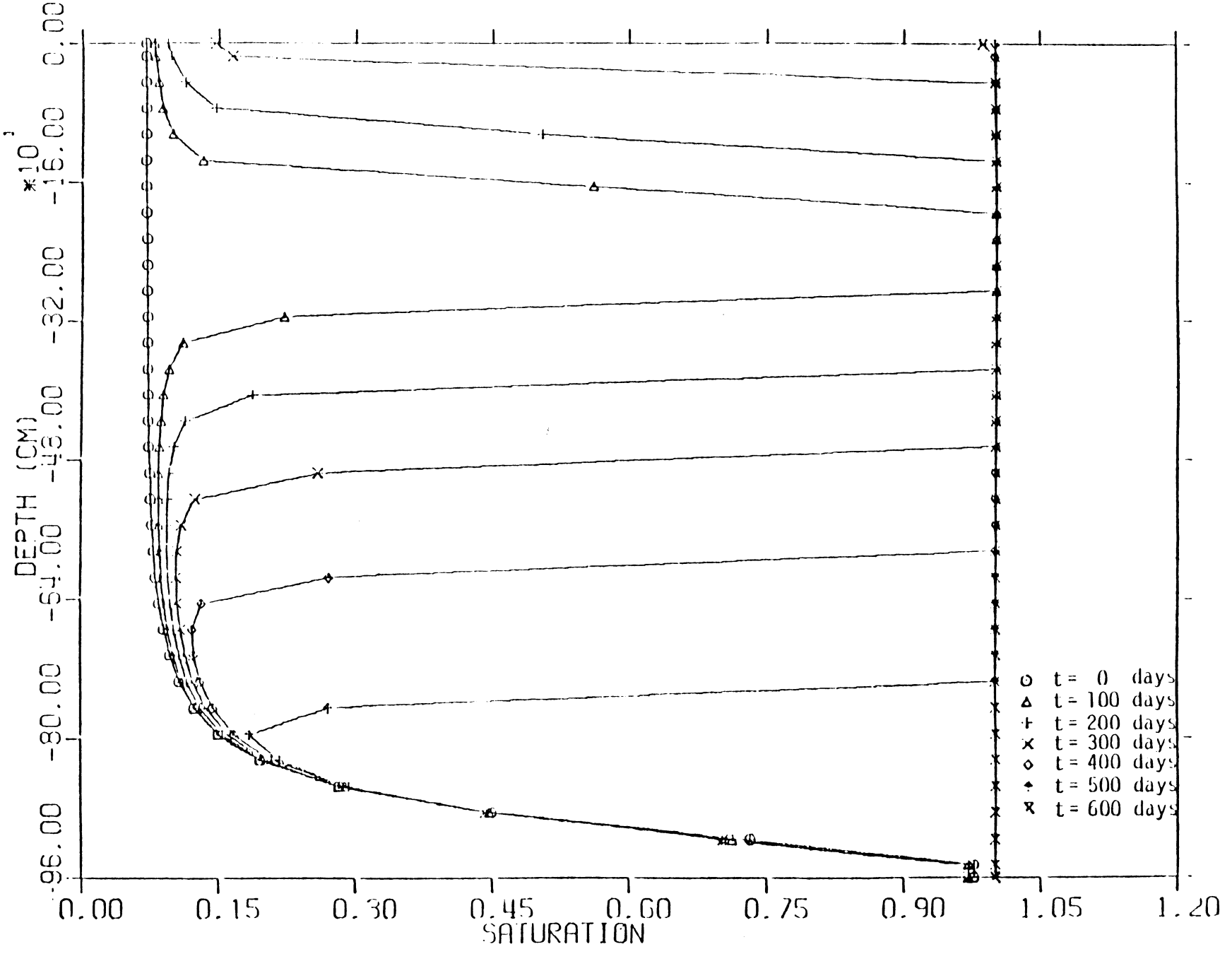

FIGURE 2.15 PROFILES OF DEGREE OF SATURATION Test Case 4

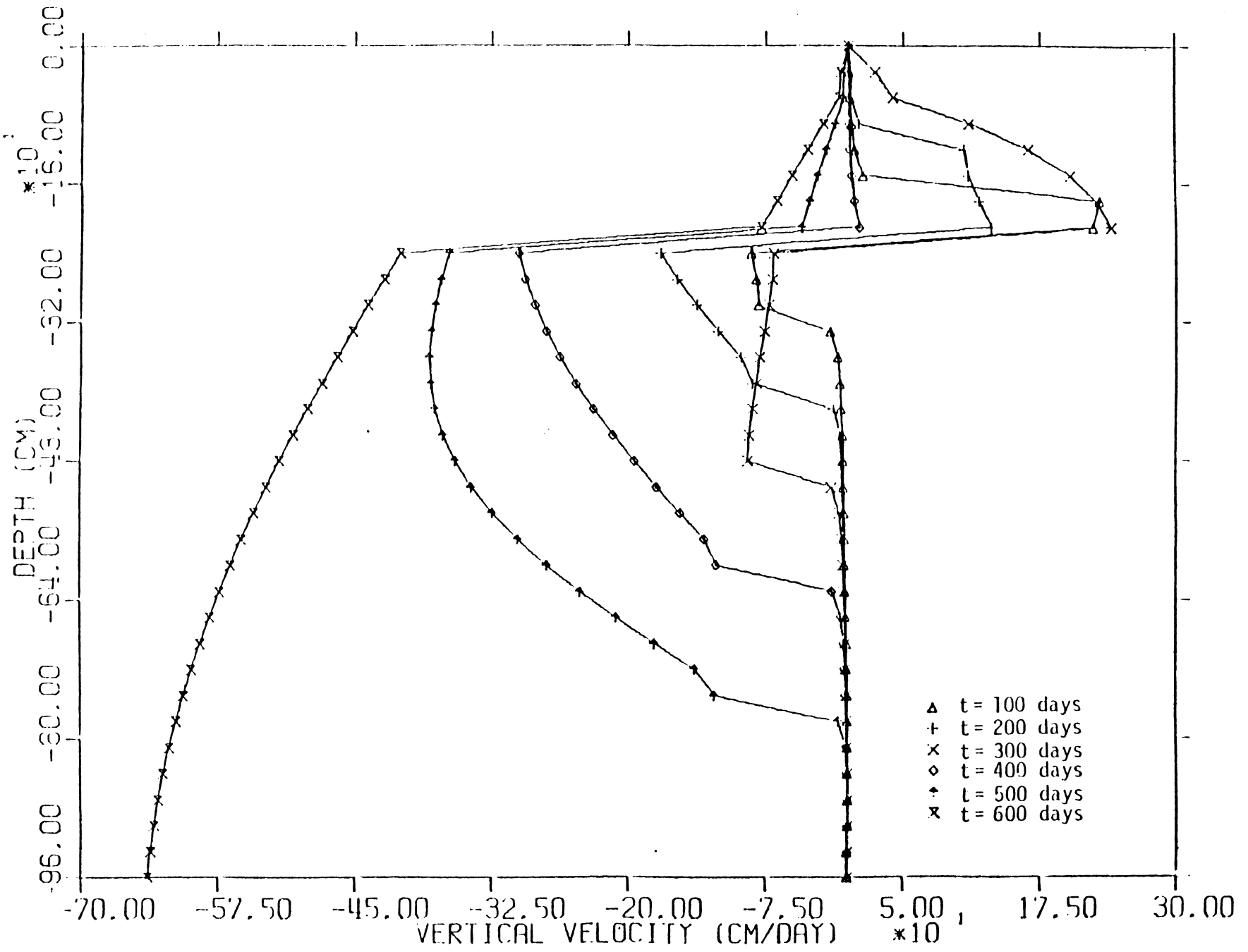

FIGURE 2.16 PROFILES OF VERTICAL VELOCITY Test Case 4

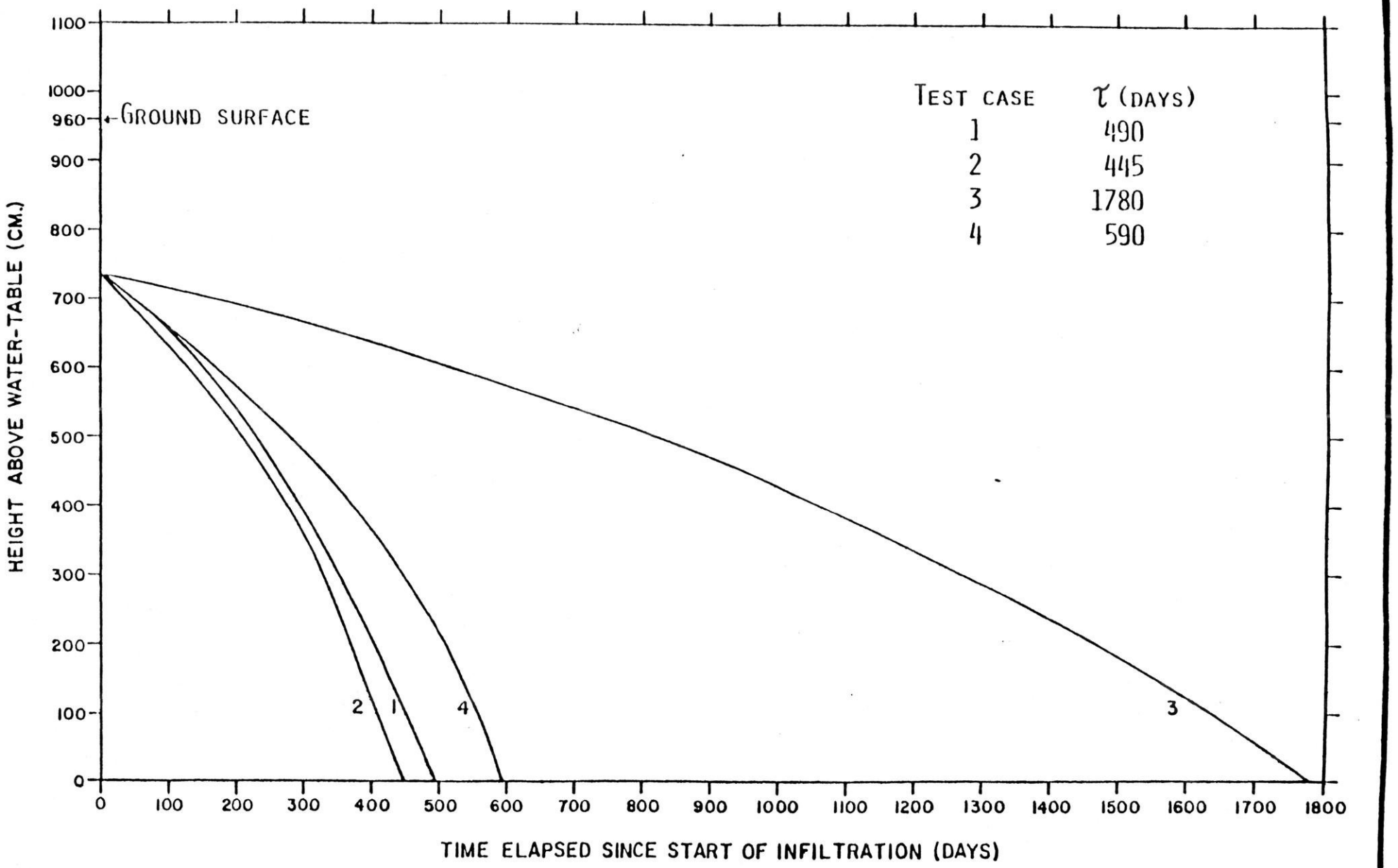

Fig. 2.17 Advance of the wetting front with time

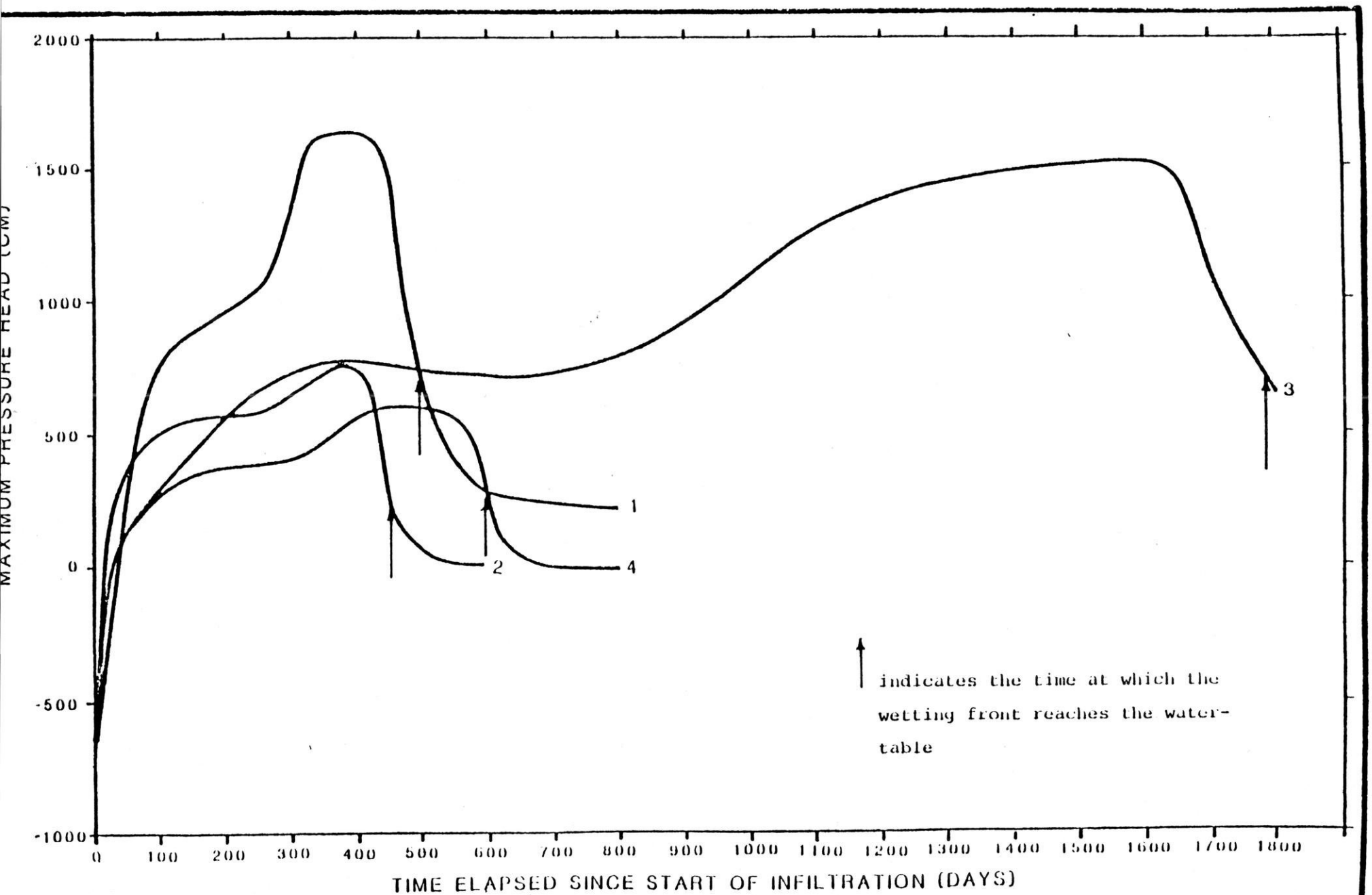

Fig. 2.18 Variation of pressure head in the infiltration bed with time

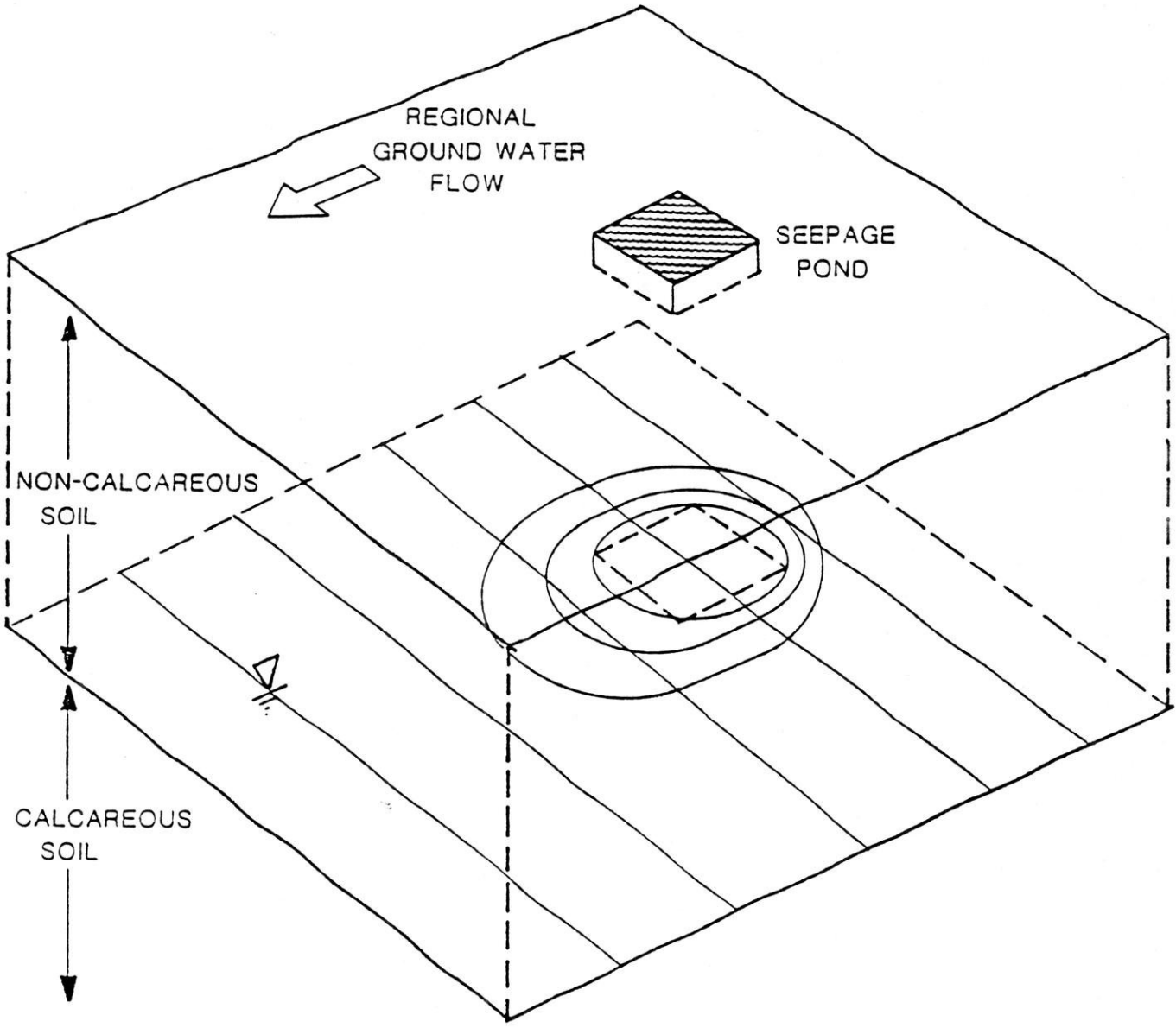

Figure 3.1 Schematic diagram of hypothetical seepage pond.

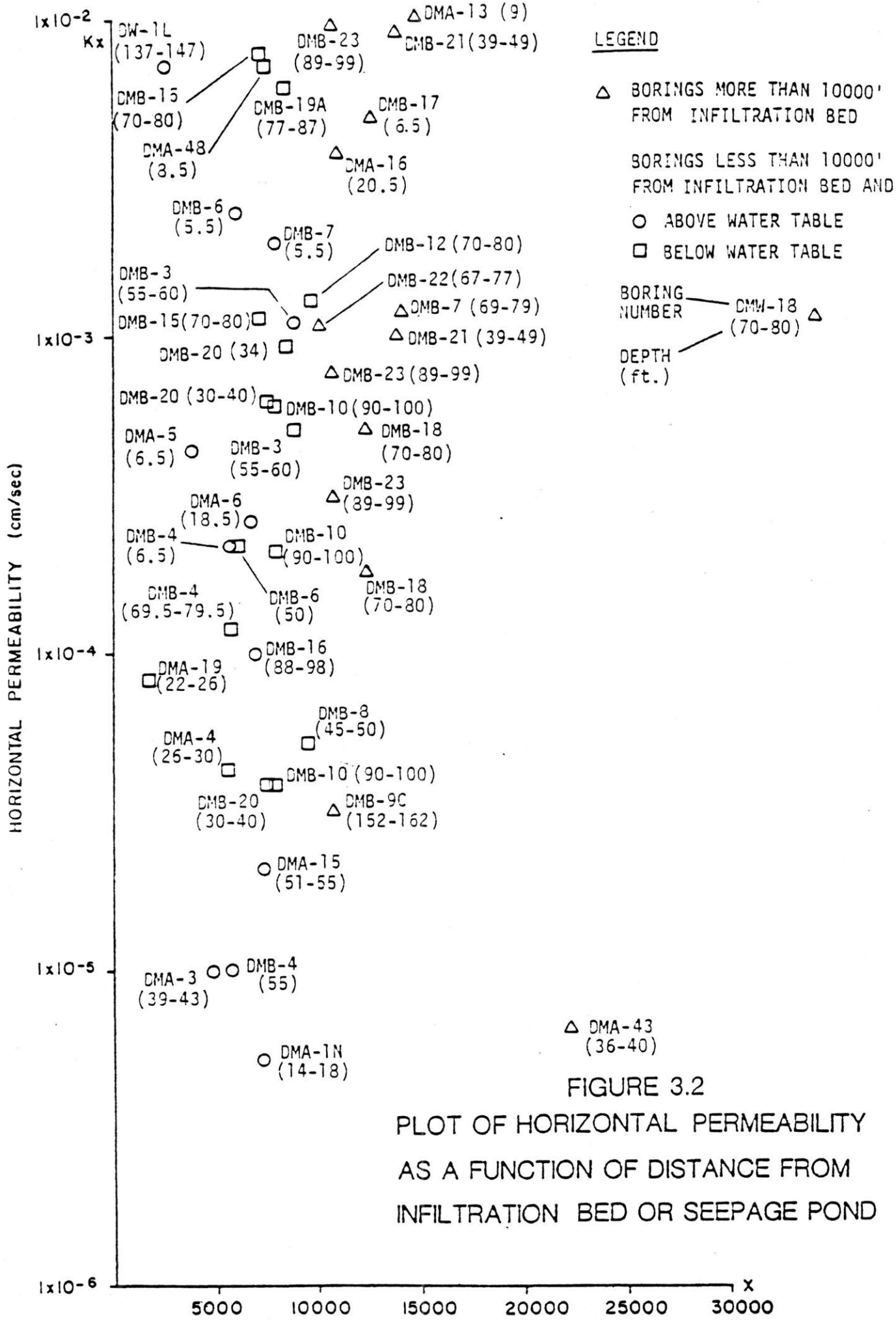

FIGURE 3.2

PLOT OF HORIZONTAL PERMEABILITY AS A FUNCTION OF DISTANCE FROM INFILTRATION BED OR SEEPAGE POND

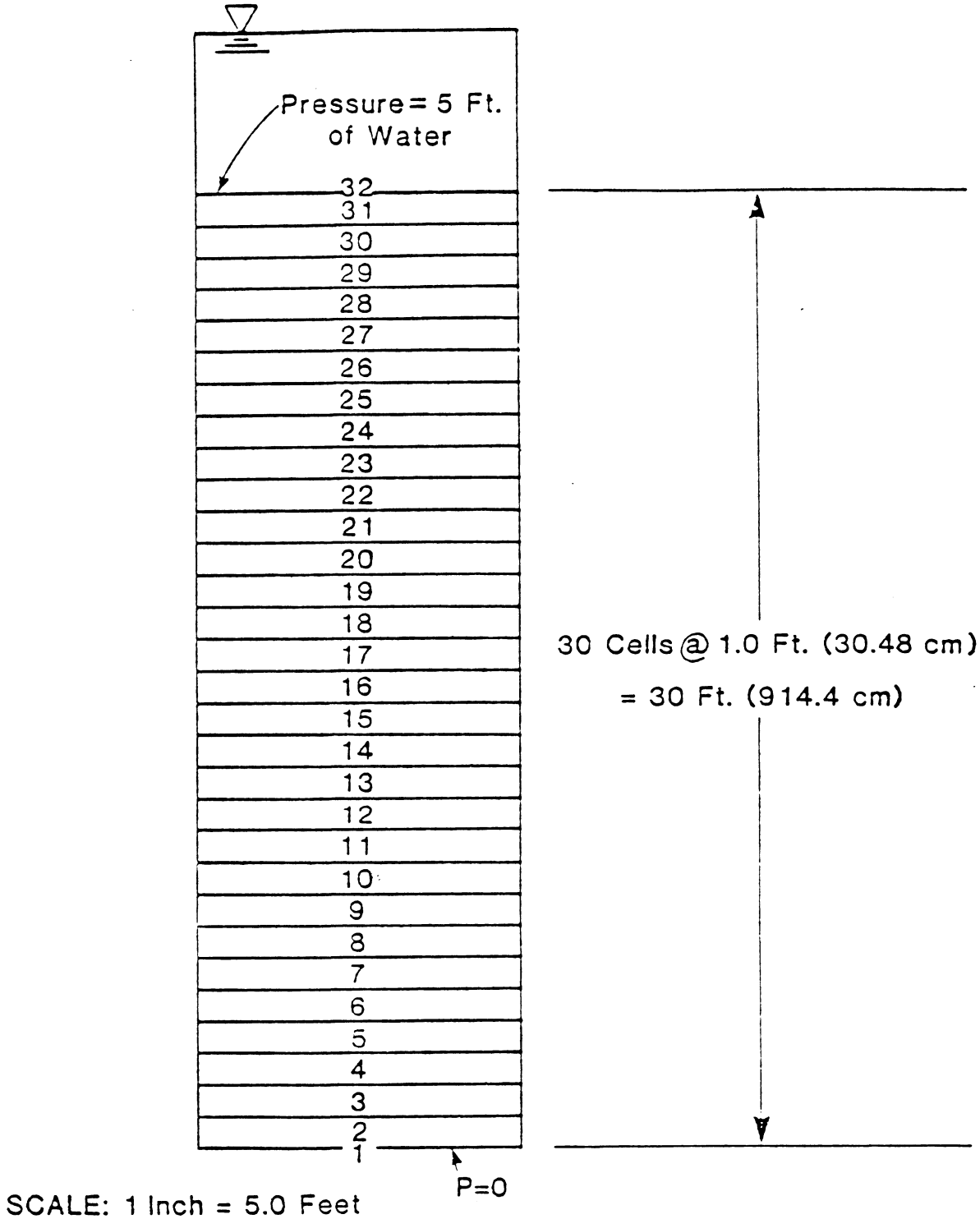

FIGURE 4.1

FINITE-DIFFERENCE MESH FOR A 1-DIMENSIONAL COLUMN OF SOIL BENEATH THE POND

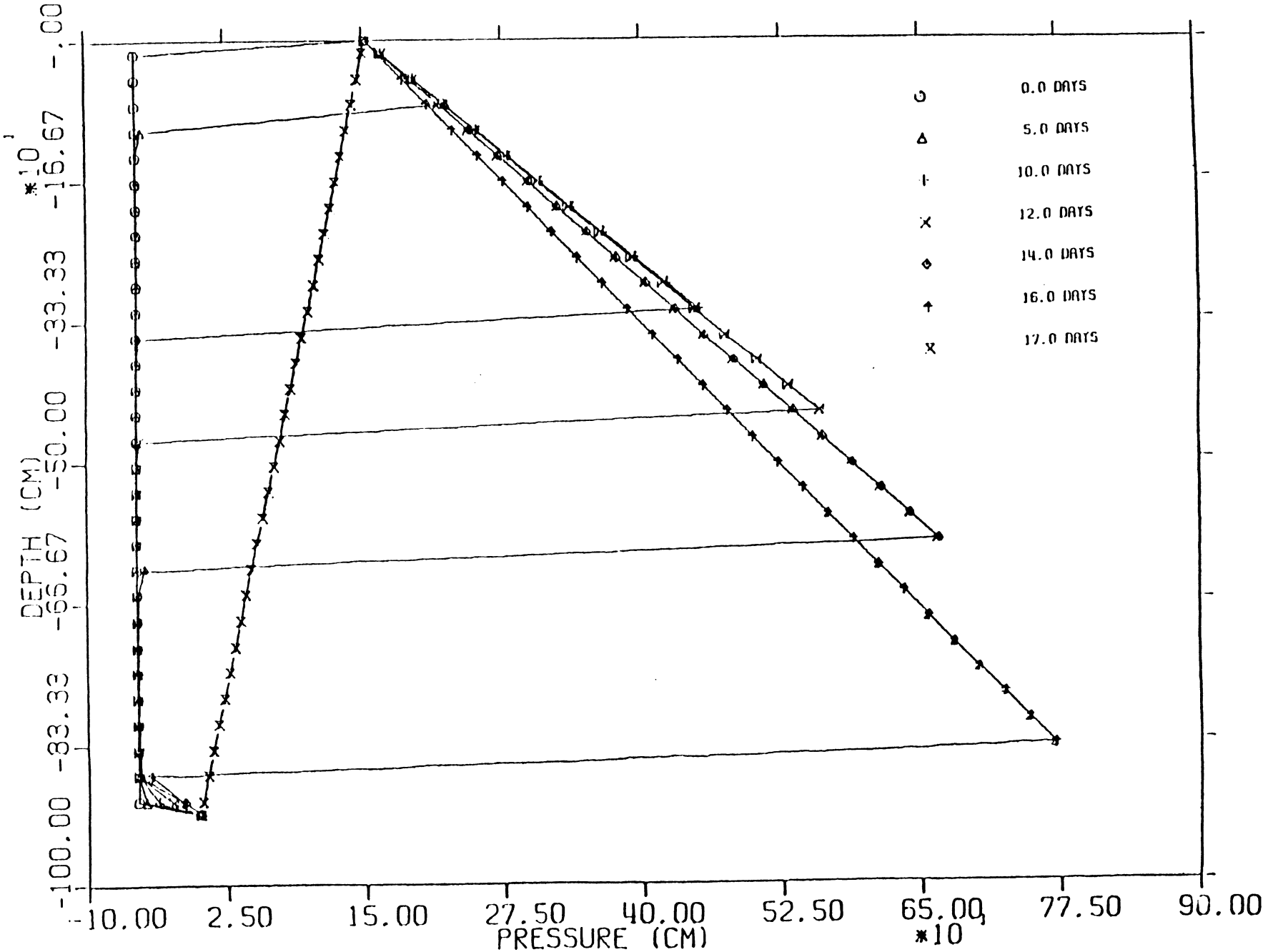

FIGURE 4.2 PRESSURE HEADS

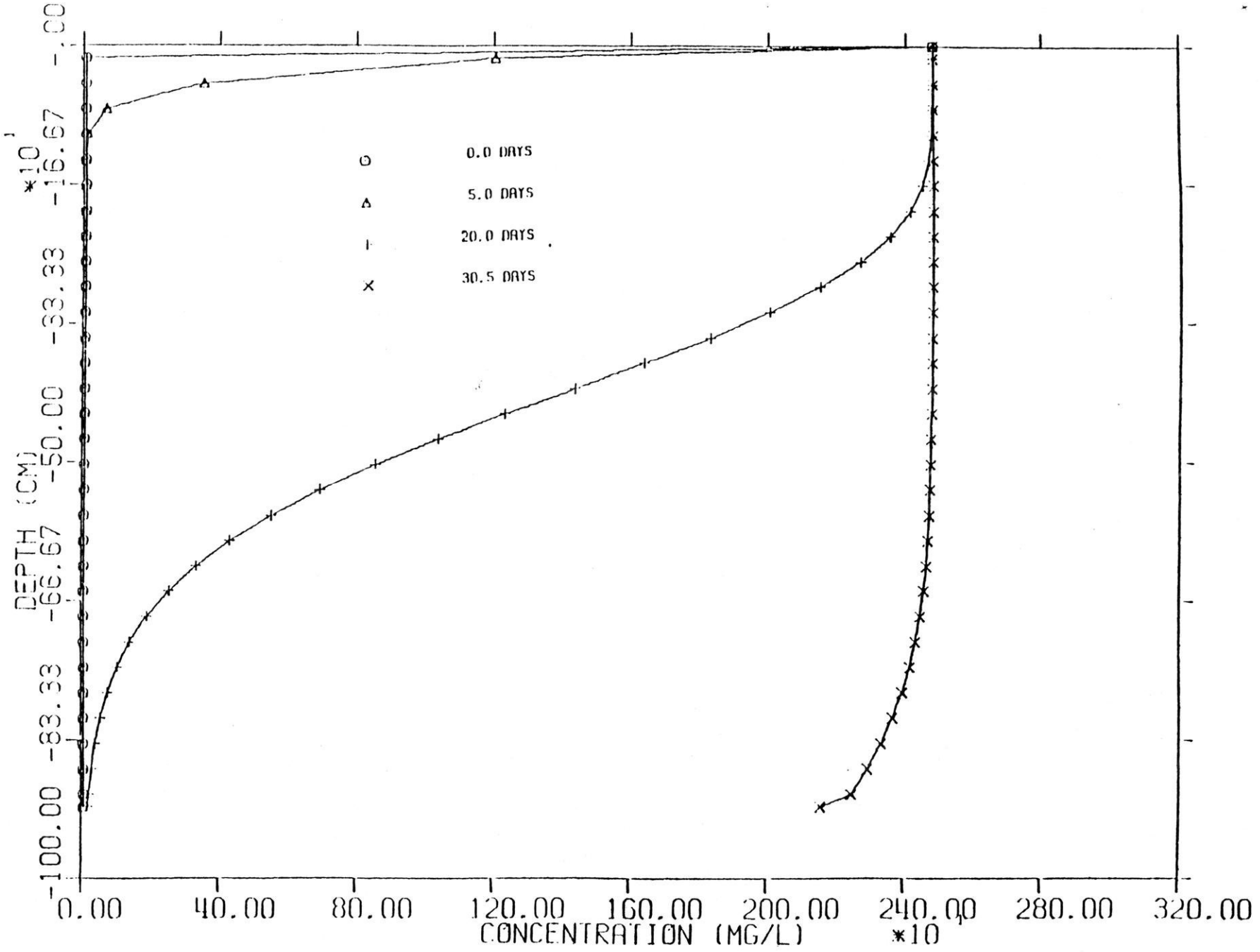

FIGURE 4.3 SO4 CONCENTRATIONS

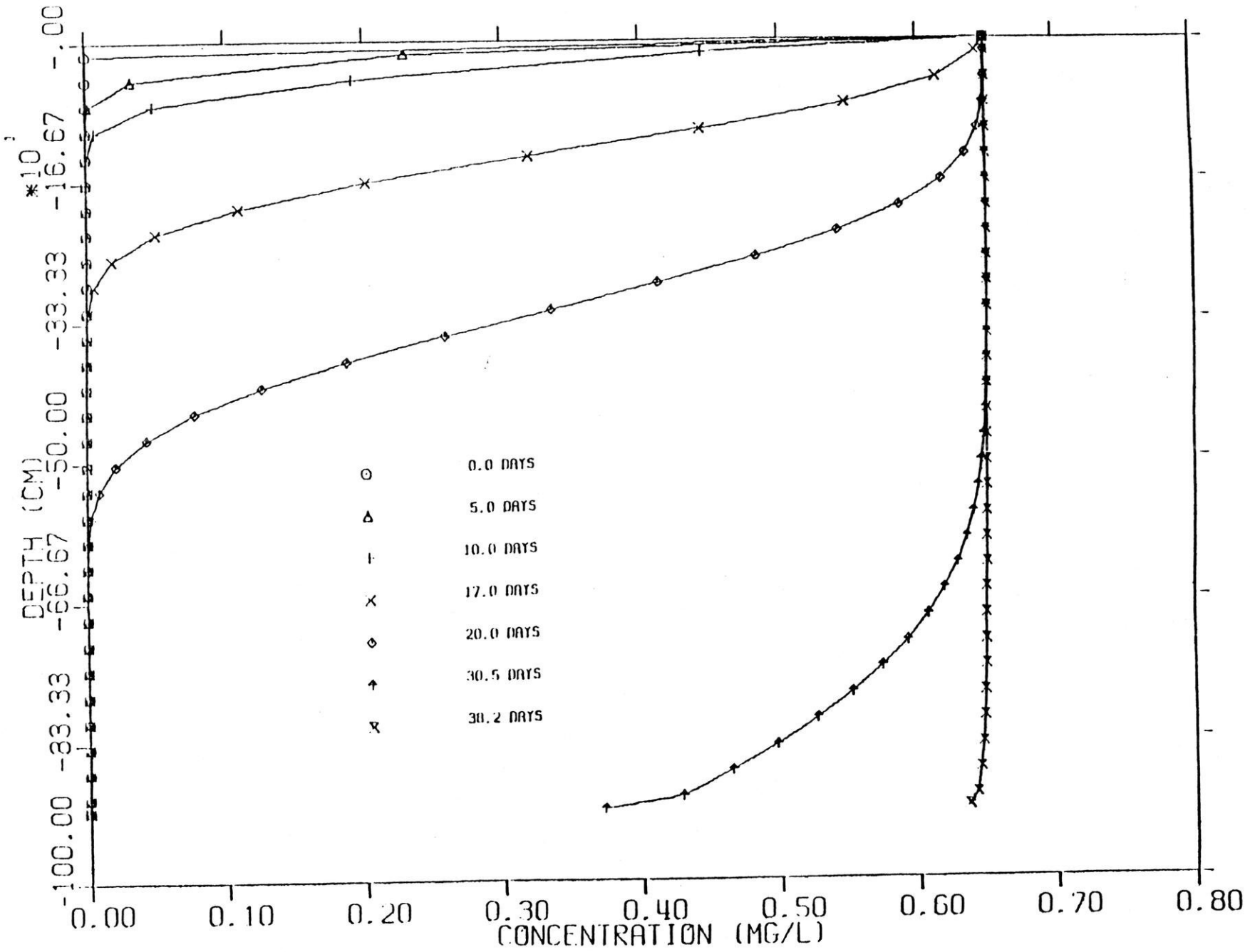

FIGURE 4.4 SE CONCENTRATIONS

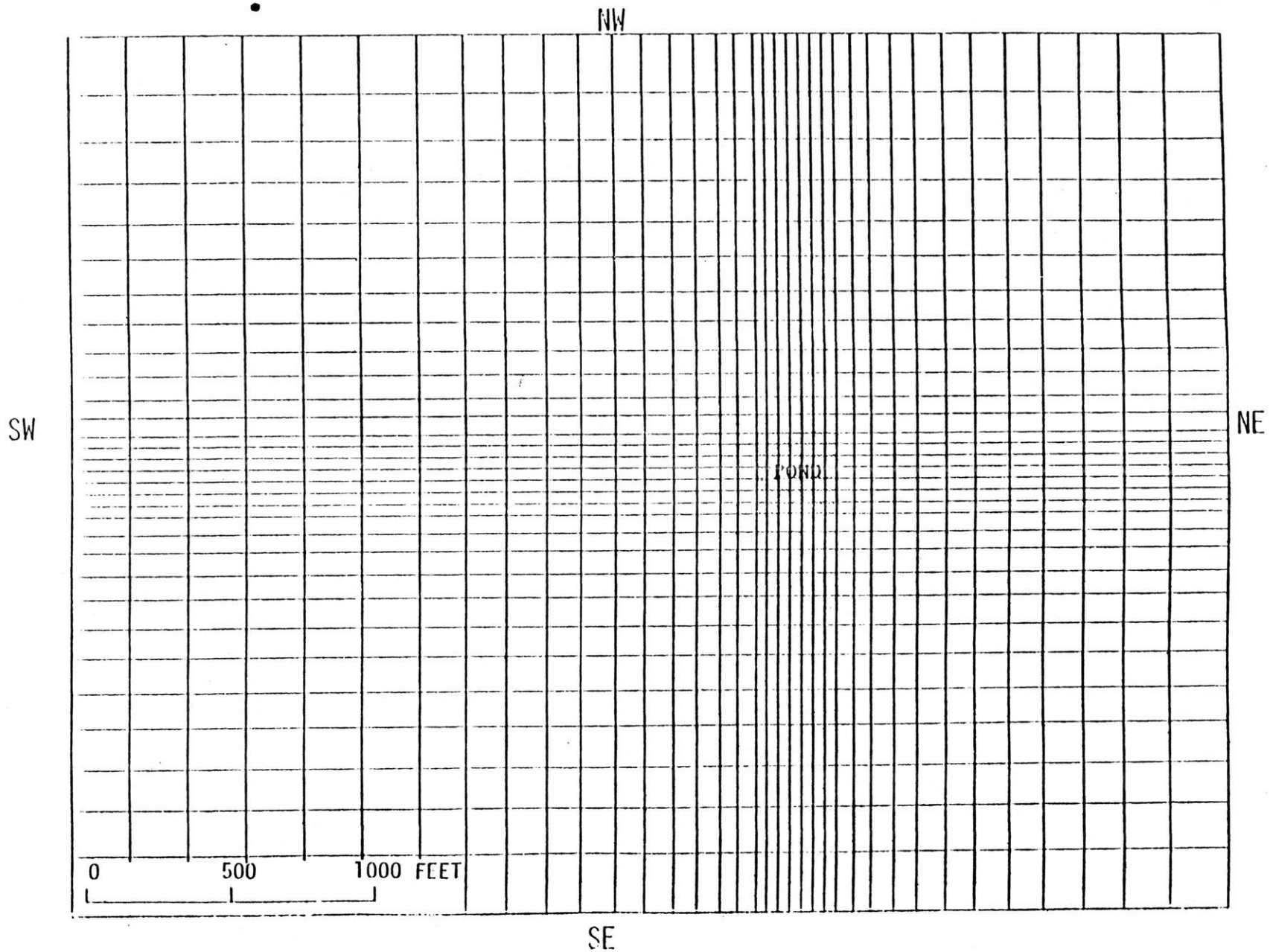

FIGURE: 4.5 Two-dimensional finite-difference grid for the area surrounding the pond.

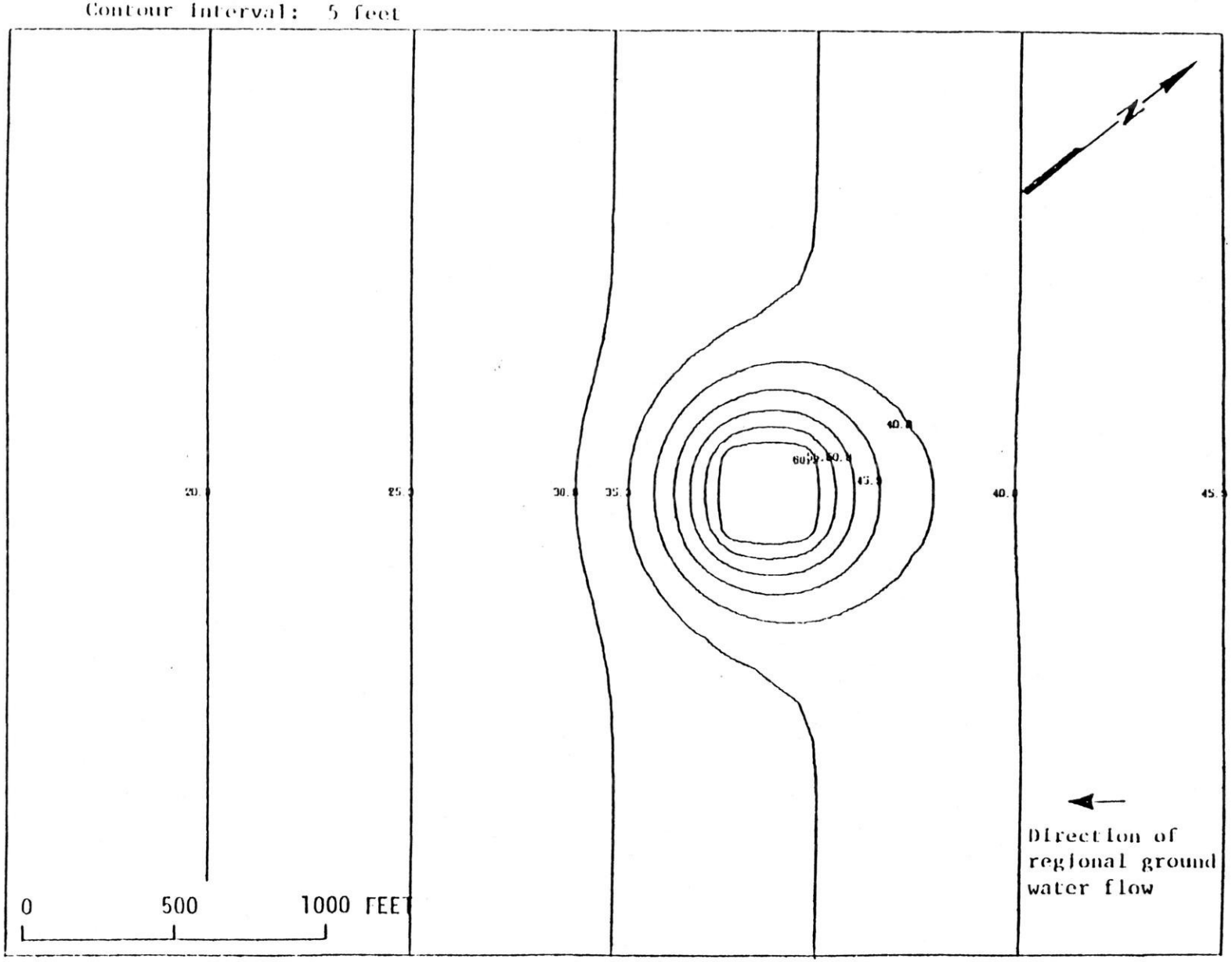

FIGURE: 4.6 Head contours after 1 year of pond operation.

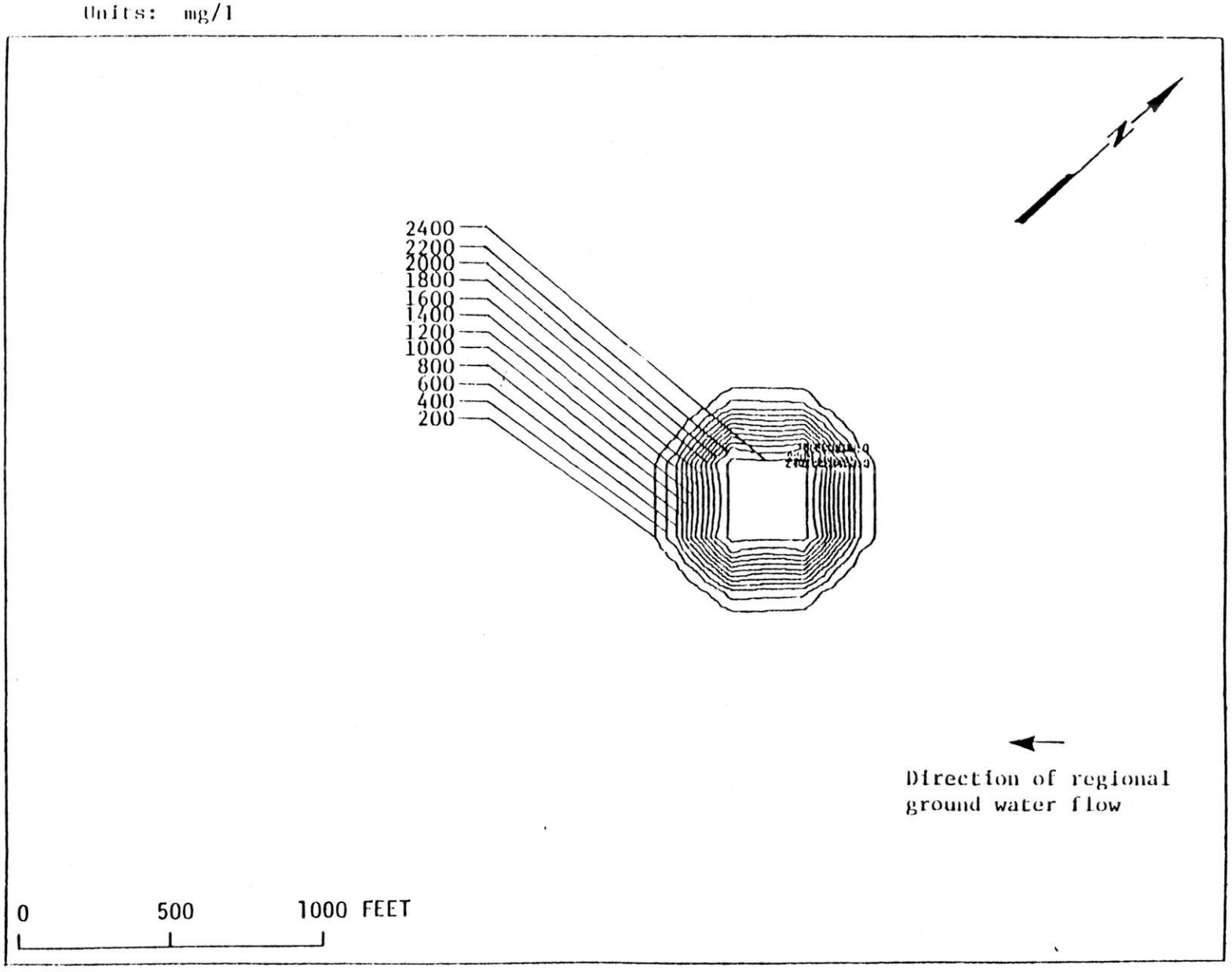

FIGURE: 4.7 Sulfate concentration distributions after 1 year of pond operation.

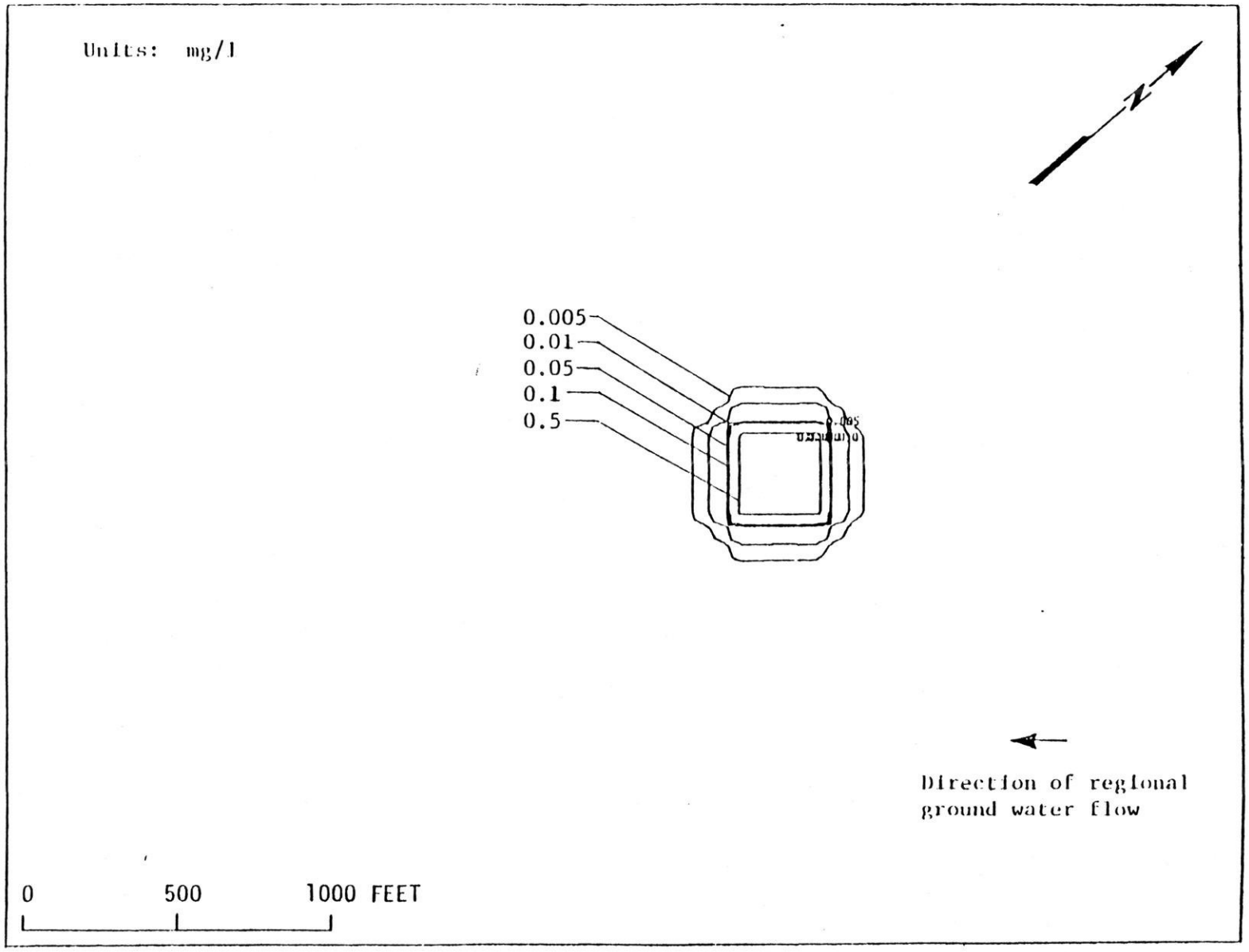

FIGURE: 4.8 Selenium concentration distributions after 1 year of pond operation.

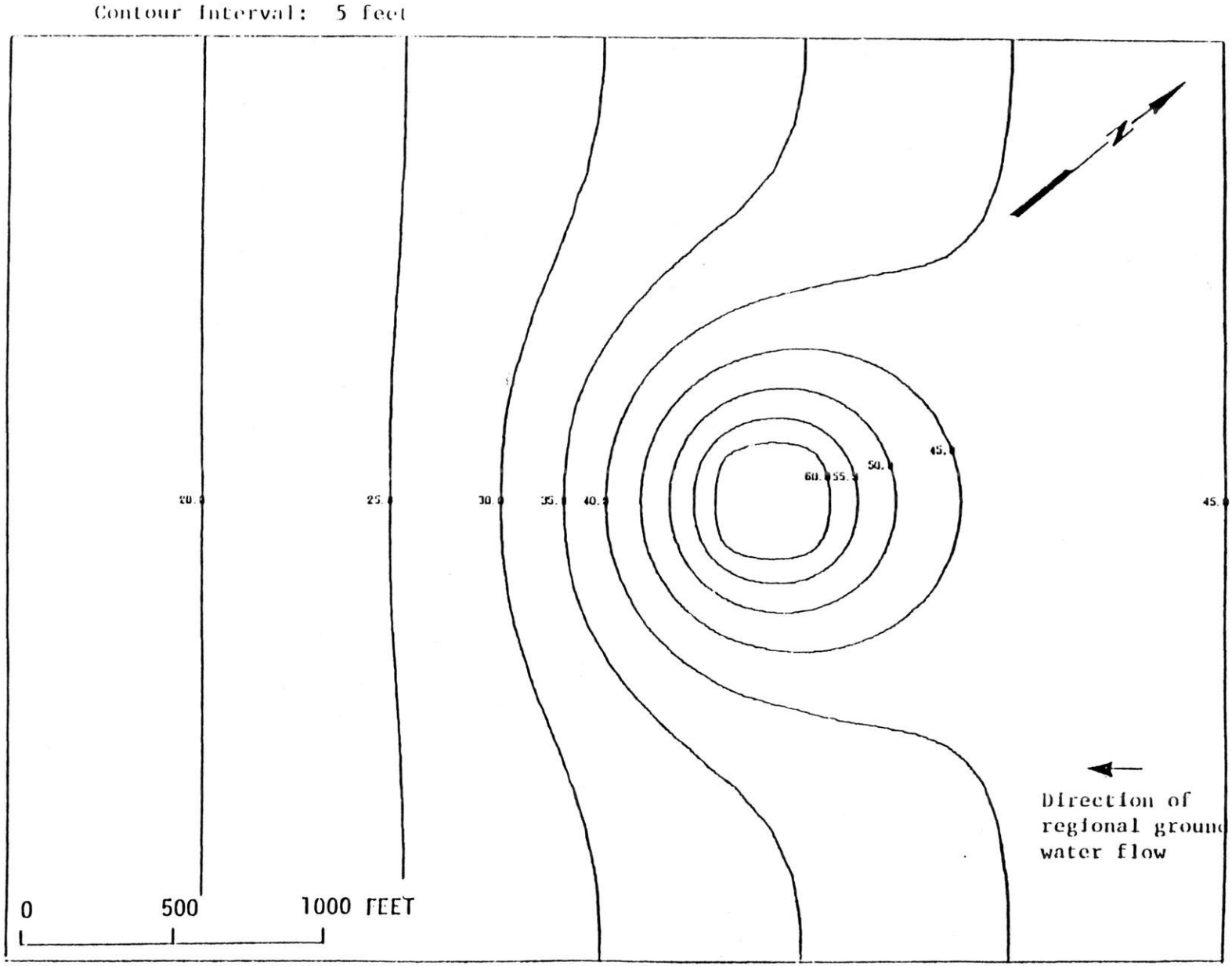

FIGURE: 4.9 Head contours after 5 years of pond operation.

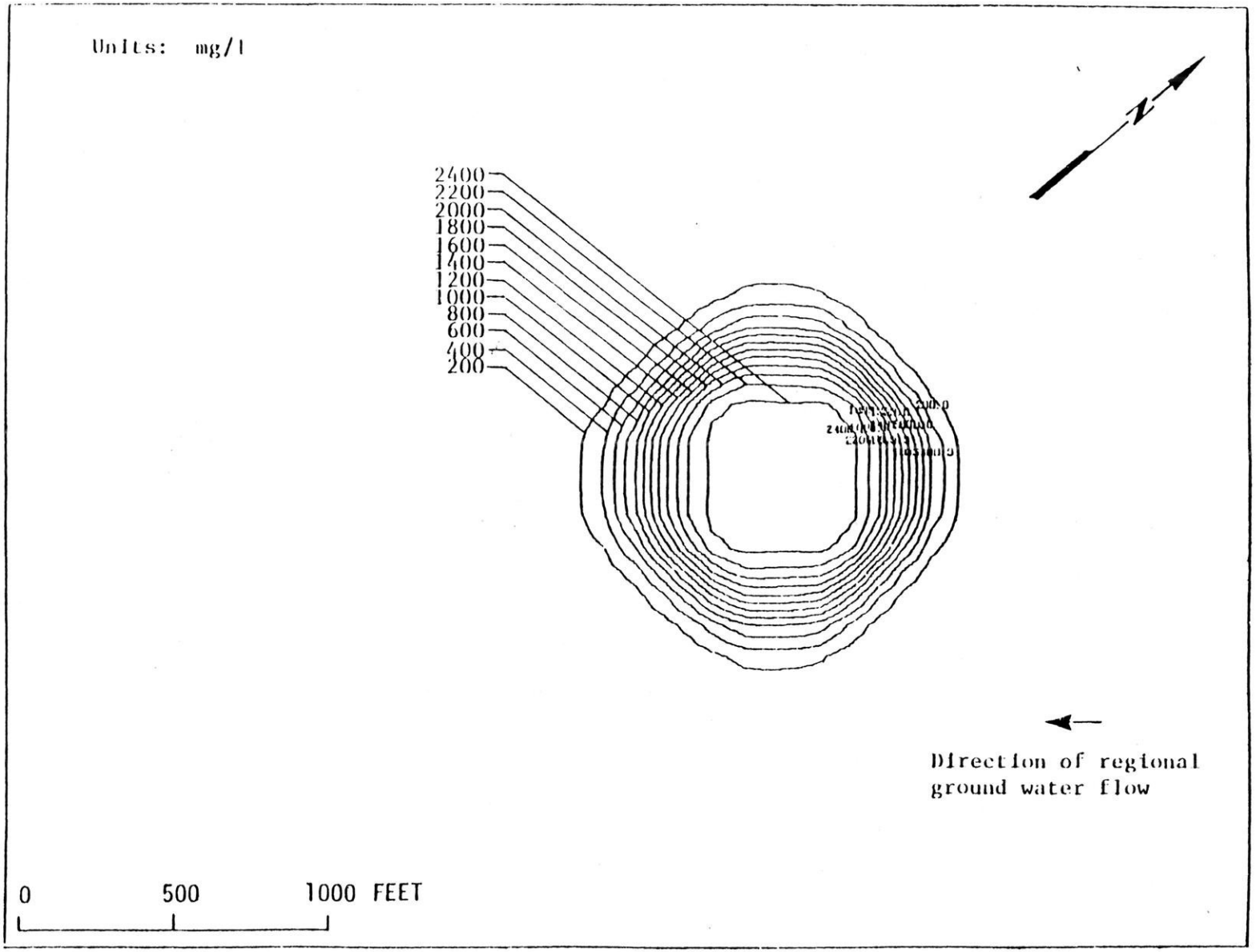

FIGURE: 4.10 Sulfate concentration distribution after 5 years of pond operation.

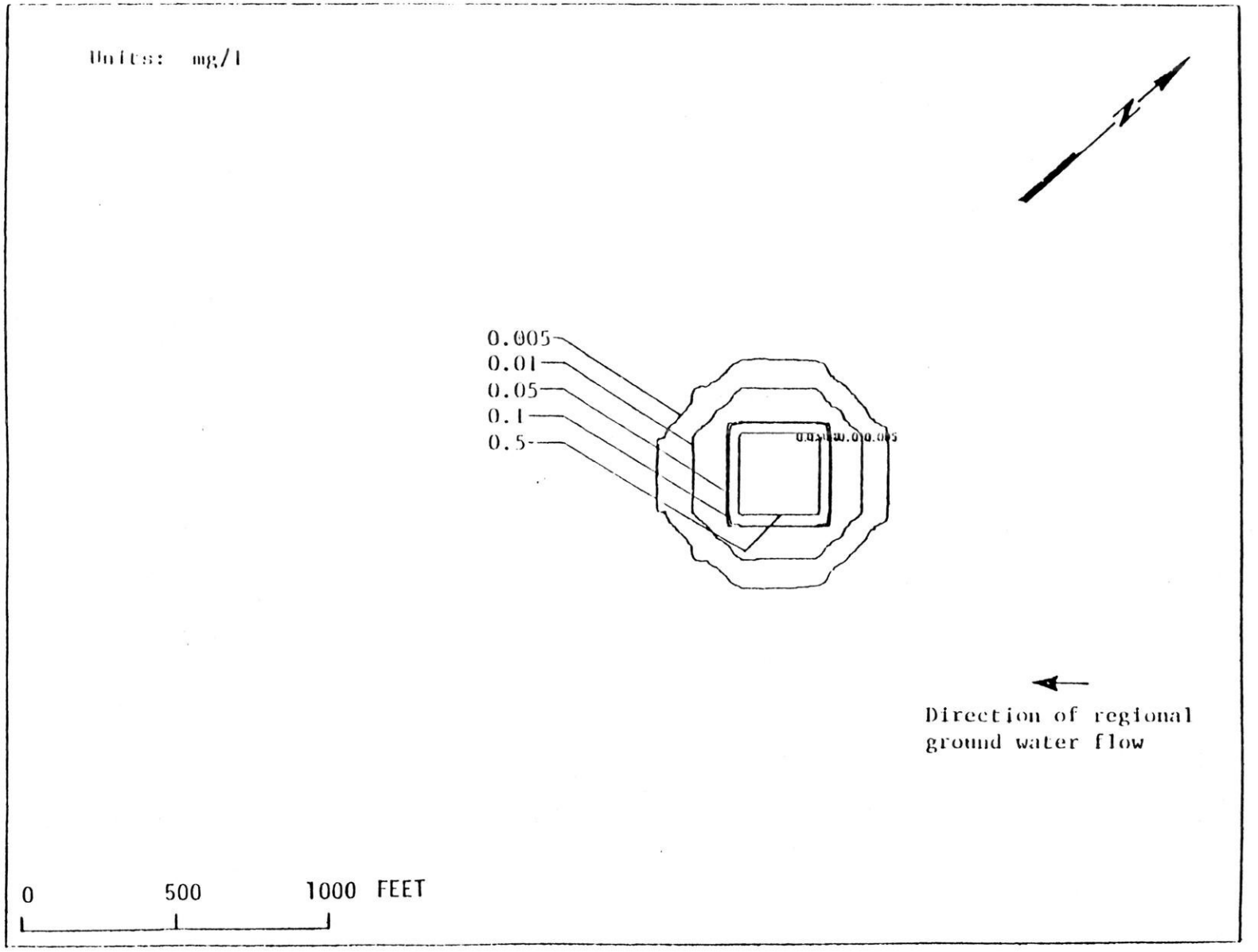

FIGURE: 4.11 Selenium concentration distribution after 5 years of pond operation.

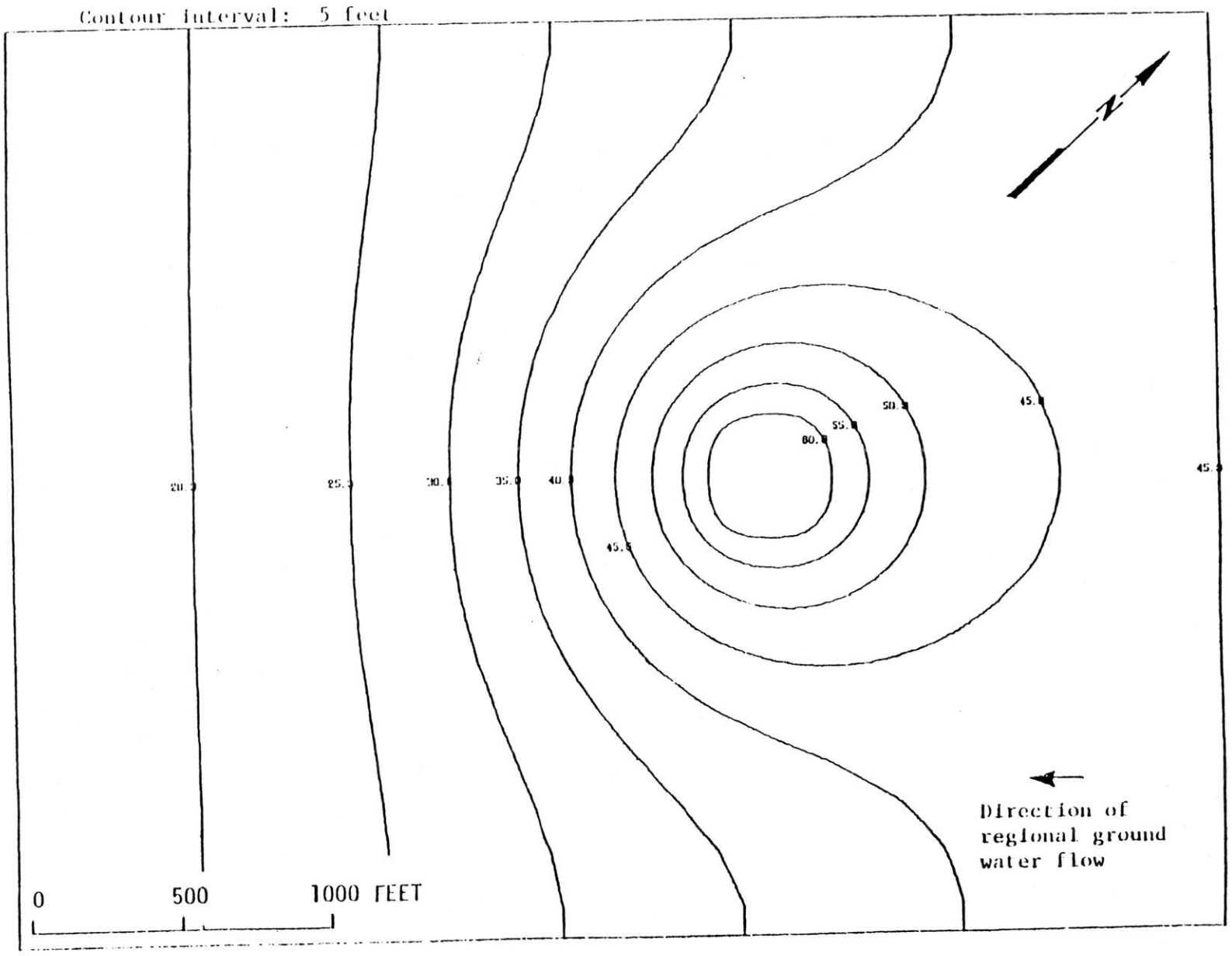

FIGURE: 4.12 Head contours after 10 years of pond operation.

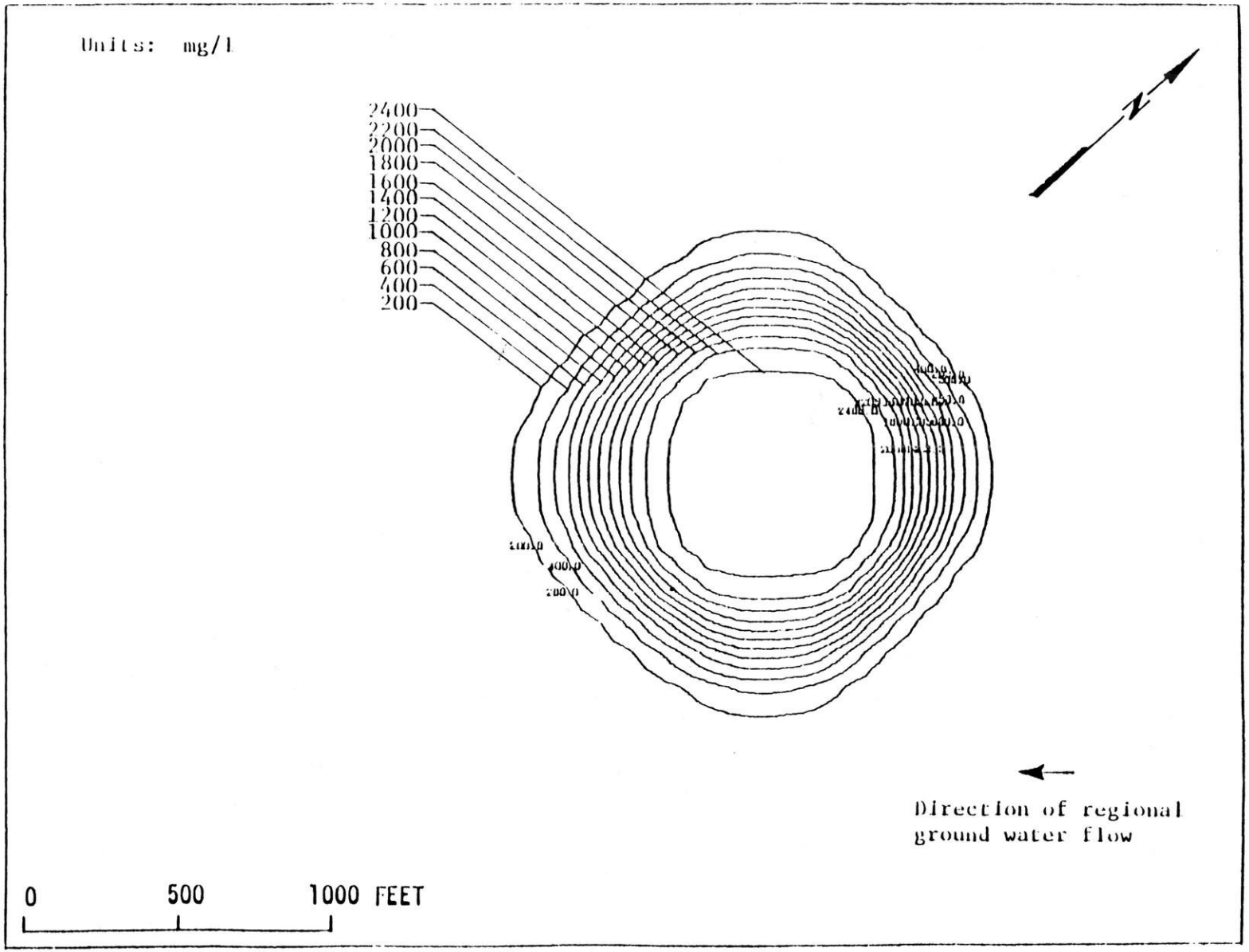

FIGURE:4.13 Sulfate concentration distribution after 10 years of pond operation.

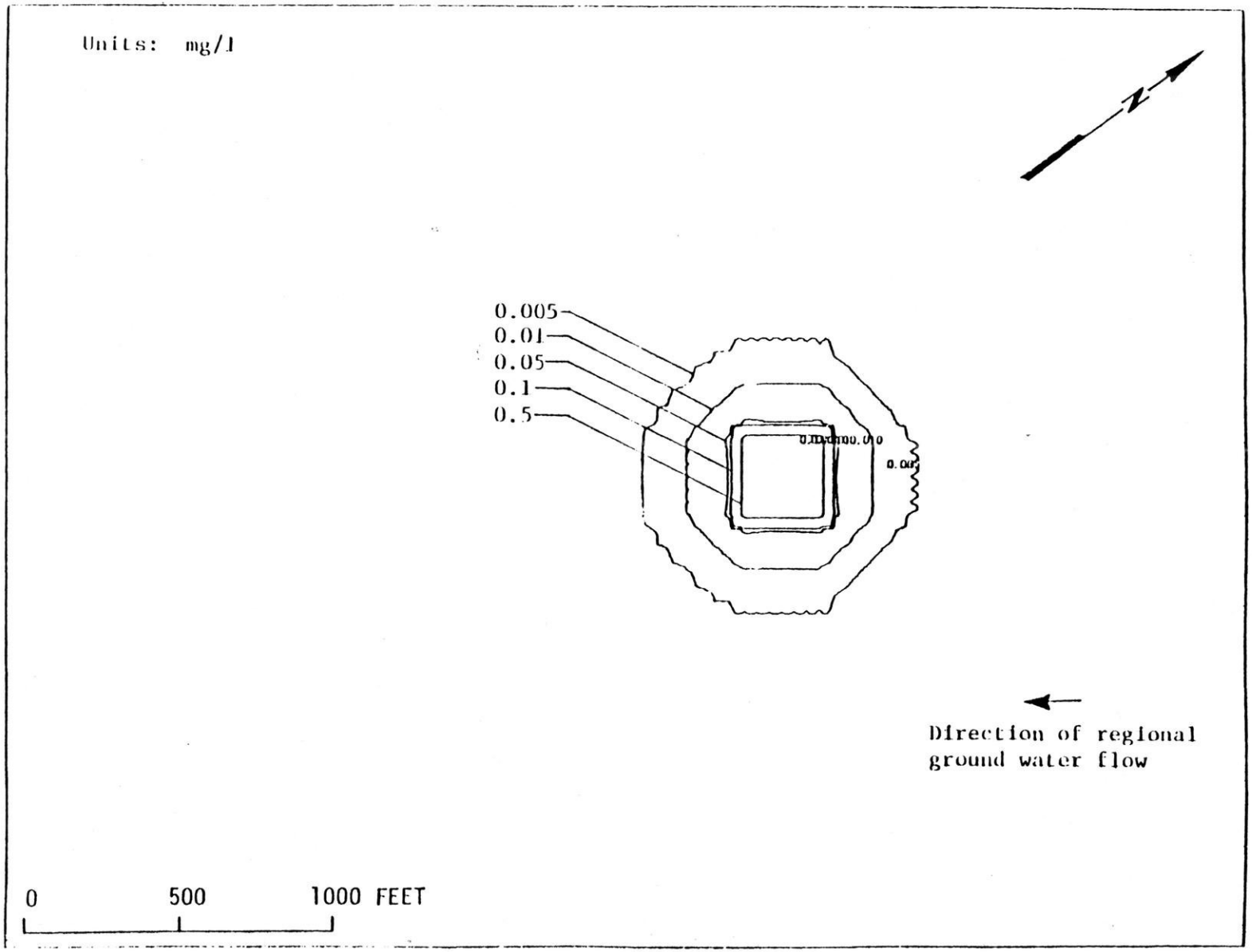

FIGURE: 4.14 Selenium concentration distribution after 10 years of pond operation.

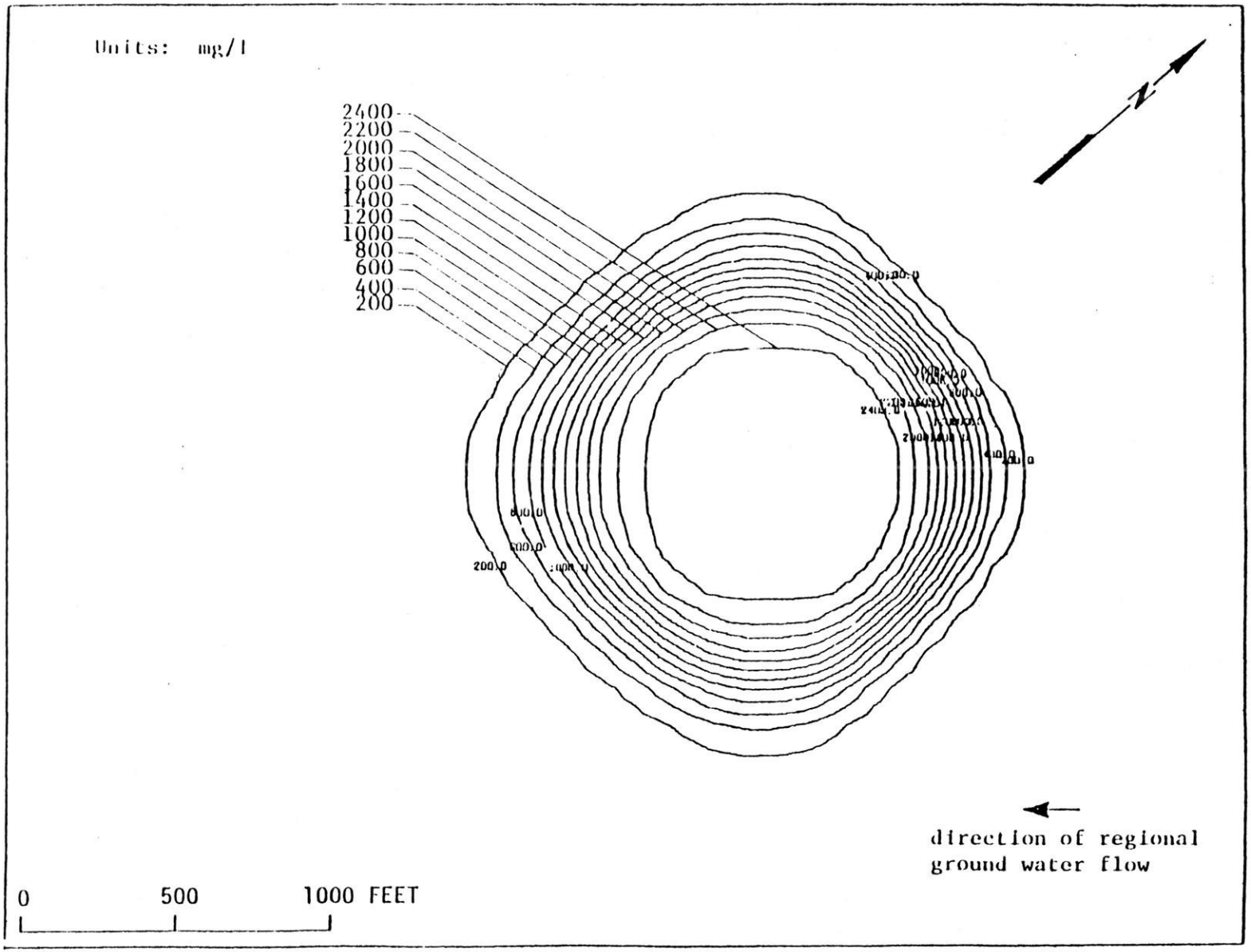

FIGURE:4.16 Sulfate concentration distribution after 15 years of pond operation.

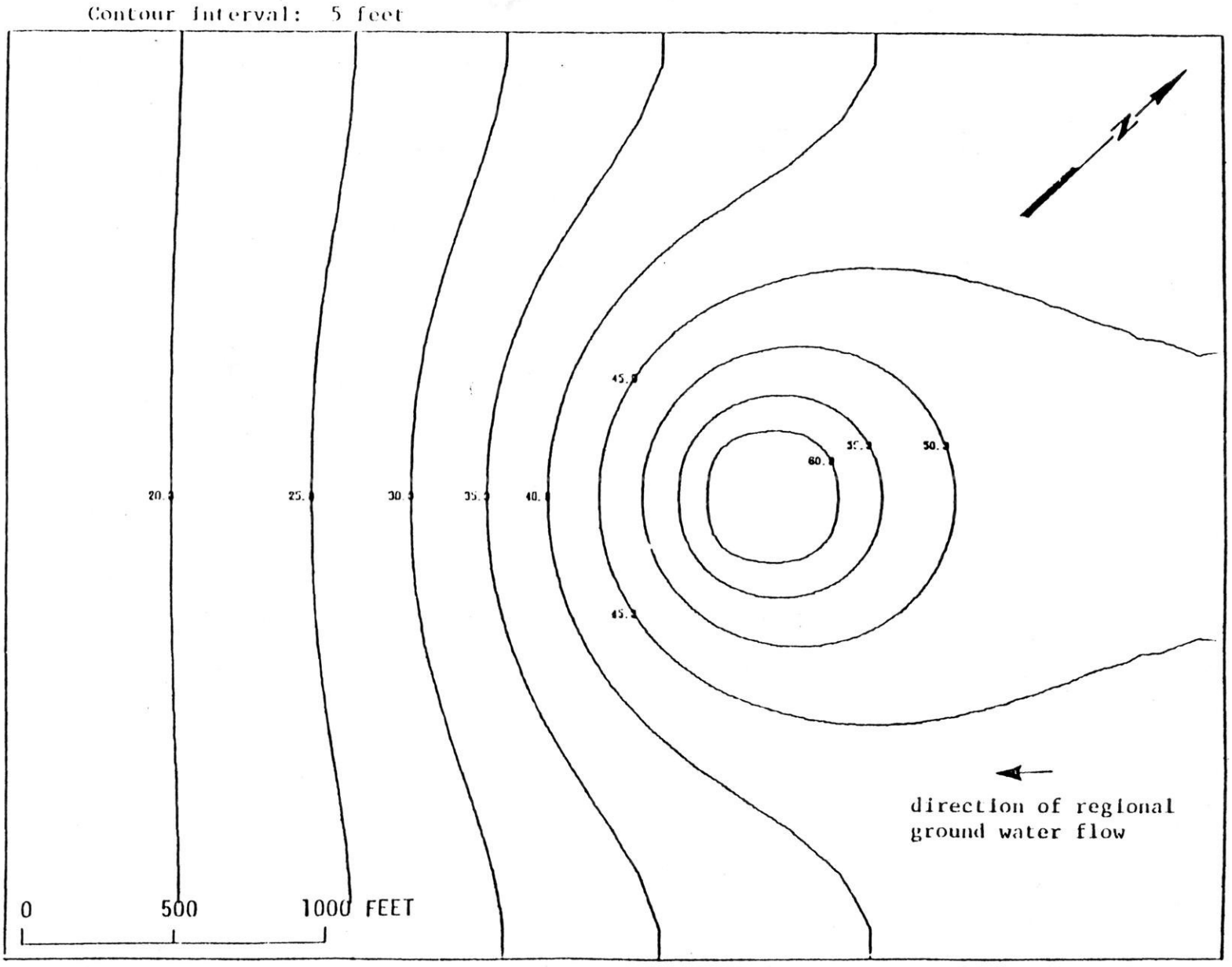

FIGURE: 4.15 Head contour after 15 years of pond operation

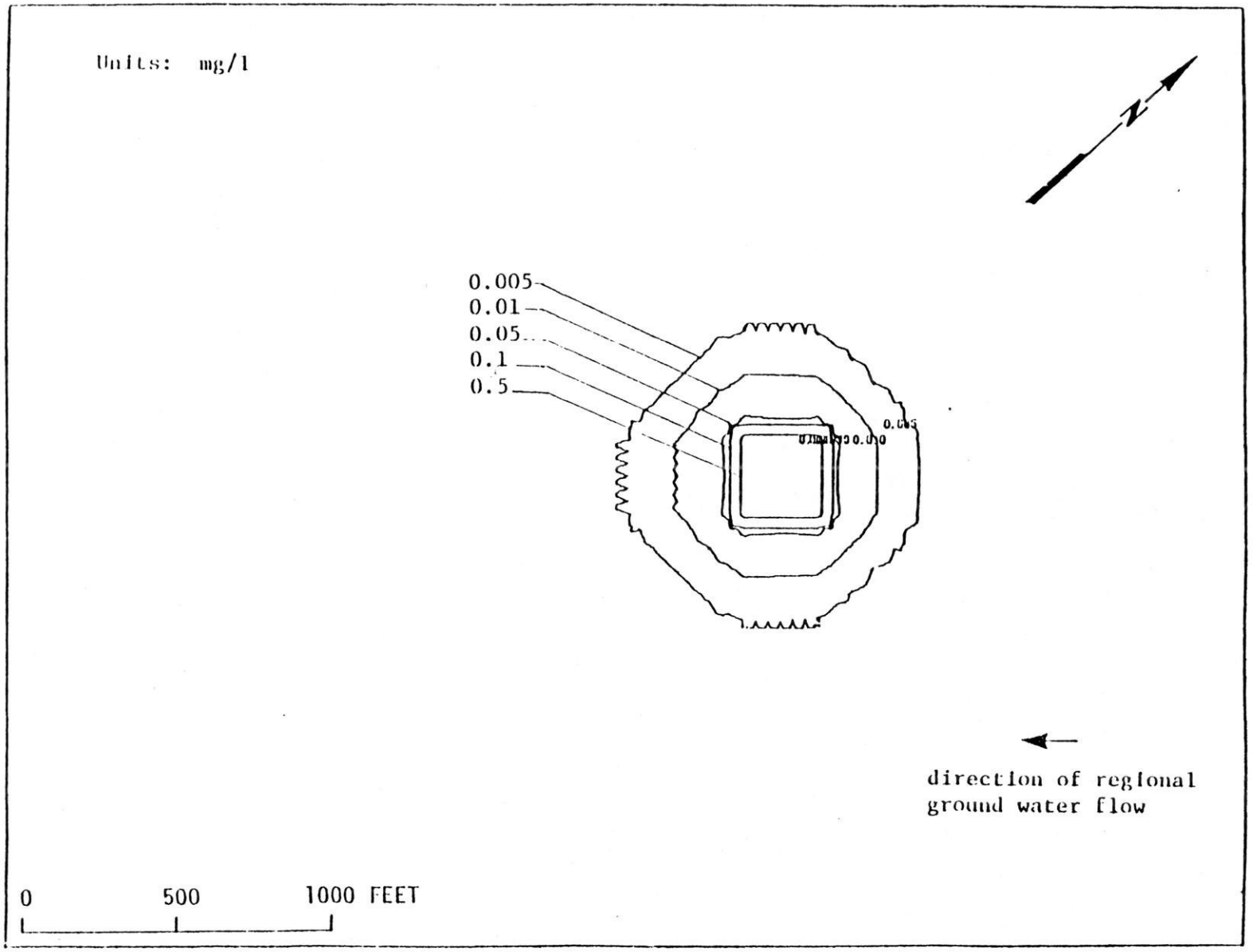

FIGURE: 4.17 Selenium concentration distribution after 15 years of pond operation.

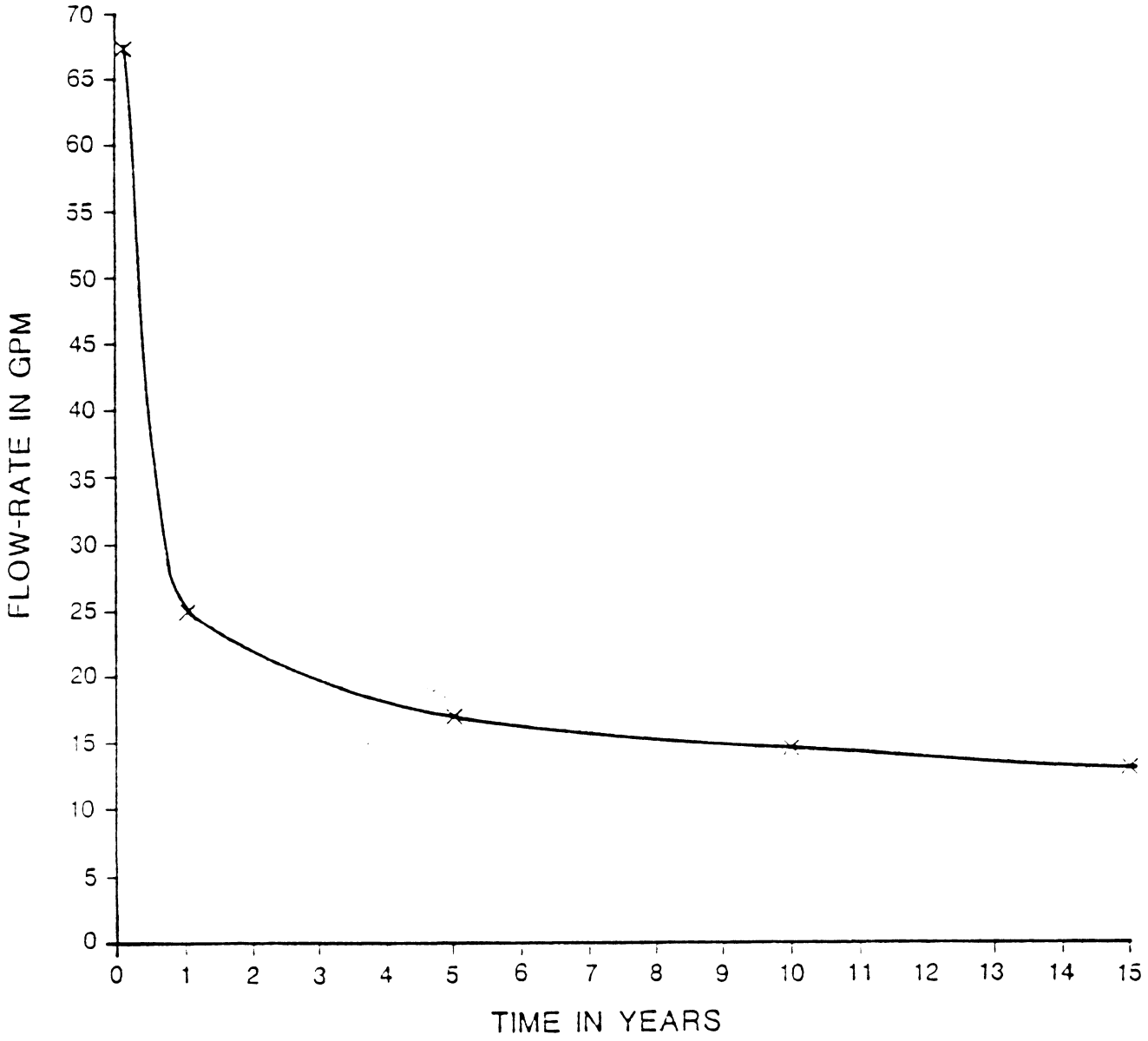

FIGURE 4.18

PREDICTED RATES OF SEEPAGE FROM THE POND AS A FUNCTION OF TIME

TABLE 1.1

DEPTH TO WATER TABLE FROM GROUND SURFACE

No.	Boring Identification	Ground Surface Elevation Z_S (ft)	Water Table Elevation Z_W (ft)	Depth to Water Table L (ft)	(cm)
1	DMI-1	1636.74	1588.77	47.97	
2	DMI-2	1629.43	1587.93	41.50	
3	DMI-3	-	-	-	
4	DMI-4	-	-	-	
5	DMI-5	-	-	-	
6	DMI-7	-	-	-	
7	DMI-8	-	-	-	
8	DMI-9	-	-	-	
9	DMI-11	-	-	-	
10	DMA-19	1597.24	1589.00	8.24	
11	DMS-1	1661.65	1591.93	69.72	
12	WW-1	-	-	-	
13	TW-1	1601.19	1590.60	10.59	
14	DW-2	1600.74	1591.07	9.67	
			Mean Values	31.28	953.4

TABLE 1.2

CALCULATED VALUES OF POROSITY AND
INITIAL DEGREE OF SATURATION

No.	Boring Sample	Depth of Sample Below Ground (ft)	n	$S_{r,i}$
1	TP-1	6.083	0.272	0.571
2	TP-2	6.083	0.374	0.285
3	TP-3	6.000	0.315	0.375
4	TP-4	6.000	0.3055	0.485

TABLE 1.3

CHARACTERISTIC PARAMETERS DESCRIBING THE RELATIONSHIP OF K_r AND S_r TO ψ

Parameter	Value	Units
θ_r	0.031	dimensionless
θ_s	0.45	dimensionless
a_{0k}	0.066	cm^{-1}
a_{1k}	5.0	dimensionless
a_{2k}	1.0	dimensionless
a_{0s}	0.017	cm^{-1}
a_{1s}	2.5	dimensionless
a_{2s}	1.0	dimensionless

TABLE 1.4

SUMMARY OF HYDRODYNAMIC ANALYSES

Test Case No.	Problem Parameters				Predicted Results				
	L (cm)	n	K_z (cm/sec)	Q (gpm)	T (days)				
1	960.	.31	3×10^{-3}	190.5	490	Fig. 2.1	Fig. 2.2	Fig. 2.3	Fig. 2.4
2	960.	.27	5×10^{-3}	190.5	445	Fig. 2.5	Fig. 2.6	Fig. 2.7	Fig. 2.8
3	960.	.375	1×10^{-3}	67.3	1780	Fig. 2.9	Fig. 2.10	Fig. 2.11	Fig. 2.12
4	960.	.27	5×10^{-3}	190.5	590	Fig. 2.13	Fig. 2.14	Fig. 2.15	Fig. 2.16

TABLE 3.1

Property Values, Associated with the Hydrodynamic Calculations, Employed in the Study

Parameter	Value
Pond Area	275 x 275 feet
Pond Depth	5 feet
Pond operating period	15 years
Vertical permeability of soil	2×10^{-4} cm/sec.
Initial degree of saturation in the unsaturated zone beneath the pond	57.1%
Thickness of initially unsaturated zone beneath the pond	30 feet
Porosity of the soil	0.25
Horizontal permeability of the soil	2×10^{-4} cm/sec.
Dry density of the soil	110 lb/ft^3
Regional ground water gradient (NE-SW)	0.0075 ft/ft

TABLE 3.2

Property Values, Associated with Chemical Species Transport, Employed in the Study

Background chemical species concentrations: -		
SO_4^{-2}		8.8 mg/l
Se		0.0005 mg/l
Assumed concentrations within the pond: -		
SO_4^{-2}		2480 mg/l
Se		0.65 mg/l
Adsorption coefficients, as employed in the Freundlich isotherm: $C_s = K_d C^m$: -		
Specie	K_d	m
SO_4^{-2}	0.0	1.00 (calcareous soil)
	0.0015	0.728 (non-calcareous soil)
Se	3467	3.01 (calcareous soil)
	0.0195	0.586 (non-calcareous soil)

TABLE 4.1

Time for Pond Concentration and Wetting Fronts to Reach the Water-table after Flooding of the Pond

	Arrival Time
Wetting Front	17 days
Sulfate Front	35 days
Selenium Front	40 days

REFERENCES

Bouwer, H. (1964)
"Unsaturated flow in ground-water hydraulics"
Journal of the Hydraulics Div., Proc. ASCE, HY5, pp. 121-144.

Dames & Moore (1980)
Groundwater hydrology portion of Chapter 2 of the Crandon Project Draft Environmental Impact Report, prepared for Exxon/Crandon.

Gillham, R.W., A. Klute and D.F. Heermann (1976)
"Hydraulic properties of a porous medium: measurement and empirical representation"
Soil Sci. Soc. Amer. Journal, 40, No. 2, pp. 203-207.

Van Genuchten, M. Th., G.F. Pinder, and W.P. Saukin (1976)
"Use of simulation for characterizing transport in soils adjacent to land disposal sites"
A. Rep. Proj. R-803827, Water Resources Prog., Princeton Univ., 89 pp.

APPENDIX A

Mathematical model for the prediction of flow distribution and, if required, chemical-species transport in unsaturated porous media.

1. INTRODUCTION

In this Appendix, a description is provided of a mathematical technique for the analysis of transient flow, and when appropriate, the transport of heat and reacting chemical species in unsaturated/saturated porous media. The description is prefaced by a brief outline of current literature on the subject, the outline being intended to place the technique described herein in perspective. Whilst the technique itself is applicable to three-dimensional problems, it is often important to focus attention on vertical components of flow. It is only for this reason the present description directs attention to a vertical one-dimensional formulation, thereby serving to highlight the salient features. In what follows, this information as embodied in a computer program which, together with the mathematical technique, is collectively referred to as the mathematical model.

2. BRIEF HISTORICAL PERSPECTIVE

The mathematical modelling of flow distributions in unsaturated porous media have been reported quite extensively in the literature covering a number of technical disciplines. The appropriate equations have been derived from fundamental principles and reviewed by Bresler et al (1971). Early work in one-dimensional systems was presented by Bresler and Hanks (1969) and Warrick et al (1971). These authors were interested in the coupled processes of flow and simultaneous transfer of inert chemical-species. However, while the former employed a simple numerical procedure, the latter present an interesting analytical solution to the equations. Freeze (1969) performed a complete review of one-dimensional models suitable for the analysis of infiltration-induced unsaturated flows. Freeze (1971) also reported a three-dimensional model based upon numerical solutions; he applied it along with certain simplifying assumptions to transient flow in a basin. Such assumptions were carefully evaluated by Gambolati (1973) who also verified their range of validity for vertical one-dimensional flows. Other analytical and algebraic models of one-dimensional vertical flows have also been applied. One such model has been deployed by Mc Worther and Nelson (1979) to predict unsaturated flows beneath uranium tailings impoundments.

In recent years more comprehensive hydrodynamic models incorporating increasingly sophisticated physical hypotheses have been reported. A well-known two-dimensional example, based upon finite-element solutions to the unsaturated flow equation, is the work by Duguid and Reeves (1976). A three-dimensional model of flow incorporating a one-dimensional consolidation theory has been presented by Narasimhan and Witherspoon (1977b). It is this model which was extended by Sharma and Hamilton (1978) as part of a continuing Research and Development program. The model is based upon an integrated finite-difference method of solution and was found to be quite effective in predicting a number of flow problems. However, a shortcoming of this model and its extensions is that it is computationally uneconomical to employ for most practical prob-

lems. Quite recently, a similar technique based on finite-element solutions, which incorporates a three-dimensional stress-field calculation, has been reported (Safai and Pinder, 1979). These and other such models have been reviewed and carefully classified by Narasimhan and Witherspoon (1977a).

It must be recognized that the more complex the mathematical models of unsaturated-media hydrodynamics, the more stringent is the requirement for reliable and accurate data on material properties to be supplied to the models. The conduct of experiments designed to obtain such data have been described by Childs and Collis-George (1950), as well as Fatt and Dykstra (1951). A more recent evaluation has been provided by Green and Corey (1971). Data, obtained for several soil samples under a wide range of conditions, have been presented by van Genuchten et al. (1977) (see Figure 1 for an example); Liakopoulos (1965) (see Figure 2 for an example of hysteresis); and Warrick et al. (1971) amongst others. The collection of data from numerous sources, their careful classification based upon soil type and casting into algebraic forms has been presented by Bouwer (1964). This work has been supplemented by the compilations of Topp (1969) and Gillham et al. (1976). The latter authors were particularly concerned with the phenomenon of hysteresis, and its mathematical expression. The above data indicate that, in general, an S-shaped relationship exists between moisture content (and also hydraulic conductivity) and suction pressure in the unsaturated flow regime. Algebraic expressions of this behaviour, correlated from a number of experiments, are supplied as "physical hypotheses" to the mathematical model.

Increasing attention is being paid to the transport of inert, reactive and radioactive chemical species as a result of natural and buoyancy-generated flows in porous media (Ames and Rao, 1978). The influences of landfill and dredge disposal, as well as solid and liquid waste disposal, in contaminating groundwater have been quantitatively evaluated (Leis et al., 1978). Studies have been made of nuclear waste disposal alternatives. Most mathematical models employed to perform the evalua-

tion are based on numerical solutions, although many analytical-solution models do exist, to the so-called convective-dispersion equation. An additional term in this equation representing the adsorption/desorption characteristics of the soil matrix has been employed by several authors to examine the attenuating capabilities of the soil. The works by Rao and Davidson (1979) and Selim et al. (1979) come under this category. Rao et al. (1979) examine several ways of representing the adsorption/desorption reaction and conclude that the non-linear Freundlich equation fitted to experimental data is both mathematically convenient and practicable.

In what follows, a mathematical model which combines the advantages of the formulations presented by Narasimhan and Witherspoon (1977b) and Safai and Pinder (1979) with that of a novel and computationally-economic solution algorithm developed recently by Sharma (1979), is presented.

3. MATHEMATICAL DETAILS

The non-linear partial differential equations as well as auxiliary equations governing the flow and transport of chemical species in unsaturated porous media are listed in a form convenient for modelling. Tensorial notation is used here for brevity and the symbols are defined in the nomenclature list.

3.1 Governing Equations

The symbols used below are defined in the nomenclature list. The equations themselves have been derived in several publications.

A) Pressure Distribution:

The partial differential equation governing the simultaneous conservation of mass and momentum in porous media is often expressed as the distribution of "pressure head". In unsaturated-saturated regions within undeformable soils the general form is (see Bear, 1972):

$$\left(\frac{\partial}{\partial\psi}(\varepsilon S_r)\right)\frac{\partial\psi}{\partial t} = \frac{\partial}{\partial x_i}\left\{MK_r K_{ij}\left(\frac{\partial\psi}{\partial x_j} + R\frac{\partial z}{\partial x_j}\right)\right\} - s^{\psi} \qquad (1)$$

This equation, in tensorial form, is valid for three-dimensional systems. However, it may be reduced to two- or one-dimensional forms through appropriate assumptions.

B) Velocity Distribution:

Implicit in the above equation is the generalised definition of Darcy velocity for unsaturated flows:

$$\varepsilon U_i = MK_r K_{ij} \left(\frac{\partial \psi}{\partial x_j} + R \frac{\partial z}{\partial x_j} \right) \qquad (2)$$

C) Distribution of Chemical Species

The general form of the equation governing the concentration transport of the l^{th} chemical species of concern is expressed thus:

$$\frac{\partial}{\partial t} \{\varepsilon S_r \rho C_l\} + \frac{\partial}{\partial t} \{[1-\varepsilon]\rho_s C_{s,l}\} + \frac{\partial}{\partial x_i} \{\varepsilon \rho U_i C_l\}$$

$$= \frac{\partial}{\partial x_i} \{\varepsilon \rho D^l_{i,j} \frac{\partial C_l}{\partial x_j}\} + s^{C_l} \qquad (3)$$

D) Distribution of Thermal Energy:

The equation governing the transport of thermal energy may be expressed, in general form, thus:

$$\frac{\partial}{\partial t} \{\varepsilon S_r \rho C_v T\} + \frac{\partial}{\partial t} \{[1-\varepsilon]\rho_s C_{v,s} T_s\} + \frac{\partial}{\partial x_i} \{\varepsilon \rho U_i C_p T\}$$

$$= \frac{\partial}{\partial x_i} \{\varepsilon K^T_{i,j} \frac{\partial T}{\partial x_j}\} + s^T \qquad (4)$$

In the above form the contribution of thermal capacitance of air within the unsaturated pores of the medium has been neglected as being small by several orders of magnitude.

E) Physical and Chemical Hypotheses

The relationship between unsaturated permeability (or relative permeability) and suction pressure, as well as that between moisture content (or degree of saturation) and suction pressure, are

usually obtained empirically for each soil type. One possible set of such relationships, amongst many that exist, due to Safai and Pinder (1979) is:

$$K_r = \left[1 + [a_{0K}(-\psi)]^{a_{1K}}\right]^{-a_{2K}} \tag{5}$$

$$S_r = \frac{\theta_R}{\theta_S} + \left(1 - \frac{\theta_R}{\theta_S}\right)\left[1 + [a_{0S}(-\psi)]^{a_{1S}}\right]^{-a_{2S}} \tag{6}$$

$$(-\infty < \psi \leq 0)$$

where the a's are constants based upon best fits to experimental data.

The density ratio R dictates the dependence of the flow distribution upon buoyancy forces. Such forces vary with spatial position because of density variations due to both temperature effects and to the effects of salinity or dissolved solids. A general expression for density is consequently necessary and a first order form is employed to denote such variations in density.

$$\rho = \rho_o + \left\{\frac{\partial \rho}{\partial T}\right\}(T - T_o) + \left\{\frac{\partial \rho}{\partial C}\right\}(C - C_o) \tag{7}$$

The pressure head is defined by:

$$\psi \equiv \frac{p}{\rho_o g} \tag{8}$$

The dispersion coefficient $D^1_{i,j}$ is obtained from empirical correlations to the velocity vector, usually with reference to laboratory-scale experiments. The adsorbed/desorbed concentration of

solute in the solid matrix is usually expressed through the assumption of an equilibrium reaction as follows.

Consider the second term of equation (3). This represents the "immobilization" of chemical-species "1" on the surfaces of grains which form the solid matrix. The processes which cause such immobilization are called "sorption" reactions. Of course, true immobilization is called adsorption; release back into solution is termed desorption. The practices currently adopted to calculate this term are based on the following assumptions:

a) The sorped concentration $C_{s,1}$ is always proportional to the concentration of solute C_1 in <u>local equilibrium</u> with it.

b) The above assumption makes it possible to determine the proportionality relationship between $C_{s,1}$ and C_1 through the conduct of appropriate laboratory-scale measurements.

c) Either "batch" or "column" measurement techniques are usually adopted. The former, involving shaking of the porous-medium sample with sufficient amounts of the solution, is more representative of the equilibrium assumption than the latter.

d) Four basic forms of the relationship are generally employed; the constants of these relationships are determined by fitting curves to the experimental data obtained by the above-mentioned experiments. These forms are:

- Linear:

$$C_{s,1} = K_d C_1 \qquad (9)$$

- Freundlich:

$$C_{s,l} = K_d C_l^{\,m} \tag{10}$$

- Langmuir:

$$\frac{1}{C_{s,l}} = 1 + \frac{1}{K_d C_l} \tag{11}$$

e) Whichever is the relationship which applies in a given circumstance, the constants must take proper account of the following parameters which control the sorption reactions:

- porous-medium characteristics, i.e. density - ρ, porosity - ε and grain size - d, and
- pH of the solution carrying the solutes C_l.

This account must, of course, come from appropriate measurements.

3.2 Initial and Boundary Conditions

In order to complete the mathematical specification of a given problem, both initial and boundary conditions are required to be specified. Initial conditions, supplied over the entire domain selected for solution, must include values of:

- moisture content θ, and when appropriate
- concentration of species l, C_l.

Boundary conditions on the boundaries of the domain must be specified in respect of:

- type of flow boundary and related flow quantities,

- nature of boundary in respect of chemical species, if appropriate, and
- sources (and/or sinks) of mass on the boundaries of or within the domain.

3.3 Numerical Solution Procedure

The numerical algorithm adopted for the set of equations (1) to (3) is based upon an integrated finite-difference technique designed to solve efficiently, partial differential equations of the general form:

$$A \frac{\partial \phi}{\partial t} + \frac{\partial (B\phi)}{\partial x_1} = \frac{\partial}{\partial x_1} \left(C \frac{\partial \phi}{\partial x_1}\right) + D \qquad (12)$$

Details of the technique are provided elsewhere (Sharma, 1979). It is emphasized here however, that the technique is particularly suited to highly non-linear forms of the above equation. Specifically, coefficients A, B, C and D can be strong functions of ϕ itself, especially for two- and three-dimensional problems. Hence, the twin requirements that the technique satisfies the finite-difference form of the above equation at a grid node P, i.e.

$$\{\sum_P A - SN_P\} \phi_P = \sum_k A_k \phi_k + SO_P \qquad (13)$$

exactly and, in addition, be iterative in order to account for the dependence of the coefficients upon the dependent variable itself, are both met.

4. COMPUTER PROGRAM DETAILS

The mathematical model outlined above has been cast into a computer program written in FORTRAN IV. This program, called TARGET-1DU for Transient Analyzer of Ground water flow and Effluent Transport in one space dimension in unsaturated media, is designed for ease of application of different types of problems. It is also to achieve this objective that the main machinery of the calculation procedure is kept separate from the input/output and user-modifiable portions of the program. Further, the numerical grid is capable of accommodating arbitrarily-spaced nodes or cells, each of which may be supplied with uniquely different material properties. A typical solution to a transient problem involving 100 grid nodes and 400 time steps requires approximately 30 seconds on a CDC 6600 computer.

5. MODEL VERIFICATION

One example amongst several test cases investigated with TARGET-1DU is steady infiltration into a uniform sand column which was assumed to be uniformly unsaturated to begin with. A one-dimensional grid selected for the investigation and the boundary condition supplied to it are illustrated in Figure 3. The typical results for this case predicted with the model are illustrated in Figure 4. In this figure, the developing profiles of moisture content and hydraulic conductivity may be observed as a wetting front at a specific instant in time.

A second example investigated was that on one-dimensional transient drainage from a sand column which is initially saturated and whose top surface is subsequently maintained as impermeable. Using a grid similar to that used for the above problem, non-linear material property relationships were supplied to the model. These relationships, illustrated in Figure 5, are due to Liakopoulos (1965). The results predicted by the model are compared with experimental data (see Figure 6) from the same reference and with the results obtained with a different approach by Narasimhan and Witherspoon (1977) which included effects of stress-induced deformation.

6. REFERENCES

Ames, L.L. and D. Rai (1978): "Radionuclide interactions with soil and rock media", Battelle P.N.W.L., Rep. EPA 520/6-78-007, 280 p.

Bear, J. (1972): "Dynamics of fluids in porous media", American Elsevier Publ., New York.

Bouwer, H. (1964): "Unsaturated flow in groundwater hydraulics", J. Hyd. Div., (ASCE), 90 HY5, pp. 121-144.

Bresler, E. and R.J. Hanks (1969): "Numerical method for estimating simultaneous flow of water and salt in unsaturated soils", Proc. Soil Sci. Soc. Amer., 33, (6), pp. 827-832.

Braester, C., G. Dagan, S. Neuman and D. Zaslavsky (1971): "A survey of equations and solutions for unsaturated flow in porous media", Ann. Rep. 1, Proj. A10-SWC-77, Israel Inst. of Tech., Haifa, 176 p.

Childs, E.C. and N. Collis-George (1950): "The permeability of porous materials", Proc. Royal Soc. (Lon.), A201, pp. 392-405.

Duguid, J.O. and M. Reeves (1976): " Material transport through porous media: a Finite-Element Galerkin model", Oak Ridge Nat. Lab., Rep. ORNL-4928, 232 p.

Fatt, I. and H. Dykstra (1951): "Relative permeability studies", Amer. Inst. Min. Met. & Pet. Eng., 192, pp. 249-255.

Freeze, R.A. (1969): " The mechanisms of natural ground-water recharge and discharge 1: one-dimensional, vertical, unsteady, unsaturated flow above a recharging or discharging ground-water flow system", Water Resources Res., 5, (1), pp. 153-171.

Freeze, R.A. (1971): "Three-dimensional transient saturated/unsaturated flow in a ground water basin", Water Resources Res., 7, (2), pp. 347-356.

Gambolati, A. (1973): "Equation for vertical one-dimensional flow of ground water - 2. Range of validity of diffusion equation", Water Resources Res., 9, (6) pp. 1385-1396.

Gillham, R.W., A. Klute and D.F. Heermann (1976): "Hydraulic properties of a porous medium: measurements and empirical representation", Soil Sci. Soc. Amer., 40, 2, pp. 203-207.

Green, R.E. and J.C. Corey (1971): "Calculation of hydraulic conductivity: a further evaluation of predictive methods", Proc. Soil Sci. Soc. Amer., 35, pp. 3-8.

Leis, W.M., W.F. Beers, J.M. Davidson, G.D. Knowles (1978): "Migration of PCB's by ground water transport - a case study of twelve landfills and dredge disposal sites in the upper Hudson Valley, New York", Proc. of Ann. Conf. on App. Res. & Pract. on Municipal and Industrial Waste, 10 p.

Liakopoulos, A.C. (1965): "Transient flow through unsaturated porous media", Dr. Eng. Thesis, Univ. of Calif., Berkeley, Calif., 186 p.

Mc Whorter, D.M. and J.D. Nelson (1979): "Seepage in the partially saturated zone beneath tailings impoundments", J. Geotech. Eng. Div. of ASCE, 105, (11), pp. 1317-1334.

Narasimhan, T.N. and P.A. Witherspoon (1977a): "Recent developments in modelling ground water systems", Lawrence Berkeley Lab., Univ. of Calif. Rep. LBL-5209, 35 p.

Narasimhan, T.N. and P.A. Witherspoon (1977b): "Numerical model for saturated/unsaturated flow in deformable porous media", Water Resources Res., 13, pp. 657-673.

Rao, P.S.C., and J.M. Davidson (1979): " Adsorption and movement of selected pesticides at high concentrations in soils", Water Res., 13, pp. 375-380.

Rao, P.S.C., J.M. Davidson, R.E. Jessup and H.M. Selim (1979): "Evaluation of conceptual models for describing non-equilibrium adsorption/desorption of pesticides during steady-flow in soils", Soil Sci. Soc. Amer. J., 43, (1), pp. 22-28.

Safai, N.M. and C.F. Pinder (1979): "Vertical and horizontal land deformation in a desaturating porous medium", Adv. in Water Resources, 2 (1), pp. 19-25.

Selim, H.M., J.M. Davidson and P.S.C. Rao (1977): "Transport of reactive solutes through multilayered soils", Soil Sci. Soc. Amer. J., 41, (1), pp. 3-9.

Sharma, D. (1979): "A comprehensive mathematical model capable of predicting flow, heat transfer as well as chemical-species transport in saturated porous media" (unpublished report).

Sharma, D. and J.L. Hamilton (1978): "A comprehensive mathematical model for the prediction of saturated/unsaturated flow in porous media", (unpublished report).

Topp, G.C. (1969): "Soil-water hysteresis measured in a sandy loam and compared with the hysteretic domain model", Soil Sci. Soc. Amer., 33, p. 645-651.

Van Genuchten, M. Th., G.P. Pinder and W.P. Sankin (1977): "Modelling of leachate and soil interactions in an aquifer", Proc. 3rd Ann. Municipal Solid Waste Res. Sym., Paper EPA-600/9-77-026, pp. 95-103.

Warrick, A.W., J.W. Biggar and D.R. Nielsen (1971): "Simultaneous solute and water transfer for an unsaturated soil", Water Resources Res., 7, (5) pp. 1216-1225.

7. NOMENCLATURE

A, B, C, D	Generalized coefficients in equation
C	Concentration of dissolved solids ($kg \cdot m^{-3}$)
C_o	Reference concentration ($kg \cdot m^{3}$)
C_v, C_p	Specific heats of water ($J \cdot kg^{-1} \cdot °C^{-1}$)
$C_{v,s}$	Constant-volume specific heat of soil ($J \cdot kg^{-1} \cdot °C^{-1}$)
a_{0K}, a_{1K}, a_{2K}...	Constants in correlations
C_l	Concentration of l^{th} chemical species ($kg \cdot m^{-3}$)
$C_{s,l}$	Immobilized concentration of l^{th} chemical species ($kg \cdot m^{-3}$)
$D^l_{i,j}$	Dispersion coefficient of species l ($m^2 \cdot s^{-1}$)
K_d	Distribution coefficient for the species l
K_{ij}	Tensorial form of saturated hydraulic conductivity ($m \cdot s^{-1}$)
K^T_{ij}	Effective thermal diffusivity of water ($J \cdot m^{-1} \cdot s^{-1}$)
K_r	Relative hydraulic conductivity of unsaturated media
m	Exponent in the chemical kinetic term of equation (3)
M	Viscosity ratio (μ/μ_o)
P	Static pressure ($N \cdot m^{-2}$)
R	Density ratio (ρ/ρ_o)
s^ϕ	Source (and/or sink) term for variable ϕ
S_r	Degree of saturation
SO, SN	Components of linearized source term in finite-difference form
t	Time (s)
T	Temperature (°C)
T_s	Temperature of soil (°C)
U_i	Velocity components in direction i ($m \cdot s^{-1}$)
x_i	Coordinate direction in direction i (m)
ψ	Static pressure expressed in head of water (m)
ϕ_i	General dependent variable at location i
ε	Porosity

θ	Volumetric moisture content ($m^3 \cdot m^{-3}$)
θ_R	Residual value of θ ($m^3 \cdot m^{-3}$)
θ_S	Saturation value of θ ($m^3 \cdot m^{-3}$)
ρ	Density of water ($kg \cdot m^{-3}$)
ρ_o	Reference density of water ($kg \cdot m^{-3}$)
ρ_S	Dry density of soil matrix ($kg \cdot m^{-3}$)
μ	Viscosity of water ($kg \cdot m^{-1} \cdot s^{-1}$)
μ_o	Reference viscosity of water ($kg \cdot m^{-1} \cdot s^{-1}$)

8. FIGURES

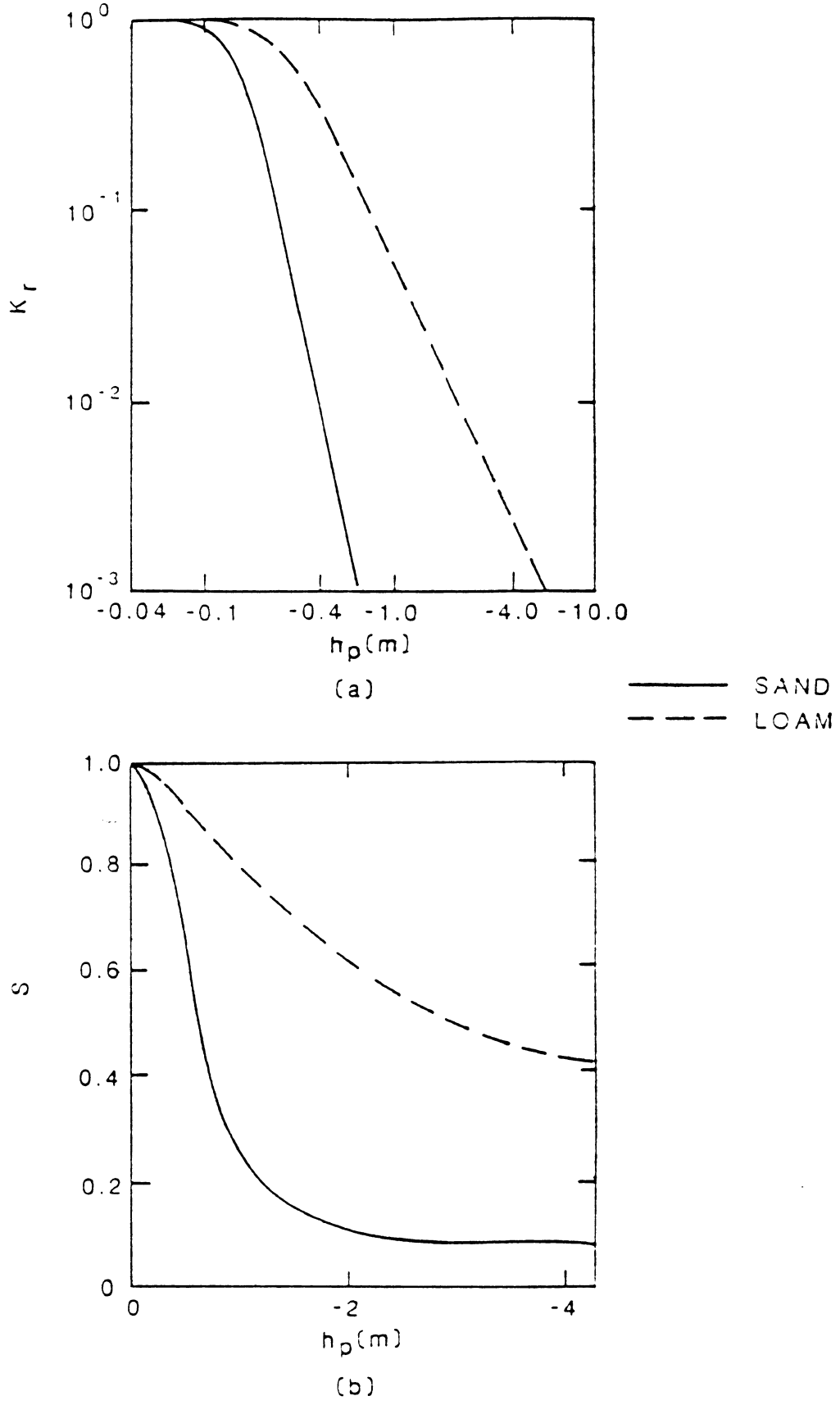

FIGURE 1. INFLUENCE OF SUCTION PRESSURE HEAD ON (a) HYDRAULIC CONDUCTIVITY AND (b) DEGREE OF SATURATION, (VAN GENUCHTEN et al., 1977)

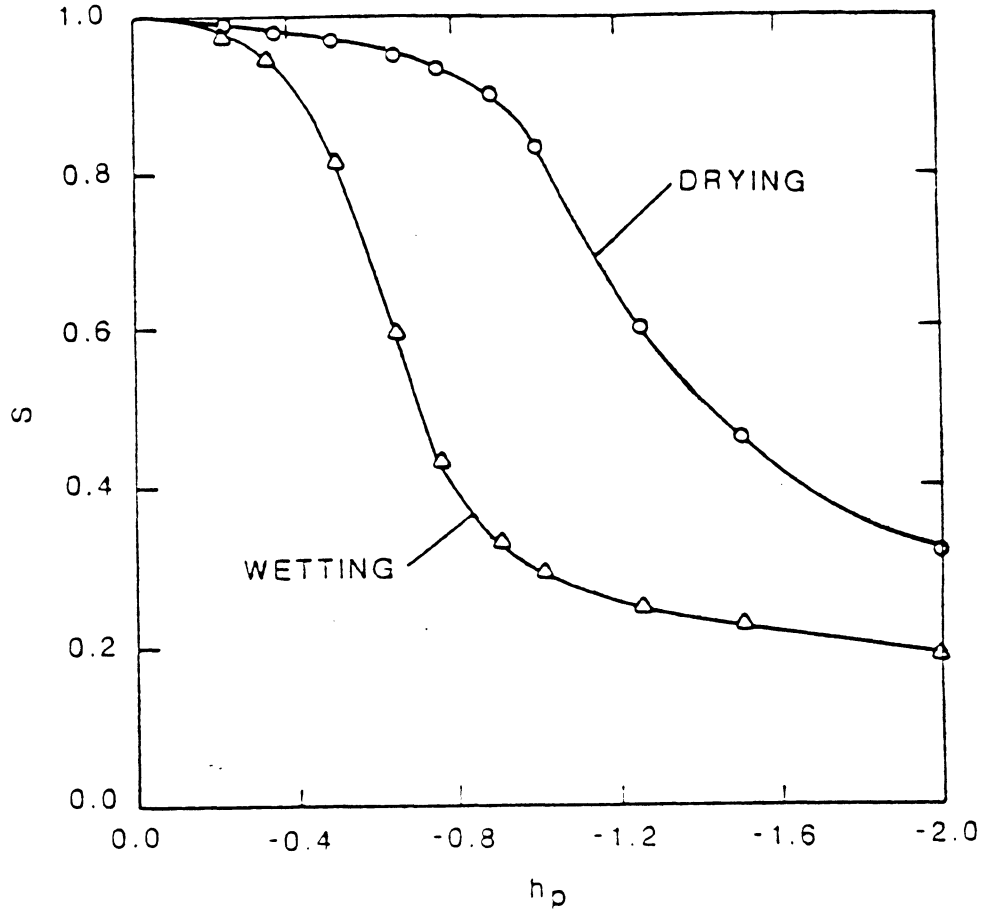

FIGURE 2. HYSTERESIS BETWEEN DEGREE OF SATURATION AND PRESSURE HEAD FOR SANDY SOILS, (LIAKOPOULOS, 1965)

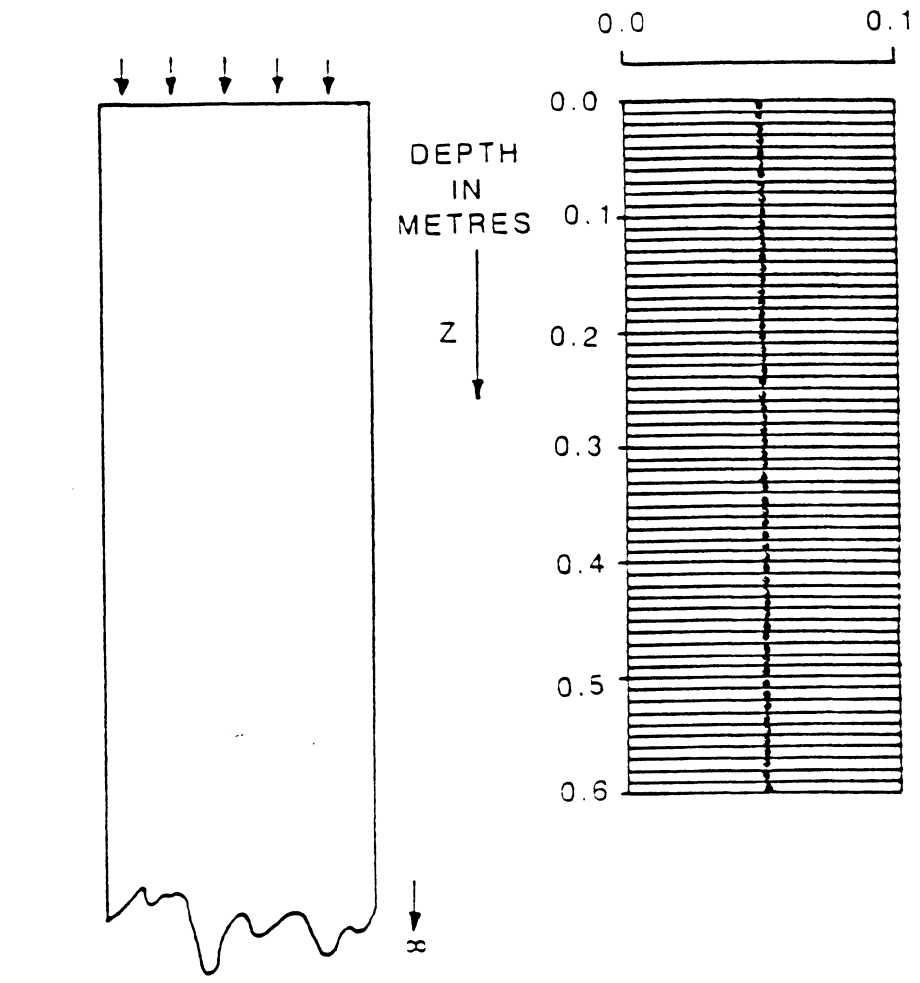

FIGURE 3. BOUNDARY CONDITIONS AND GRID FOR CONSTANT INFILTRATION TEST PROBLEM

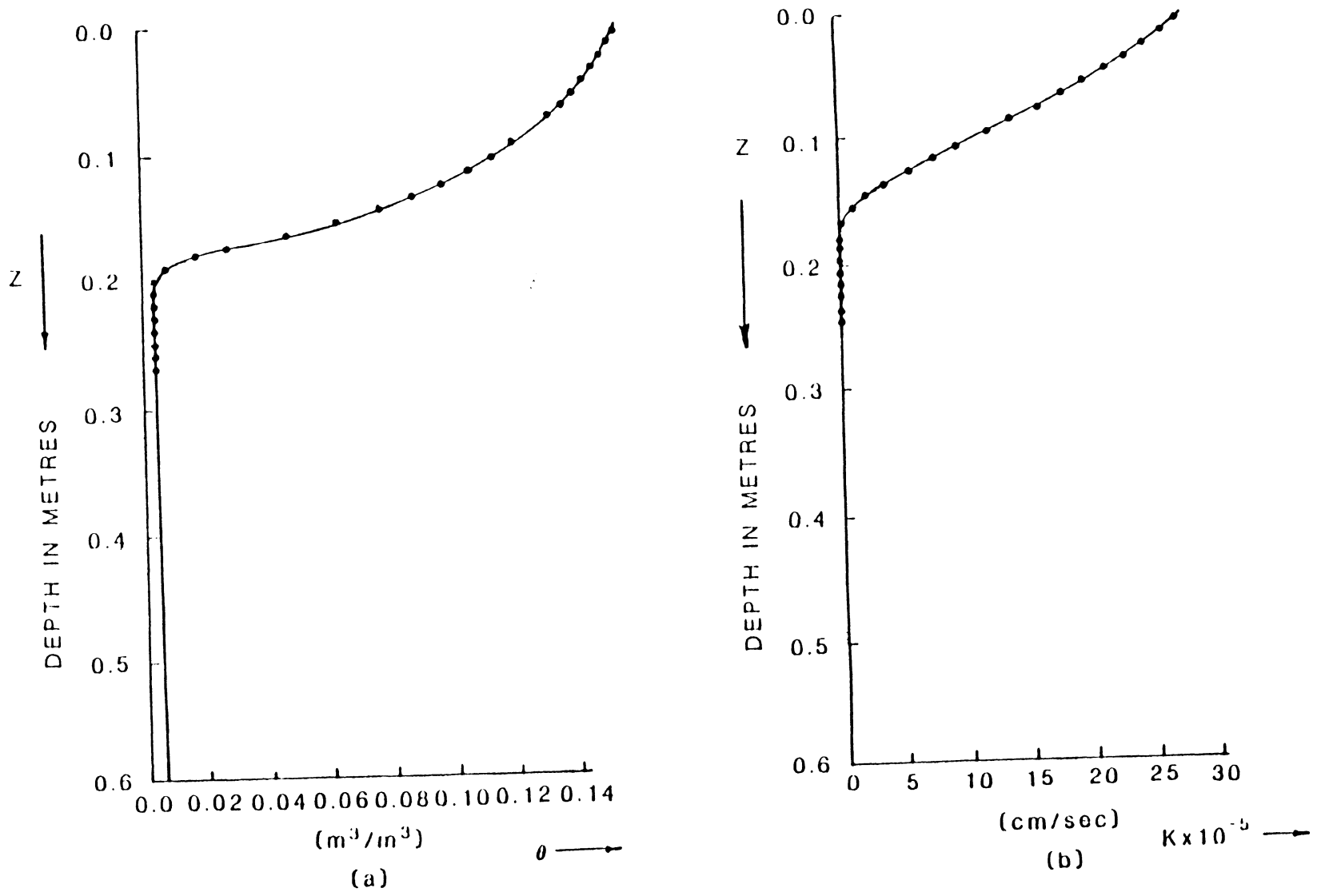

FIGURE 4. PREDICTED VARIATION OF (a) MOISTURE CONTENT, AND (b) HYDRAULIC CONDUCTIVITY WITH DEPTH AT t= 5625 SEC

DAMES & MOORE

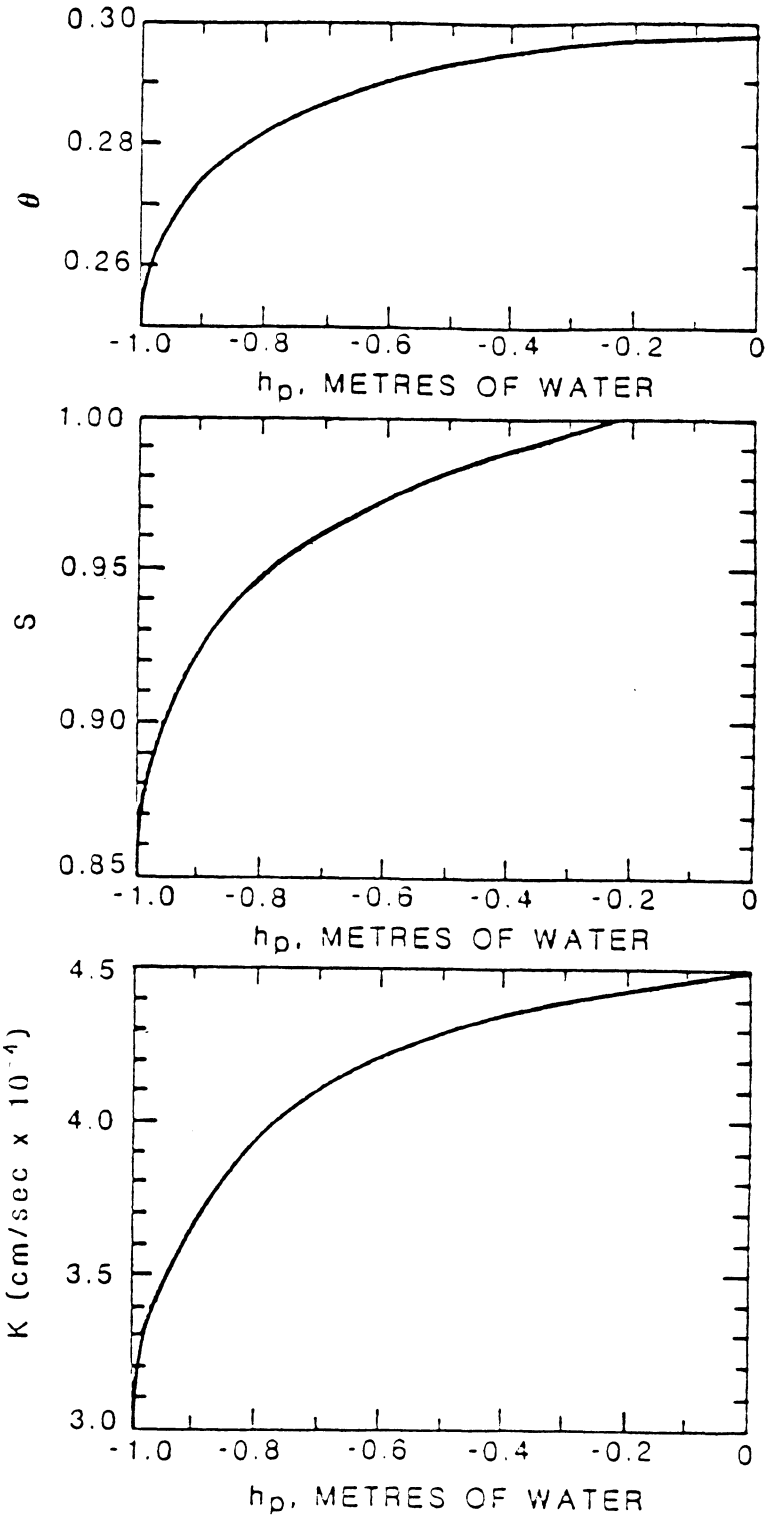

FIGURE 5. MATERIAL PROPERTIES OF SAND SUPPLIED TO MODEL (LIAKOPOULOS, 1965)

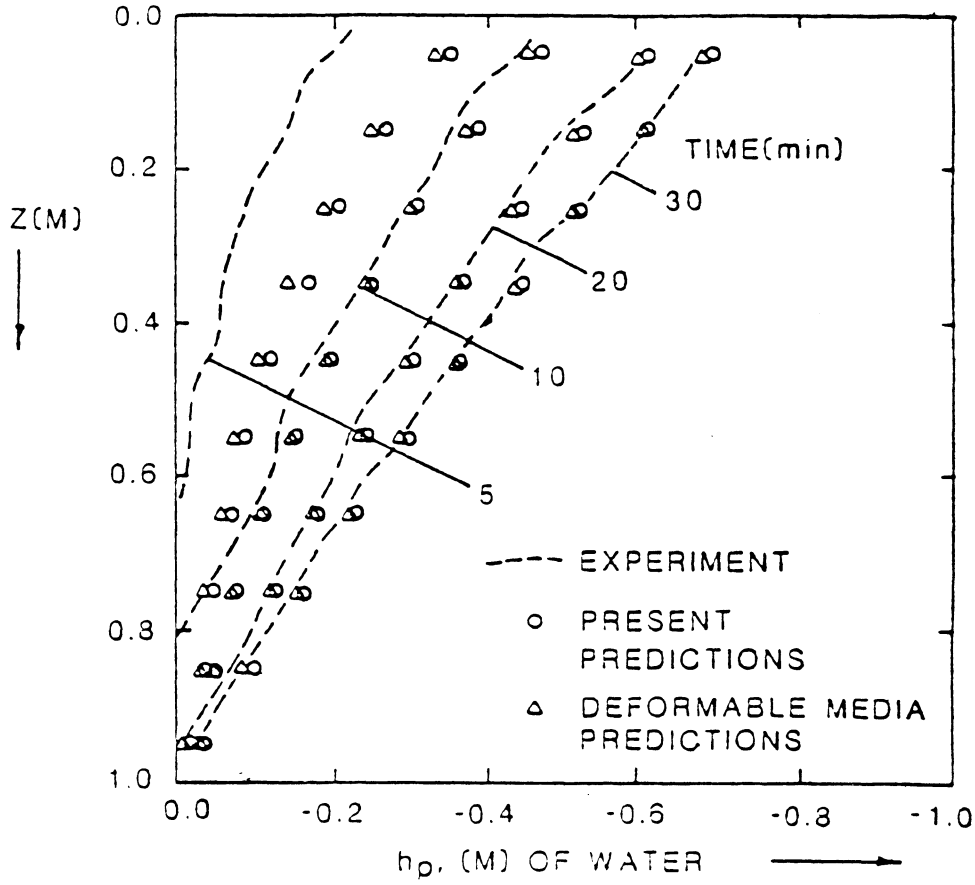

FIGURE 6. COMPARISON OF PREDICTED PORE PRESSURES IN A ONE-DIMENSIONAL DRAINING SAND COLUMN WITH EXPERIMENTAL DATA

APPENDIX B

A comprehensive mathematical model suitable for the prediction of coupled hydrodynamics, heat transfer and chemical-species transport in saturated porous media.

1. INTRODUCTION

The purpose of this appendix is to present a description of a comprehensive mathematical model for the prediction of momentum, heat and mass transfer in porous media. This presentation is prefaced by a review of recently published literature concerning prediction procedures for flows in porous media coupled with heat and/or mass transfers. Underground porous media are the primary subjects of concern here, and the review is intended to provide an overview of the state-of-the-art. For this reason, it is necessarily brief.

The prediction procedures considered here include both analytical solution techniques for simplified governing equations as well as mathematical models based upon numerical solution techniques for sets of coupled and uncoupled governing differential equations. Attempts have not been made to prepare here a detailed classification of these procedures based upon rigorous mathematical criteria. The intention rather is to present a coherent summary which highlights the salient features and recent advances.

It is recognized that in preparing this review complete attention may not have been paid to the degree of validation, in respect of reliable field and laboratory data, that each available procedure may have been subjected to. The degree of sophistication and flexibility built into these procedures which permit them to accept such data in some convenient form, will be considered sufficient for purposes of this review. This is largely due to the paucity of data, in sufficient quantity and of suitable quality, readily available for purposes of validation.

In the following subsections, reviews are separately presented for hydrodynamic aspects, aspects of chemical-species transport, and heat-transfer aspects respectively. This loose sub-division is maintained purely for reasons of convenience in presentation.

1.1 Hydrodynamics

Analytical techniques for solving simplified equations of groundwater mass and momentum balance have been employed now for a number of years. These techniques involve basic assumptions about the geometric configuration of the flow domain and the uniformity of material properties. The employment of these techniques usually results in closed-form expressions for hydraulic head as a function of space and time. The velocity fields are then extracted by the appropriate use of Darcy's law, which has been incorporated into the mass balance equation.

The deployment of such analytical techniques for the flow distribution in multiple inter-connected aquifers has been reported by Bredehoeft and Pinder (1970). A more recent and elegant treatment of so-called leakage flow between aquifers is presented by Dever and Cleary (1979). The principal assumption involved in the above procedures is that the flow field in each aquifer is entirely saturated and two-dimensional. The analysis of the more difficult problem of unsaturated flows under similar conditions has received relatively little quantitative attention. Braester et al. (1971) have prepared a comprehensive survey of governing equations for unsaturated flows. Gambolati (1973) has presented a discussion of vertical unsaturated flow analyses. It may be concluded, however, that versatile analytical procedures for saturated/unsaturated flow predictions do not, in general, exist. A simple one-dimensional semi-empirical procedure for predicting purely unsaturated flows has, however, recently been reported by Mc Whorter and Nelson (1979) who have applied it to the prediction of seepage beneath uranium tailings ponds.

Recent years have seen the proliferation of mathematical models based upon numerical schemes for solving the non-linear form of the mass-conservation equation. Narasimhan and Witherspoon (1977) present a critical review of much of the current literature on the subject and indicate that both finite-difference and finite-element techniques have been employed, each with varying degrees of success. The premier ones of

the former variety are those developed by Bredehoeft and Pinder (1970), Prickett and Lonnquist (1971), Cooley (1974), Trescott et al. (1976), and Sharma (1979).

Of the latter variety, the works by Narasimhan et al. (1976), Neuman (1973) and Pinder (1973) represent the principal ones. Trescott and Larson (1977), in a series of numerical experiments, compare the efficacy of iterative methods used to solve sets of algebraic equations resulting from arbitrary forms of numerical discretization.

Numerical procedures particularly suited to the prediction of saturated/unsaturated flows have also been developed (see for example Freeze, 1971; Narasimhan et al. (1977); Sharma and Hamilton (1978); etc.). The numerical formulation of leakage interactions between elements of a multiple aquifer system are extensively discussed by Frind (1979). The numerical simulation of individual wells of arbitrary size as well as the interactions amongst them have been reported by Prickett and Lonnquist (1971) and Akbar et al. (1974).

An assessment of these and other similar procedures, in formulation and especially in implementation, has been prepared recently by Weston (1978). In agreement with this assessment, it is argued here that numerical procedures, of sufficient degrees of comprehensiveness are presently available for application to the range of problems currently encountered. The major areas of weakness in such applications are: the prediction of flows in porous media with superposed fracture distributions; and, the supply of adequate amounts of reliable data to calibrate the procedures. The state-of-the-prediction art for such flows has been thoroughly reviewed recently by Gringarten (1979).

1.2 Mass Transfer

The use of the term mass transfer here is intended to signify the transport of inert and/or reacting chemical species within porous media by the complex interaction of several physical and chemical mechanisms. The set of such mechanisms, loosely termed as sorption in the literature, considered here as a basis for review is:

- convection
- diffusion and dispersion
- buffering of pH
- chemical precipitation by reactions with the solid matrix as well as the interstitial water
- hydrolysis and precipitation
- oxidation-reduction reactions
- radioactive decay
- volatilization
- mechanical filtration
- biological degradation
- cation-exchange reactions

It must be emphasized that specialized knowledge of the in-situ effects of individual mechanisms are understood only to a limited extent. The set of sophisticated measurements necessary to quantify these influences for each geological medium and chemical specie are currently being made in a variety of contexts. It is thus reasonable to suppose that the data obtained from these measurements will be available within a few years for purposes of refining the available mathematical models.

Analytical solutions to the convective dispersion equation have been developed by a number of authors, each of whom has been interested in specific geometric configurations and specific chemical species. The deployment of these solutions has been governed to a large extent by the requirements of the technical discipline within which each problem has

been tackled. For instance, a one-dimensional solution including adsorption effects has been developed, on the one hand, by Gupta and Greenkorn (1973) as a tool in soil chemistry. The work by Aikens et al. (1979), on the other hand, presents a variety of useful analytical solutions which take radioactive decay into account. Such solutions are indeed simple to use, and provide order-of-magnitude results in respect of concentration distributions with a modicum of effort. However, as geometries, material properties or the reactive mechanisms themselves become more complex, it is more convenient to employ mathematical models based upon numerical solution techniques.

One-dimensional models of this type abound in the literature. An interesting work by Selim et al. (1977) is concerned with finite-difference simulations of reactive solute transport through multilayered soils. Davidson et al. (1978) report the recent extension of this work to the finite-difference treatment of coupled adsorption, convective dispersion as well as biological degradation. This work represents an excellent study of the effects of pesticides in soils. The recent publication by Konikow and Bredehoeft (1978) describes a two-part finite-difference procedure for solving the coupled flow and chemical species transport equations. A comprehensive, coupled procedure employing a sophisticated hybrid differencing scheme, has been developed by Sharma (1979). These procedures are typical of several available schemes, of varying degrees of computational economy, being currently reported. To be entirely valid, each such procedure must be supplied with reliable physical and chemical data, appropriate to a given application.

In like fashion, finite-element based numerical methods have been developed by researchers for predicting chemical-species transport in porous media. Rubin and James (1973) present one such method which uses the Galerkin approach. Duguid and Reeves (1976) document another similar method which has had numerous practical applications. Gray and Pinder (1976) discuss the efficacy of this and other finite-element approaches, and in addition compare their relative accuracies. The application of

finite-element approach by Pinder (1973) to groundwater contamination in Long Island is a meticulously-documented study augmented by field measurements. The application of finite-element methods to other types of problems involving transport of chemical species has also been achieved. A good example of such an application by Kealy et al. (1974) involves the analysis of seepage from tailings ponds. It is in this connection that the work by Duguid and Reeves (1976) is well known. Weston (1978) presents a comprehensive review of currently available models of the above types and, based upon their degree of validation and use, commends some for routine application. In short, a wide range of models covering a range of applicability is presently available for use in predicting the transport of reacting chemical species. The data requirements for these models are not always met to the same level of quality.

1.3 Heat Transfer

The analysis of heat transfer coupled with fluid flow in porous media, has also been conducted using both analytical and numerical techniques. The analytical solutions, depending on specific boundary conditions, which are implicitly incorporated into them, have much in common with those for transport of inert chemical species. However, the range of application of both analytical and numerical solutions for heat transfer is limited when compared with transport of chemical species. The limitation is primarily due to the recent nature of public interest in energy application in underground media.

The work by Harlan (1973) on the prediction of freezing in soils is an excellent early example of the use of a numerical procedure for the analysis of freezing fronts in porous media. Likewise, Holst and Aziz (1972) as well as Rubin and Roth (1979) examine aspects of thermally-induced convection in porous media and the stability of such flows. The former authors present a detailed investigation of three dimensional flows. Special attention has been paid by Runchal et al. (1978) to the problem of heat-transfer effects, resulting from the disposal of

high-level radioactive waste, upon groundwater motion. They treated this phenomenon as essentially decoupled. All such procedures depend, of course, on the supply of adequate field data, of sufficient quantities and of sufficient quality for purposes of input and validation. Such data, in respect of heat transfer, is extremely sparse, and hence most heat transfer models must be considered to be in a state of development. A recent example of field measurements of temperature effects in porous-media flows is that by Molz et al. (1978). These measurements were specifically made in connection with thermal energy storage in aquifers. The problems involved in such storage have been discussed by Werner and Kley (1977). Theoretical studies of this problem, using both finite-difference and finite-element methods have been reported. Amongst the former is the work by INTERCOMP (1976); examples of the latter are: Mercer et al. (1975); and, Papadopulos and Larson (1978).

2. MATHEMATICAL FOUNDATIONS

2.1 Preamble

In what follows, a mathematical description is provided of a general version of the computational procedure embodied in a computer program collectively termed "the model". Two-dimensional versions of the model have been successfully employed in a variety of engineering applications. A simple three-dimensional version of the model has also been developed, tested and applied recently by Sharma (1979), and Hamilton and Sharma (1979). The procedure is economical of computational effort, and, whilst retaining the sophistry of physical and chemical formulations, embedded in other models mentioned above, maintains mass conservation to desired levels at each time instant of interest.

In what follows, a two-dimensional version of the procedure is described. This version illustrates the significant features whilst keeping algebraic details to manageable proportions.

2.2 Governing Equations

The symbols used in the following equations are defined in the nomenclature list. Their derivation has been documented extensively elsewhere.

a) Mass Conservation

It can be shown (Bear, 1972) that the primitive form of the continuity equation can be combined with the generalised definition of Darcy velocity field to yield the partial differential equation governing flow with piezometric head as the dependent variable. Expressed in general two-dimensional form, principally for convenience of understanding, this equation is:

$$S_c \frac{\partial h}{\partial t} = \frac{\partial}{\partial x}\left\{\Gamma_x^h \frac{\partial h}{\partial x}\right\} + \frac{\partial}{\partial y}\left\{\Gamma_y^h \frac{\partial h}{\partial y}\right\} + s^h \qquad (1)$$

Specific forms of this general equation are outlined below. The coordinate directions used in these forms imply that y is used interchangeably for one horizontal or the vertical coordinate direction. For vertical-plane flows (y-positive upwards), the following definitions apply:

$$\left.\begin{aligned} \Gamma_x^h &\equiv K_{xx}M \\ \Gamma_y^h &\equiv K_{yy}M \\ s^h &\equiv -\frac{\partial}{\partial y}(K_{yy}MR) + \dot{q}''' \\ M &\equiv \frac{\mu_o}{\mu} \\ R &\equiv 1 - \frac{\rho}{\rho_o} \end{aligned}\right\} \qquad (2)$$

For horizontal-plane flows under confined conditions the following definitions apply:

$$\left.\begin{aligned} \Gamma_x^h &\equiv K_{xx}MS_t \\ \Gamma_y^h &\equiv K_{yy}MS_t \\ s^h &\equiv \dot{q}'' \\ M &\equiv \frac{\mu_o}{\mu} \text{ and } R = 0 \end{aligned}\right\} \qquad (3)$$

For horizontal-plane flows under unconfined conditions with M and R defined as in (3) the following definitions apply:

$$\left.\begin{aligned} \Gamma_x^h &= K_{xx} Mh \\ \Gamma_y^h &\equiv K_{yy} Mh \\ s^h &\equiv \dot{q}'' \end{aligned}\right\} \qquad (4)$$

b) Fluid Velocity Components

The well-known Darcy hypothesis is used to relate the velocity components to distributions of total head, h.

$$\left.\begin{aligned} h &\equiv \frac{p}{\rho_o g} + z \\ \varepsilon U &\equiv - K_{xx} M \frac{\partial h}{\partial x} \\ \varepsilon V &\equiv - K_{yy} M \frac{\partial h}{\partial y} + K_{yy} MR \end{aligned}\right\} \qquad (5)$$

c) Chemical-Species Conservation

It has been shown (Sharma, 1979) that the two-dimensional form of the general convective transport equation for the conservation of chemical species, l is:

$$\frac{\partial}{\partial t}(\varepsilon\rho C_l) + \frac{\partial}{\partial t}\{[1-\varepsilon]\rho_s C_{s,l}\} + \frac{\partial}{\partial x}\{\varepsilon\rho U C_l\} + \frac{\partial}{\partial y}\{\varepsilon\rho V C_l\}$$

$$= \frac{\partial}{\partial x}\{\varepsilon\rho D_{x,l} \frac{\partial C_l}{\partial x}\} + \frac{\partial}{\partial y}\{\varepsilon\rho D_{y,l} \frac{\partial C_l}{\partial y}\} + s^{C_l} \qquad (6)$$

d) Thermal Energy Conservation

Likewise, the conservation of thermal energy is:

$$\frac{\partial}{\partial t}(\varepsilon\rho C_v T) + \frac{\partial}{\partial t}\{[1-\varepsilon]\rho_s C_{v,s} T_s\} + \frac{\partial}{\partial x}\{\varepsilon\rho U C_p T\} + \frac{\partial}{\partial y}\{\varepsilon\rho V C_p T\}$$

$$= \frac{\partial}{\partial x}\{\varepsilon K_{x,T} \frac{\partial T}{\partial x}\} + \frac{\partial}{\partial y}\{\varepsilon K_{y,T} \frac{\partial T}{\partial y}\} + s^T \qquad (7)$$

The source terms s^{C_1} and s^T in equations (6) and (7) account for supply and/or annihilation of the respective variables due both to natural and man-made events.

2.3 Initial and Boundary Conditions

Initial and boundary conditions, respectively within and on the boundary of the solution domain, must be supplied for each of the dependent variables in order to complete the mathematical specification of the problem.

Initial conditions designate the distribution of h, C_1 and T, over the entire solution domain of interest, at the commencement of the solution. Such conditions may be obtained from the results of a field-measurement program and extrapolations thereof, as for example would be the regional piezometric head distribution. Alternatively, they may be obtained from laboratory-scale experiments, as for example the ambient concentration of chemical species in ground water. They may also be supplied from the results of previous calculations of a similar nature.

Boundary conditions represent variations of the dependent variables, their fluxes or combinations thereof, at the boundaries of the solution domain. Such conditions may also be obtained from the results of a field-measurement program, as would be the case, for instance, with recharge boundaries. It is important to note that boundary conditions

may vary with time. As a result, they influence the accuracy of results obtained with, and hence the numerical algorithms embodied in, computational solution procedures.

In addition to the above it must be noted that certain man-made as well as natural influences affect the distribution of h, C_1 and T within the solution domain. Such influences include discharging (and/or recharging) wells; artificial and natural barriers to flow (as well as heat and mass transfer) occurring locally within the domain.

It may be noted at this point that significant advantages accrue from a comprehensive mathematical formulation such as that outlined above. The advantages, principally in respect of flexibility in model applications to a large variety of problems, can be maintained only if the numerical algorithm selected for solution of the equations exhibits equally versatile features. Just such an algorithm is described below.

3. NUMERICAL SOLUTION PROCEDURE

3.1 General

The numerical procedure adopted in the present model, in its one-, two- or three-dimensional versions is of the integrated finite-difference (IFD) variety. The origins of this procedure lie in an earlier work on computational fluid mechanics and heat transfer (Sharma, 1974). Details of the present procedure are available in Sharma (1979). A brief description, however, is provided in this section.

3.2 Numerical Grid and Variable Locations

An illustration of the numerical grid adopted in the x-y plane is illustrated in Figure (1). In this figure the faces of control volumes, used in deriving the discretised equations, are indicated as dashed lines. The intersections of grid lines which are termed grid nodes, are chosen to lie at the geometric center of the associated control volumes. An exception is made at the boundaries of the domain where the nodes lie on the boundaries themselves.

All problem variables, with the exception of the velocity components U, and V, are presumed to be located at grid nodes. The x-direction velocity components U are presumed to lie on the intersections of the control-volume faces in the y-direction with the x-direction grid lines. Likewise, the y-direction velocity components V are presumed to lie on the intersections of the control-volume faces in the x-direction with y-direction grid lines. In general, with the flexibility of using variable grid spacings in any given direction, it is important to note that velocity components in any given direction do not lie exactly midway between grid nodes in that direction. This feature influences the numerical algorithm in a significant way.

3.3 The Discretised Equations

Discretised forms of the partial-differential equations (1), (6) and (7) are obtained by integrating them over the above-mentioned control volumes. It is presumed for purposes of this integration that the dependent variables vary linearly between successive grid nodes. Furthermore one such discretised algebraic equation, per dependent variable, may be derived in this manner for each control volume within the solution domain. It is precisely such an algebraic equation which represents, in finite-difference form, the conservation of mass, thermal energy or of chemical species. The preservation of these conservation principles in the simultaneous solution of the algebraic equations permits, in the present procedure, an exact accounting of mass, energy and momentum to be made. It is of great importance to note that such precise accounting of chemical species is vital in problems concerned with the limited disposal of waste at a given site. Many, otherwise praiseworthy mathematical models, do not ensure that this is the case.

The discretised equations, at an arbitrary grid node P with its neighbours at E, W, N and S, have the following forms:

a) Piezometric Head:

$$\left(\sum_{P} A^{h} - SN_{P}^{h} \right) h_{P} = \sum_{\substack{i= \\ E,W,N,S,O}} A_{i}^{h} h_{i} + SO_{P}^{h} \qquad (8)$$

b) Species Concentration:

$$\left(\sum_{P} A^{C_l} - SN_{P}^{C_l} \right) C_{l,P} = \sum_{\substack{i= \\ E,W,N,S,O}} A_{i}^{C_l} C_{l,i} + SO_{P}^{C_l} \qquad (9)$$

c) Temperature:

$$\left(\sum_{P} A^{T} - SN_{P}^{T}\right) T_{P} = \sum_{\substack{i= \\ E,W,N,S,O}} A_{i}^{T} T_{i} + SO_{P}^{T} \qquad (10)$$

In the above, A's denote coefficients computed from known (or sometimes temporarily presumed known) values of hydraulic conductivity, dispersion coefficients etc.; and SO, SN are components of a linearised source term; i denotes respectively the neighbouring grid nodes in space; and, O denotes the coefficient associated with the previous-time value of the appropriate dependent variable.

3.4 The Solution Algorithm

The sets of simultaneous algebraic equations noted above are solved by the efficient application of an alternating-direction, heavily-implicit, line-by-line solution algorithm coupled, for three-dimensional problems, to a plane-by-plane block correction procedure. Details are provided by Sharma (1979). This algorithm applied iteratively leads to relatively monotonic solutions for most problems with commonly-encountered boundary conditions.

Brief details of computer programs which embody the above described numerical procedure are provided below.

4.0 COMPUTER-PROGRAM DETAILS

The algorithm mentioned above has been incorporated into a set of computer programs written for one-, two- and three-dimensional problems. In the programs a serious attempt has been made to preserve the flexibility of the mathematical and of the numerical solution procedure. In keeping with this objective, the main machinery of the calculation procedure is kept entirely separate from the problem-specific and user-modifiable portions of the programs. Thus, they are versatile and relatively easy to employ.

These programs, called TARGET-S (for Transient Analyser of Reacting Ground Water Effluent Transport in saturated porous media), are written in standard FORTRAN-IV. They are thus capable of being run on most available computers. On a CDC-6600 machine a typical computer run for an unsteady two-dimensional problem requires approximately 60 seconds of central processor time.

5. SOME PREDICTED RESULTS

For purposes of testing the computer program TARGET-S and to demonstrate the accuracy of results predicted thereby, a few test runs were first made of a selected problem. The problem posed is that of unsteady convective dispersion in a homogeneous, saturated porous media in one space dimension.

Grid-dependency tests were first conducted to determine the effect of grid-size upon numerical accuracy. It was observed in that sufficiently accurate results may be obtained with a number of grid nodes which is also compatible with reasonable computing effort. Further tests investigating the dependence of accuracy upon the chosen time-step were conducted. The results of these are illustrated in Figures 2 and 3, which indicate that for desired levels of accuracy a sufficiently small time-step must be chosen. Subsequently predictions of concentrations of a moving solute front were made. For a given set of parameters, the predicted results for this case may be observed in Figure 3 to compare very favourably with the corresponding exact analytical solution.

TARGET-S has undergone numerous other tests, not reported here, to ensure that the program is essentially correct and that the results predicted with it are both plausible and valid. The validation tests are continuing.

The application of TARGET-S to a few representative problems is illustrated in Figures 4 to 8. In Figure 4, plots of piezometric head at successive time instants illustrates the achievement of steady-state leakage from a river to an underlying aquifer due to a continuously-operating pumping well. Figure 5 illustrates the performance of a set of dewatering wells employed to reduce pressures around an open pit mine. Figures 6 and 7 illustrate, respectively via piezometric heads and corresponding velocity vectors, the effect of a slurry wall in preventing flow to a chemically-contaminated portion of an aquifer.

Figure 8a, 8b and 8c illustrate the transient nature of chemical specie transport from an in-pit disposal system for wastes from a lignite-gasification facility. In addition to the above applications, TARGET-S is currently being applied to problems of radioactive and toxic waste disposal alternatives.

6. REFERENCES

Aikens, A.E. Jr, R.E. Berlin, J. Clancy and O.I. Oztunali (1979): "Generic methodology for assessment of radiation doses from groundwater migration of radionuclides in LWR wastes in shallow land burial trenches".

Akbar, A.M., M.E. Arnold and O.E. Harvey (1974): "Numerical simulation of individual wells in a field simulation model", Soc. Pet. Eng. J., pp. 315-320.

Bear, J. (1972): "Dynamics of fluids in porous media", American Elsevier, New York.

Braester, C., G. Dagan, S. Newman and D. Zaslawsky (1971): "A survey of the equations and solutions of unsaturated flow in porous media", Ann. Rep. 1, Proj. A 10-SWC-77, Israel Institute of Technology, Haifa, 176 p.

Bredehoeft, J.D. and G.F. Pinder (1970): "Digital analysis of areal flow in multi-aquifer ground water systems: a quasi three-dimensional model", Water Resources Res., 6, (30), pp. 883-888.

Cooley, R.L. (1974): "Finite-element solutions for the equations of ground water flow", Des. Res. Inst., Univ. of Nevada, Tech. Rep. Series H-W, Pub. No. 18, 134 p.

Davidson, J.M., L-T Ou, and P.S.C. Rao (1978): "Adsorption, movement and biological degradation of high concentrations of selected pesticides in soils", Proc. 4th Annual Res. Symp. on Land Disposal of Hazardous Wastes, pp. 233-244.

Dever, R.J. and R.W. Cleary (1979): "Unsteady-state, two-dimensional response of leaky aquifers to stream stage fluctuations", Adv. Water Resource, 2, (1), pp. 13-18.

Duguid, J.O. and M. Reeves (1976): "Material transport through porous media: A finite-element Galerkin model", Oak Ridge National Laboratory Report ORNL-4928.

Freeze, R.A. (1971): "Three-dimensional, transient, saturated/unsaturated flow in a ground water system", Water Resources Res., 7, (2), pp. 347-366.

Frind, E.O. (1979): "Exact aquitated response functions for multiple aquifer mechanics", Adv. Water Resource, 2, (2), pp. 77-82.

Gambolati, G. (1973): "Equation for one-dimensional vertical flow of ground water: 1, the rigorous theory", Water Resources Res., 9, (4), pp. 1022-1028.

Gray, W.G. and G.F. Pinder (1976): "An analysis of the numerical solution of the transport equation", Water Resources Res., 12, (3), pp. 547-555.

Gringarten, A.C. (1979): "Flow test evaluation of fractured reservoirs", presentation at the symposium on recent trends in hydrology, Berkeley, California.

Gringarten, A.C. and J.P. Sauty (1975): "A theoretical study of heat extraction from aquifers with uniform regional flow", J. Geophys. Res., 80, (35), pp. 4956-4962.

Gupta, S.P. and R.A. Greenkorn (1973): "Dispersion during flow in porous media with bilinear adsorption", Water Resources Res., 9 (5), pp. 1357-1368.

Hamilton J.L. and D. Sharma 1979: "Applications of a comprehensive mathematical model (TARGET) capable of predicting flow and chemical-species transport in porous media. Report under preparation.

Harlan, R.L. (1973): "Analysis of coupled heat/fluid transport in partially frozen soil", Water Resources Res., 9 (5), pp. 1314-1323.

Holst, P.H. and Aziz, K. (1972): "Transient three-dimensional natural convection in confined porous media", Int. J. Heat Mass Transfer 15, pp. 73-88.

Intercomp Resources Development and Engineering Inc. (1976): "A model for calculating effects of liquid waste disposal in deep saline aquifers", US Geol. Surv. Water Res. Invest., pp. 76-81.

Kealy, C.D., R.A. Busch and M.M. McDonald (1976): "Seepage - environmental analysis of the slime zone of a tailings pond", US Bureau of Mines, Rep. 7939, 89 p.

Konikow, L.F. and J.D. Bredehoeft (1978): "Computer model of two-dimensional solute transport and dispersion in ground water", USGS, Techniques of Water Resource Investigations, book 7, ch. C2.

McWhorter, D.B. and J.D. Nelson (1979): "Unsaturated flow beneath tailings impoundments", Journal of the Geotechnical division ASCE, 105, (11), pp. 1317-1334.

Mercer, J.W., G.F. Pinder and I.G. Donaldson (1975): "A Galerkin finite element analysis for hydrothermal system at Wairakei, New Zealand", J. Geophys. Res., 80, pp. 2608-2621.

Molz, F.J., J.C. Warman and T.E. Jones (1978): "Aquifer storage of heated water: Part I - A field experiment", Ground Water, 16, pp. 234-241.

Narasimhan, T.N. (1975): "A unified numerical model for saturated/unsaturated ground water flow", Ph.D. dissertation, Univ. of Calif., Berkeley, California.

Narasimhan, T.N. and P.A. Witherspoon, (1977): "Recent developments in modelling ground water systems. Rep. L3L-5209, Lawrence Berkeley Lab., Univ. of Calif., Berkeley, Calif.

Papadopulos, S.S. and S.P. Larson (1978): "Aquifer storage of heated water: Part II - Numerical simulation of field results", Ground Water 16, pp. 242-248.

Pinder, G.F. (1973): "A Galerkin - finite element simulation of ground water contamination on Long Island, New York", Water Resources Res., 9, (6), pp. 1657-1669.

Prickett, T.A. and C.G. Lonnquist (1971): "Selected digital computer techniques for ground water resource evaluation", Ill. State Water Survey, Bull. 55, 62 p.

Rubin, E. and C. Roth (1979): "On the growth of instabilities in ground water due to temperature and salinity gradients", Adv. Water Resources, 2, (2), pp. 69-76.

Rubin, J. and R.V. James (1973): "Dispersion-affected transport of reacting solutes in saturated porous media: Galerkin method applied to equilibrium-controlled exchange in uni-directional steady water flow", Water Resources Res., 9, (5), pp. 1332-1356.

Runchal, A.K., J. Treger and G.S. Segal (1978): "Two-dimensional coupled thermal and fluid-flow analysis in porous media", Dames & Moore, Advanced Techn. Group Rep. TN-LA-34.

Selim, H.M., J.M. Davidson and P.S.C. Rao (1977): "Transport of reactive solutes through multi-layered soils", Soil. Sci. Soc. of Amer. J., 41, (1), pp. 3-10.

Sharma, D. (1974): "Turbulent convective phenomena in straight reactangular-sectioned diffusers", Ph.D. Thesis, Imp. College, London, U.K.

Sharma, D. (1979): "A comprehensive mathematical model capable of predicting flow, heat transfer as well as chemical species transport in porous media". (Unpublished report).

Sharma, D. and J.L. Hamilton (1978): "A comprehensive mathematical model for the prediction of saturated/unsaturated flow in porous media. (Unpublished report).

Trescott, P.C., G.F. Pinder and S.P. Larson (1976): "Finite-difference model for aquifer simulations in two dimensions with results of numerical experiments", USGS, Tech. of Water Resource Investigations, Book 7, Ch. C1.

Trescott, P.C. and S.P. Larson (1977): "Comparison of iterative methods of solving two-dimensional groundwater flow equations", Water Resource Res., 13, (1), pp. 125-135.

Werner O., and W. Kley (1977): "Problems of heat storage in aquifers", J. Hydrology, 34, pp. 37-43.

Weston, R.F. (1978): "Pollution prediction techniques for waste disposal siting: a state of the art assessment", Rep. prepared for office of solid waste hazardous waste management division, USEPA.

7. NOMENCLATURE

A_i^{ϕ}	Coefficients representing hydraulic conductivity or dispersion coefficients etc., for variable ϕ at grid position i
C_l	Chemical species concentration of species l ($kg \cdot m^{-3}$)
C_p	Specific heat capacity at constant pressure ($J \cdot kg^{-1} \cdot °C^{-1}$)
C_v	Specific heat capacity at constant volume ($J \cdot kg^{-1} \cdot °C^{-1}$)
$C_{v,s}$	Specific heat capacity of the solid at constant volume ($J \cdot kg^{-1} \cdot °C^{-1}$)
$D_{x,l}$	Dispersion coefficient for species l in x-direction ($m^2 \cdot s^{-1}$)
$D_{y,l}$	Dispersion coefficient for species l in y-direction ($m^2 \cdot s^{-1}$)
h	hydraulic or piezometric head (m)
K_{xx}	x-direction hydraulic conductivity ($m \cdot s^{-1}$)
K_{yy}	y-direction hydraulic conductivity ($m \cdot s^{-1}$)
$K_{x,T}$	x-direction thermal conductivity ($J \cdot s^{-1} \cdot m^{-1} \cdot °C^{-1}$)
$K_{y,T}$	y-direction thermal conductivity ($J \cdot s^{-1} \cdot m^{-1} \cdot °C^{-1}$)
M	Viscosity ratio
$\dot{q}'''$	Point source of mass ($m^3 \cdot s^{-1} \cdot m^{-3}$)
R	Density ratio deficit
S_c	Storage coefficient (m^{-1})
S_t	Saturated thickness (m)
s^{ϕ}	Source term for variable ϕ
SO_P^{ϕ}	Component of linearized source term for variable ϕ at node P
SN_P^{ϕ}	Component of linearized source term for variable ϕ at node P
T	Temperature (°C)
t	time (s)
U	x-direction velocity ($m \cdot s^{-1}$)
V	y-direction velocity ($m \cdot s^{-1}$)
x,y,z	Cartesian coordinate directions (m)
ε	Porosity
μ	Viscosity ($kg \cdot m^{-1} \cdot s^{-1}$)
μ_o	Reference viscosity ($kg \cdot m^{-1} \cdot s^{-1}$)

Γ^{ϕ}_{x} Effective diffusion coefficient for variable ϕ, in direction x

ρ Density ($kg \cdot m^{-3}$)

ρ_o Reference density ($kg \cdot m^{-3}$)

8. FIGURES

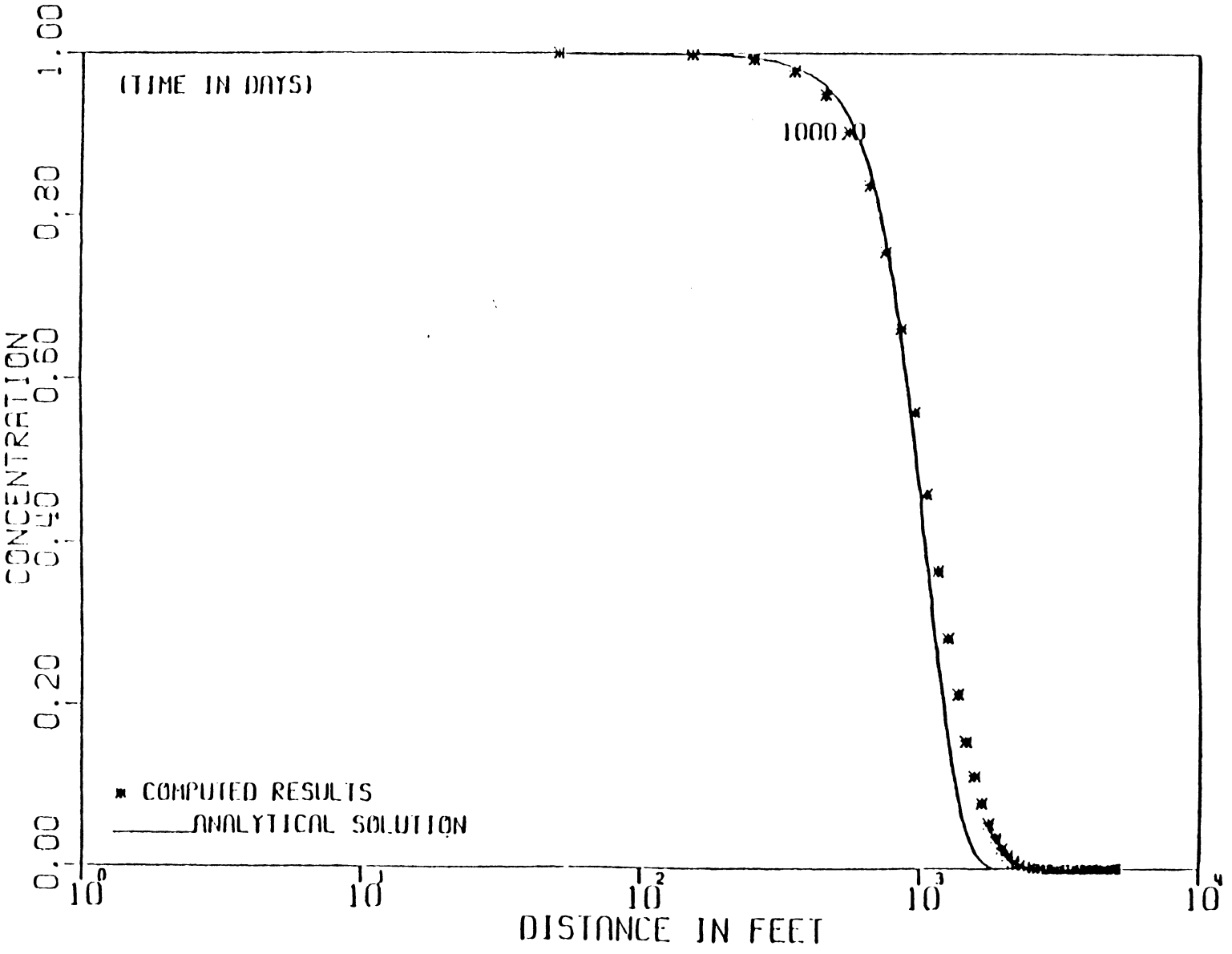

Figure 2 TIME DEPENDENCE OF CONCENTRATION DISTRIBUTIONS

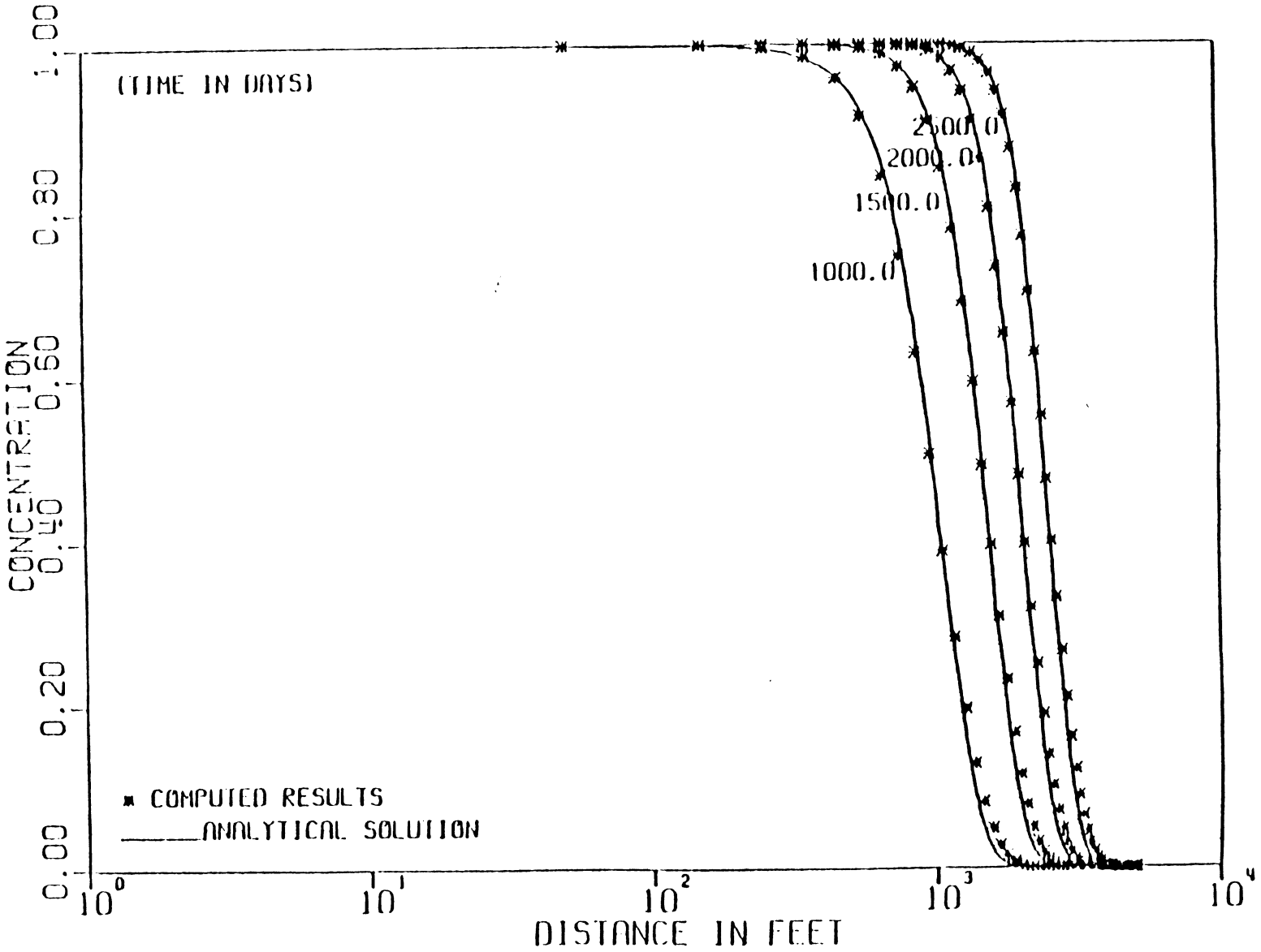

Figure 3 TIME DEPENDENCE OF CONCENTRATION DISTRIBUTIONS

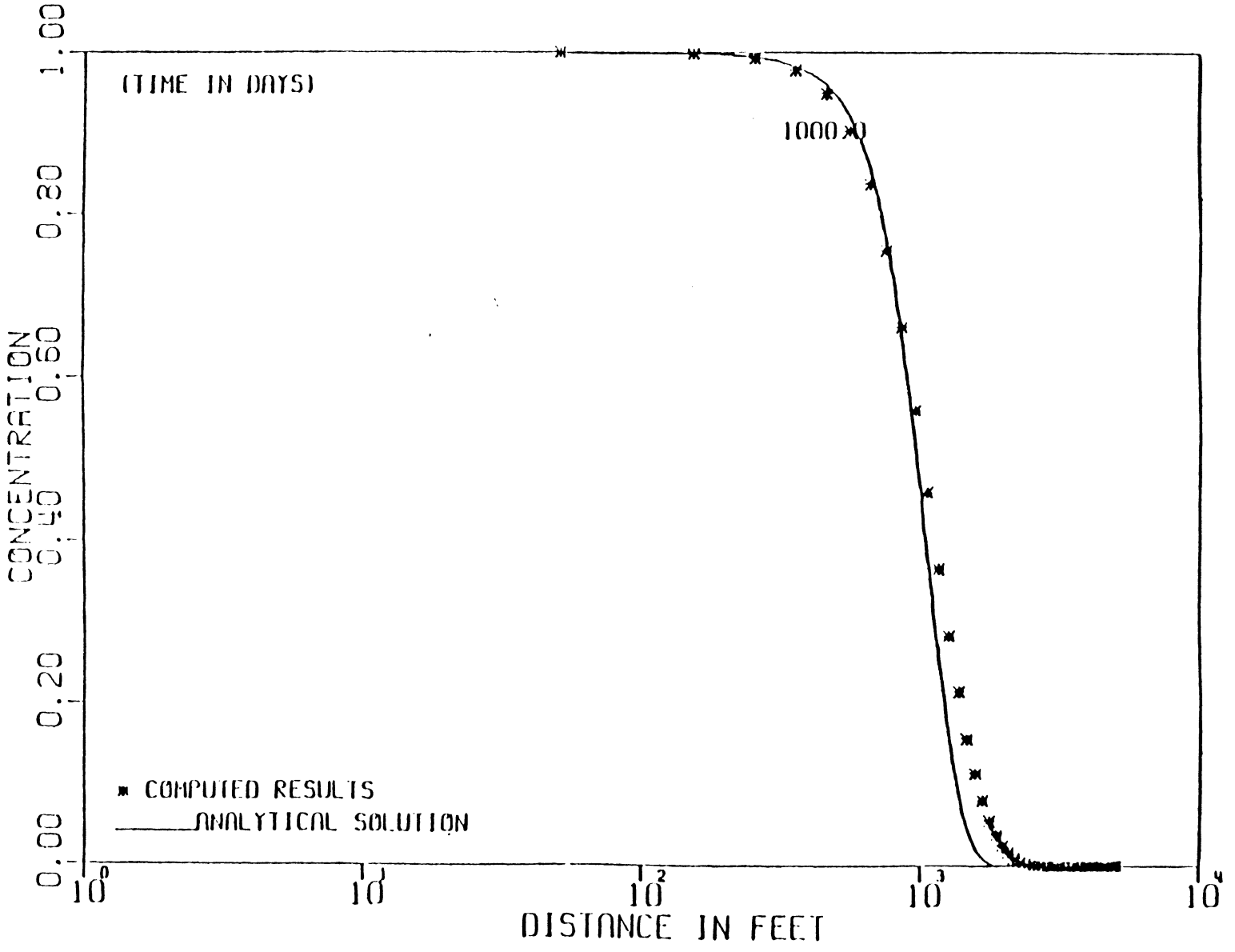

Figure 2

TIME DEPENDENCE OF CONCENTRATION DISTRIBUTIONS

Figure 3 TIME DEPENDENCE OF CONCENTRATION DISTRIBUTIONS

Figure 4

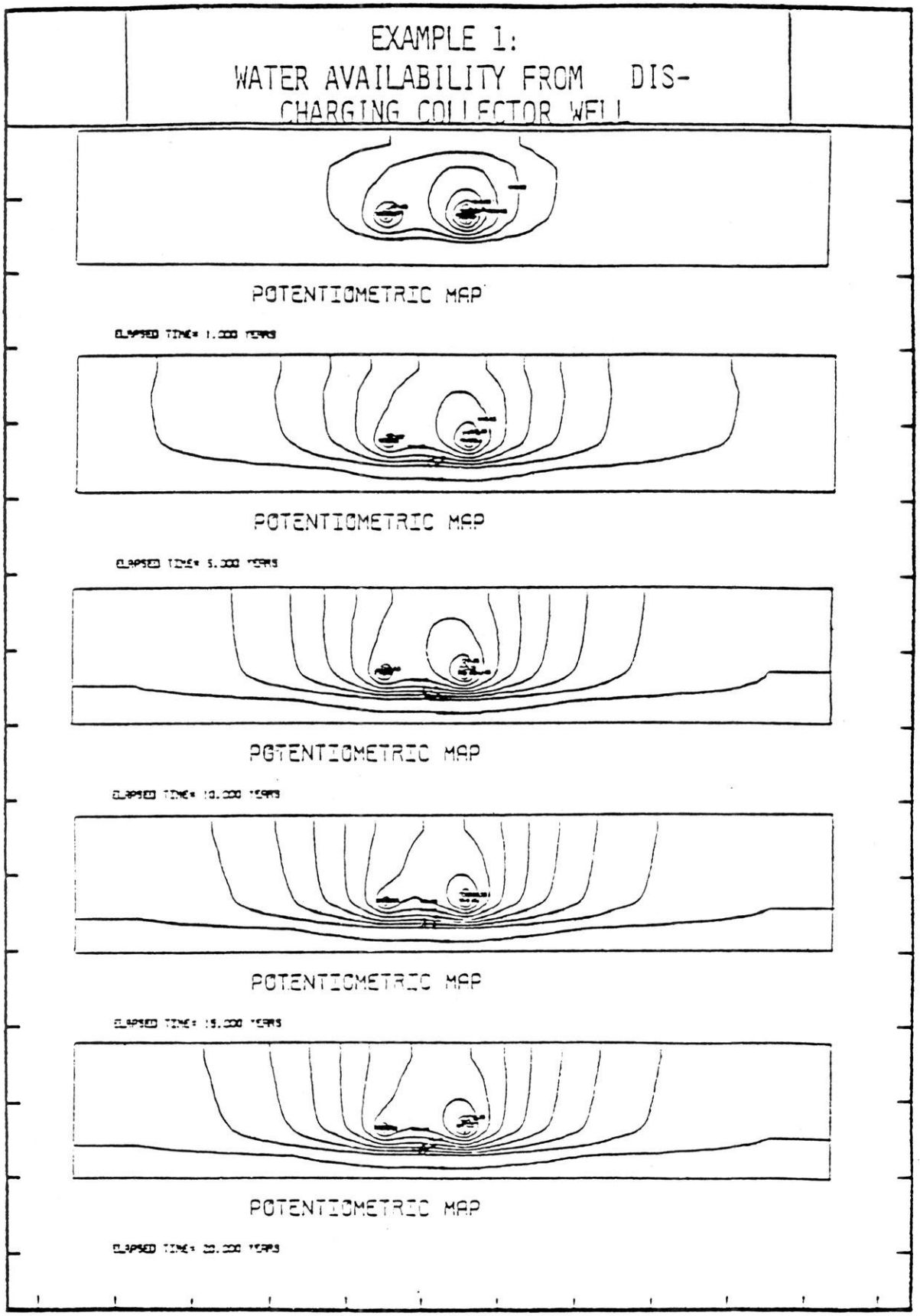
EXAMPLE 1:
WATER AVAILABILITY FROM DIS-
CHARGING COLLECTOR WELL
POTENTIOMETRIC MAP
POTENTIOMETRIC MAP
POTENTIOMETRIC MAP
POTENTIOMETRIC MAP
POTENTIOMETRIC MAP

Figure 5

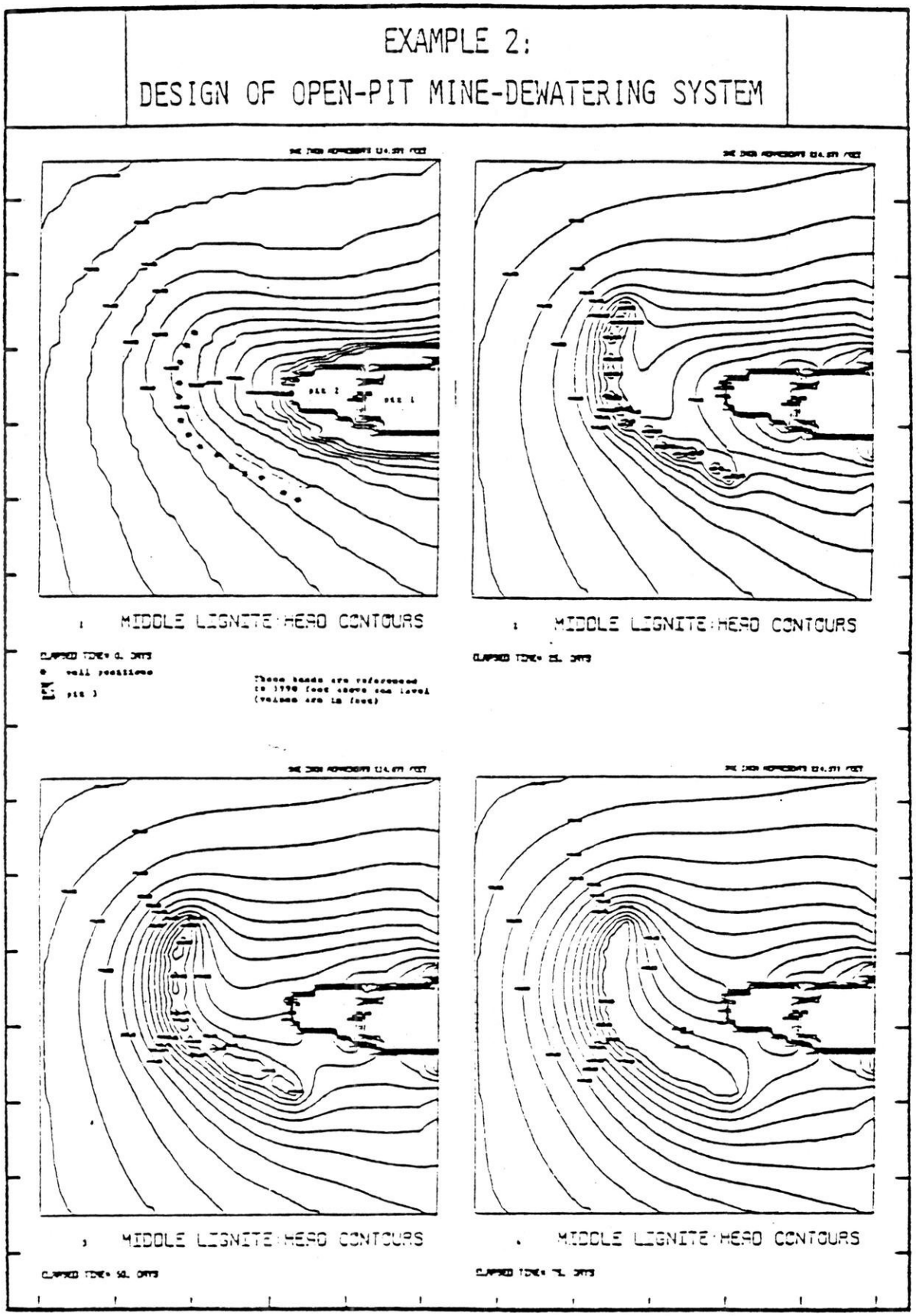
EXAMPLE 2:
DESIGN OF OPEN-PIT MINE-DEWATERING SYSTEM
MIDDLE LIGNITE HEAD CONTOURS
MIDDLE LIGNITE HEAD CONTOURS
MIDDLE LIGNITE HEAD CONTOURS
MIDDLE LIGNITE HEAD CONTOURS

Figure 6: Predicted contours of piezometric heads due to presence of slurry wall

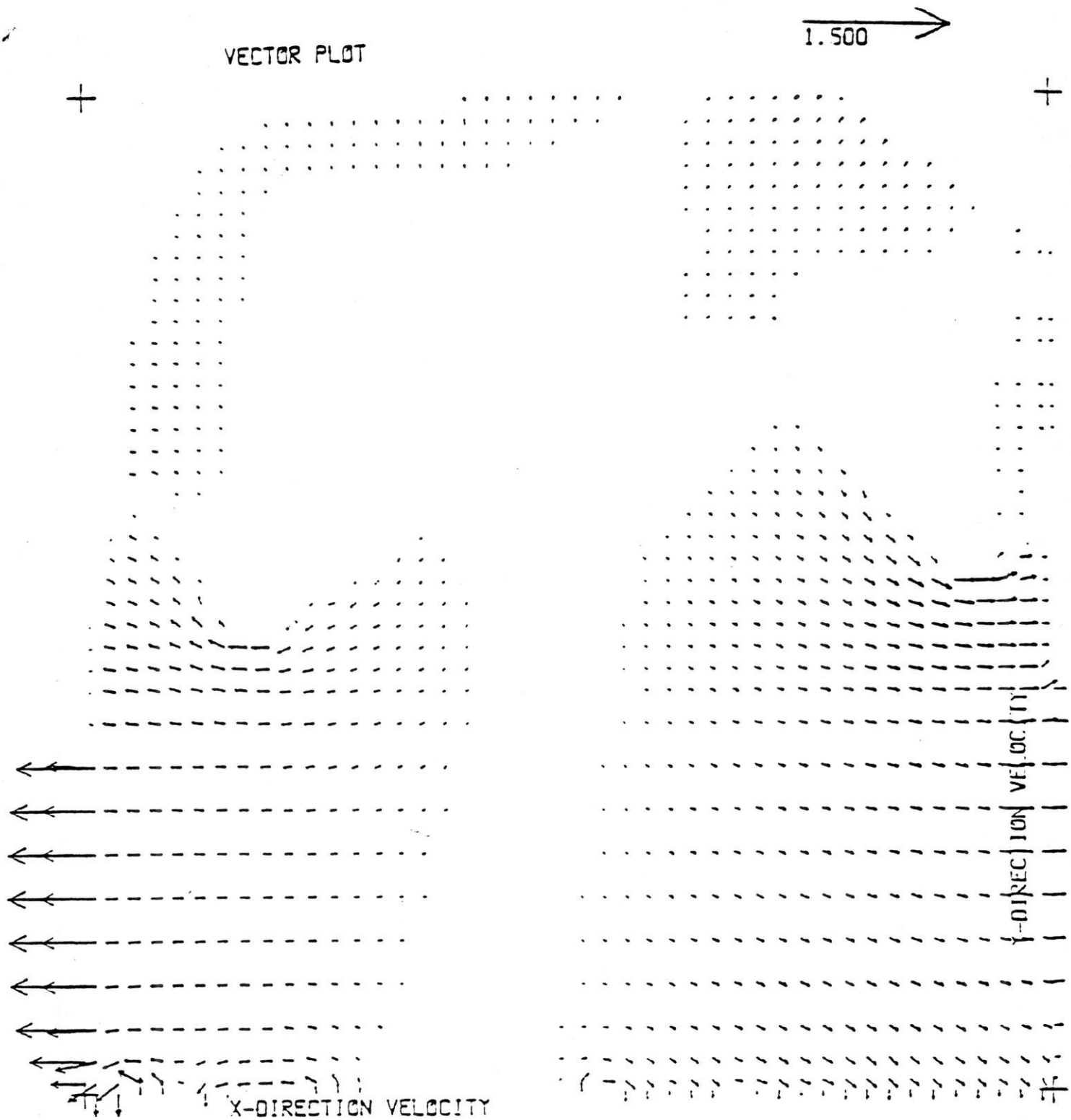

Figure 7: Velocity vectors corresponding to Figure 6.

Figure 8a

EXAMPLE 3: CONTD.
CHEMICAL-SPECIES TRANSPORT
D) CONCENTRATION DISTRIBUTIONS

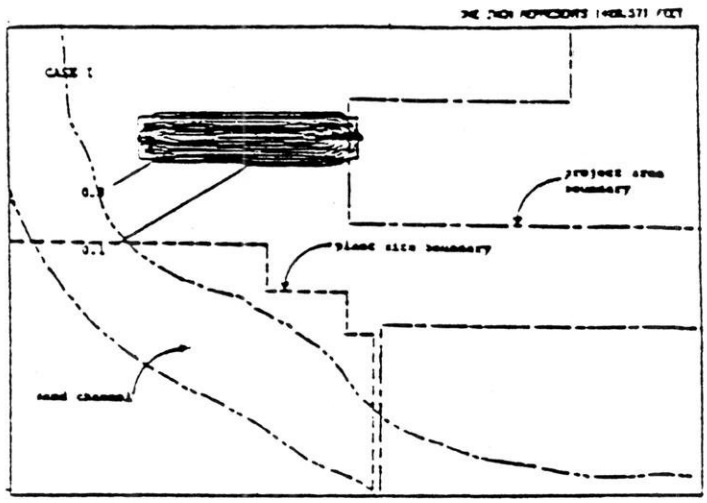

CONTOURS OF CONCENTRATION $\left(\frac{C-C_0}{C_1-C_0}\right)$

TIME= 2 YEARS

waste deposit

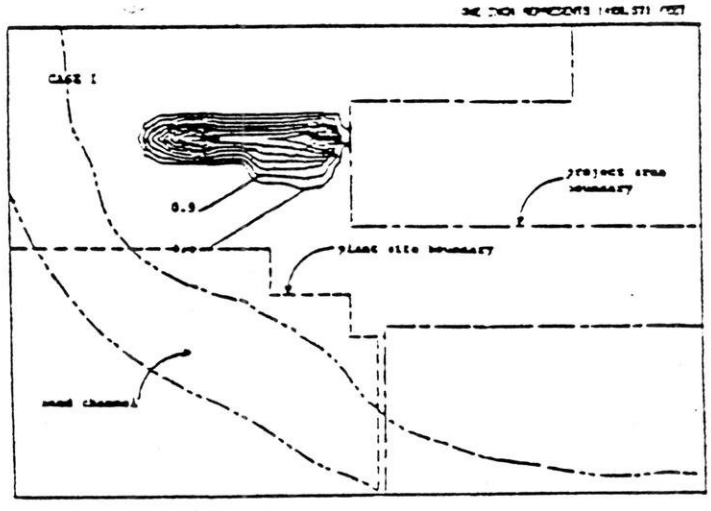

CONTOURS OF CONCENTRATION $\left(\frac{C-C_0}{C_1-C_0}\right)$

TIME= 10 YEARS

waste deposit

Figure 8b

EXAMPLE 3: CONTD.
CHEMICAL-SPECIES TRANSPORT
D) CONCENTRATION DISTRIBUTIONS

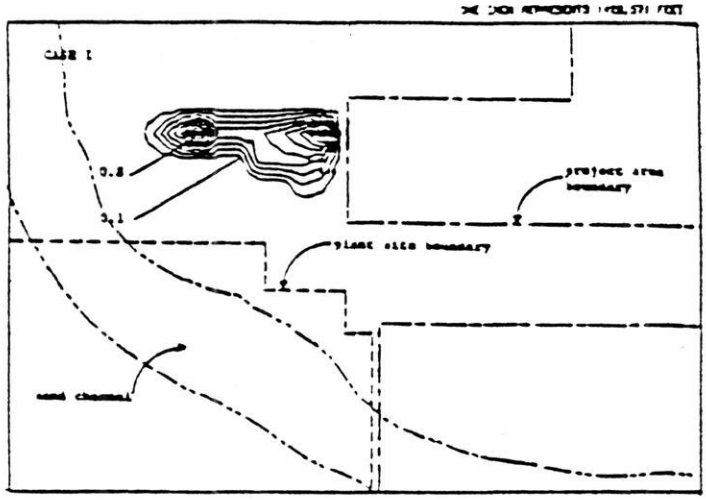

CONTOURS OF CONCENTRATION $\left(\frac{C-C_0}{C_0-C_1}\right)$

TIME= 20 YEARS
wake deposit

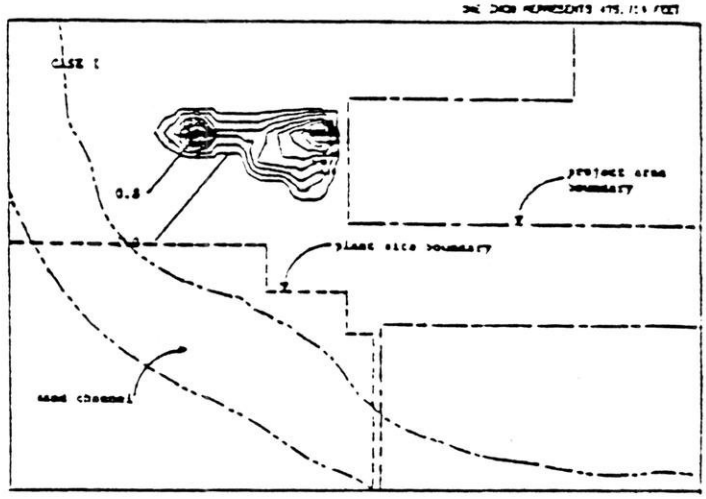

CONTOURS OF CONCENTRATION $\left(\frac{C-C_0}{C_0-C_1}\right)$

TIME= 30. YEARS
wake deposit

Figure 8c

EXAMPLE 3: CONTD.
CHEMICAL-SPECIES TRANSPORT
D) CONCENTRATION DISTRIBUTIONS

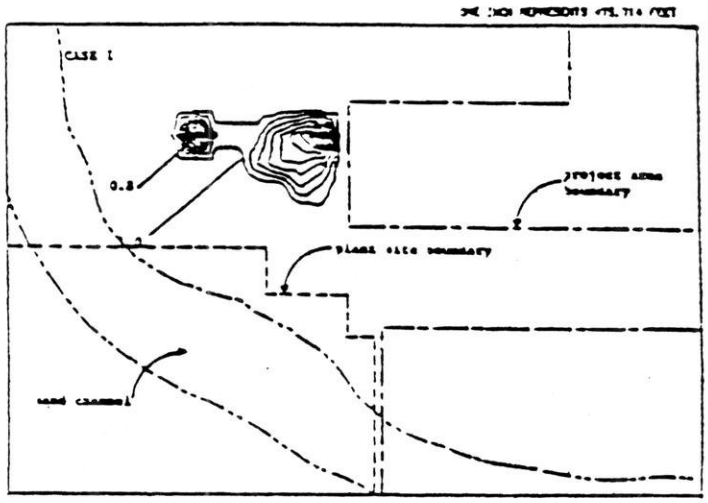

CONTOURS OF CONCENTRATION $\left(\frac{C-C_0}{C_1-C_0}\right)$

TIME= 40. YEARS

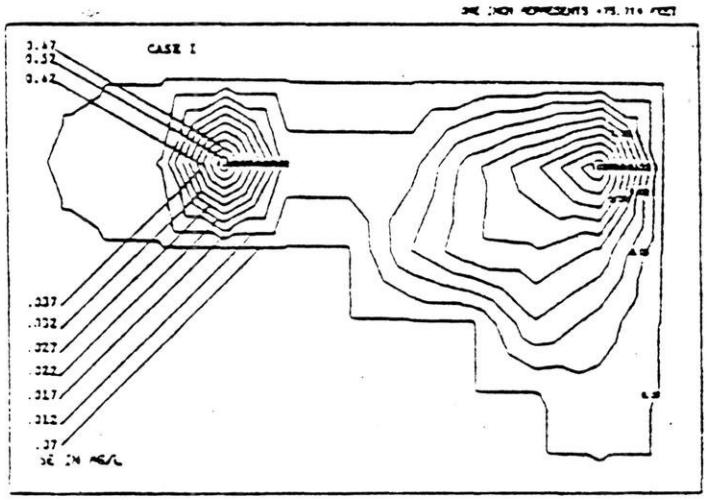

CONTOURS OF CONCENTRATION

TIME= 40. YEARS